Fall 2010

Posttranslational regulation of protein function and stability at the mitochondria and beyond

Shanna Katherine Nifoussi
University of Iowa

POSTTRANSLATIONAL REGULATION OF PROTEIN FUNCTION AND STABILITY AT THE MITOCHONDRIA AND BEYOND

by

Shanna Katherine Nifoussi

An Abstract

Of a thesis submitted in partial fulfillment
of the requirements for the Doctor of
Philosophy degree in Pharmacology
in the Graduate College of
The University of Iowa

December 2010

Thesis Supervisor: Associate Professor Stefan Strack

The goal of this dissertation research is to determine how post translational modifications of Mitofusin 2 (Mfn2), dynamin related protein 1 (Drp1) and Protein Phosphatase 2A (PP2A) B'β regulate protein function and stability. Mfn2 and Drp1 work in opposing manners to balance mitochondrial morphology and maintain organelle function. Loss of balanced fission and fusion results in mitochondrial dysfunction, a major contributor to the pathology of many neurodegenerative diseases and cancer. While regulation of fission is mediated through the reversible posttranslational modifications of Drp1, there are currently no known post-translational modifications of Mfn2 that regulate fusion. The first two experimental chapters of this thesis focus on the regulation of PKA induced phosphorylation of mitochondrial fission and fusion proteins. In Chapter 2 I utilize a Mfn2 phospho Ser442 specific antibody to determine the phosphorylation state of both over-expressed and endogenous neuronal Mfn2. Using this technique I found that under the conditions studied, Mfn2 is not PKA phosphorylated on Ser442. To look at the requirement of Mfn2 Ser442 in promoting mitochondrial elongation and protecting hippocampal neurons from excitotoxic cell death, Hela cells and primary hippocampal neurons (PHN) were evaluated by immunofluorescence. Results from these studies suggest Mfn2's neuroprotective effects require Ser442, and are separate from its function to promote mitochondrial fusion, and independent of PKA phosphorylation. Chapter 3 utilizes biochemical and immunofluorescence techniques to determine whether the PKA induced phosphorylation of Drp1 on Ser656 and the nitrosylation of Drp1 on Cys663 are mutually competing events. While previous work demonstrated the requirement of Drp1 Cys663 in mediating nitric oxide (NO) induced mitochondrial fragmentation and cell

death, results presented herein demonstrate Cys663 and Ser656 act independently to blunt, but not inhibit, mitochondrial fragmentation following NO treatment. Additional work demonstrated that the Drp1 Cys663Val mutant that blocks nitrosylation shows increased PKA phosphorylation of Ser656 by both biochemical and morphological assays, while direct Drp1 nitrosylation had no effect. These results show Cys663 to be a structurally important residue, but suggest Drp1 nitrosylation at Cys663 is not required for NO induced mitochondrial fragmentation.

The final chapter characterizes the formation of a novel E3 ubiquitin ligase complex, composed of KLHL15 and Cul3, that mediates the specific degradation of protein phosphatase 2A (PP2A) regulatory subunit B'β. PP2A B'β is expressed in neurons where it functions to regulate catecholamine synthesis through the dephosphorylation and inactivation of tyrosine hydroxylase (TH). Here I establish the role of a novel kelch domain containing protein, KLHL15, which serves as an adaptor molecule, bridging the E3 ubiquitin ligase Cul3, through the N-terminal BTB domain, with the substrate B'β through the C-terminal kelch domain. Additionally, the requirement of B'β Tyr52 for its interaction with KLHL15 suggests Tyr phosphorylation of this residue might regulate the inclusion of PP2A B'β in the complex, ultimately regulating downstream dopamine synthesis.

Abstract Approved:

_____
Thesis Supervisor

_____
Title and Department

_____
Date

POSTTRANSLATIONAL REGULATION OF PROTEIN FUNCTION AND STABILITY AT THE MITOCHONDRIA AND BEYOND.

by

Shanna Katherine Nifoussi

A thesis submitted in partial fulfillment
of the requirements for the Doctor of
Philosophy degree in Pharmacology
in the Graduate College of
The University of Iowa

December 2010

Thesis Supervisor: Associate Professor Stefan Strack

Graduate College
The University of Iowa
Iowa City, Iowa

CERTIFICATE OF APPROVAL

_____

PH.D. THESIS

_____

This is to certify that the Ph.D. thesis of

Shanna Katherine Nifoussi

has been approved by the Examining Committee
for the thesis requirement for the Doctor of Philosophy
degree in Pharmacology at the December 2010 graduation.

Thesis Committee: _____
Stefan Strack, Thesis Supervisor

_____
Donna Hammond

_____
Michael Dailey

_____
David Sheff

_____
Yuriy Ushachev

To Matt, Tyson and Tegan

I may not have gone where I intended to go, but I think I have ended up where I intended to be.

Douglas Adams

ACKNOWLEDGMENTS

First, I would like to thank my mentor Dr. Stefan Strack for providing me with a laboratory which to call home during my graduate school career. While my path towards graduation was not as smooth and straight as I would have preferred, I could not have navigated the bumps, curves, and changes in direction without your wealth of knowledge and seemingly unending support.

I would also like to thank my thesis committee members, Drs Michael Dailey, Yuriy Usachev, Donna Hammond and David Sheff for their guidance and encouragement over the years, as well as the letters of recommendation that have allowed me to not only receive a Pre-doctoral fellowship, but also given me the opportunity to choose my future direction. I would especially like to thank Dr. Sheff for his support and mentoring during my last year of graduate school. I want to thank Kate, Linda, Sue G, Sue B and Lisa for all of your help providing the simplest of assistance, which would be impossible without you. I also want to thank the faculty and students of the Department of Pharmacology for always keeping me on my toes during seminars, and for providing invaluable technical and reagent support. I would also like to thank the American Heart Association for my research funding.

I would like to thank the other Strack lab members, both past and present, especially Tom, Ron and Mike for their technical support, scientific wisdom, small talk when science was just too much, and for increasing my knowledge of all things fishy. Lastly, I want to thank my fellow classmates Jenna and Dice for their friendship and for traveling this long and difficult path by my side.

I would especially like to thank my family. My mom Bridget for always being there for moral support, providing a far off sanctuary, and most importantly for helping me see the forest for the trees. My dad Roy for his unending

encouragement, and my brother Ian for following in my footsteps (sort of) and always providing good humor. My in-laws for their support and for providing a loving weekend getaway. Most importantly, I would like to thank my children Tyson and Tegan for their comic relief, and for reminding me why I get up in the morning. Finally, I want to thank my husband Matt, for his never-ending support and encouragement, and for following me all over the country in pursuit of my dreams while his take a back seat. I truly wish I can live up to his expectations, and provide as much support for him in reaching his goals as he has for me.

ABSTRACT

The goal of this this dissertation research is to determine how post translational modifications of Mitofusin 2 (Mfn2), dynamin related protein 1 (Drp1) and Protein Phosphatase 2A (PP2A) B'β regulate protein function and stability. Mfn2 and Drp1 work in opposing manners to balance mitochondrial morphology and maintain organelle function. Loss of balanced fission and fusion results in mitochondrial dysfunction, a major contributor to the pathology of many neurodegenerative diseases and cancer. While regulation of fission is mediated through the reversible posttranslational modifications of Drp1, there are currently no known post-translational modifications of Mfn2 that regulate fusion. The first two experimental chapters of this thesis focus on the regulation of PKA induced phosphorylation of mitochondrial fission and fusion proteins. In Chapter 2 I utilize a Mfn2 phospho Ser442 specific antibody to determine the phosphorylation state of both over-expressed and endogenous neuronal Mfn2. Using this technique I found that under the conditions studied, Mfn2 is not PKA phosphorylated on Ser442. To look at the requirement of Mfn2 Ser442 in promoting mitochondrial elongation and protecting hippocampal neurons from excitotoxic cell death, Hela cells and primary hippocampal neurons (PHN) were evaluated by immunofluorescence. Results from these studies suggest Mfn2's neuroprotective effects require Ser442, and are separate from its function to promote mitochondrial fusion, and independent of PKA phosphorylation. Chapter 3 utilizes biochemical and immunofluorescence techniques to determine whether the PKA induced phosphorylation of Drp1 on Ser656 and the nitrosylation of Drp1 on Cys663 are mutually competing events. While previous work demonstrated the requirement of Drp1 Cys663 in mediating nitric oxide (NO) induced mitochondrial fragmentation and cell death, results presented herein

demonstrate Cys663 and Ser656 act independently to blunt, but not inhibit, mitochondrial fragmentation following NO treatment. Additional work demonstrated that the Drp1 Cys663Val mutant that blocks nitrosylation shows increased PKA phosphorylation of Ser656 by both biochemical and morphological assays, while direct Drp1 nitrosylation had no effect. These results show Cys663 to be a structurally important residue, but suggest Drp1 nitrosylation at Cys663 is not required for NO induced mitochondrial fragmentation.

The final chapter characterizes the formation of a novel E3 ubiquitin ligase complex, composed of KLHL15 and Cul3, that mediates the specific degradation of protein phosphatase 2A (PP2A) regulatory subunit B'β. PP2A B'β is expressed in neurons where it functions to regulate catecholamine synthesis through the dephosphorylation and inactivation of tyrosine hydroxylase (TH). Here I establish the role of a novel kelch domain containing protein, KLHL15, which serves as an adaptor molecule, bridging the E3 ubiquitin ligase Cul3, through the N-terminal BTB domain, with the substrate B'β through the C-terminal kelch domain. Additionally, the requirement of B'β Tyr52 for its interaction with KLHL15 suggests Tyr phosphorylation of this residue might regulate the inclusion of PP2A B'β in the complex, ultimately regulating downstream dopamine synthesis.

TABLE OF CONTENTS

LIST OF TABLES

LIST OF FIGURES

LIST OF ABBREVIATIONS

AC	Adenylate Cyclase
AKAP1	A-Kinase anchoring protein 1
BACK	BTB and C-terminal Kelch
BSA	Bovine Serum Albumin
BTB	bric a brac, tramtrack, broad complex
Bt_2 cAMP	Dibutyryl cAMP
C	Catalytic subunit
cAMP	cyclic adenosine monophosphate
caPKA	constitutively active PKA
cDNA	complimentary deoxyribonucleic acid
Cdk	cyclin dependent kinase
CMT	Charcot Marie Tooth disease
Cul	Cullin
DIV	Days *in vivo*
DMSO	dimethyl sulfoxide
DNA	Deoxyribonucleic Acid
DOA	Dominant optic atrophy
Drp1	Dynamin related protein 1
Erk	Extracellular regulated kinase
F/R	Forskolin and rolipram
FRAP	Fluorescence Recovery After Photobleaching
GED	GTPase Effector Domain

GFP	Green Fluorescent Protein
GPCR	G protein coupled receptors
GST	Glutathione S Transferase
HA	Hemaglutinin
HEAT	Huntingtin, elongation, A subunit, TOR
IF	Immunofluorescence
IP	Immunoprecipitation
IMM	Inner Mitochondrial Membrane
mGFP/omGFP	Outer mitochondrial targeted GFP
MAPK	Mitogen activated protein kinase
MD	Middle Domain
Mfn1	Mitofusin 1
Mfn2	Mitofusin 2
mtDNA	Mitochondrial DNA
NO	Nitric Oxide
NOS	Nitric Oxide Synthase
NT2	N-tera 2 cells
OA	Okadaic Acid
OMM	Outer Mitochondrial Membrane
omPKA	Outer mitochondrial targeted PKA
Opa1	Optic Atrophy 1
PAGE	Polyacrylamide gel electrophoresis
PBS	Phosphate buffered saline

PFA	Paraformaldehyde
PHN	Primary Hippocampal Neurons
PI	Propidium Iodide
PP2A	Protein Phosphatase 2A
PKA	Protein Kinase A
R	Regulatory Subunit
RIPA	Radioimmunoprecipitation Assay
RNA	Ribonucleic Acid
RNAi	RNA interference
SCA	Spinocerebellar Ataxia
shRNA	short hairpin RNA
SNOC	S-nitrosocysteine
TH	Tyrosine hydroxylase
TTBS	Tris Buffered Saline containing Triton X-100
VD	Variable Domain
VSMC	Vascular Smooth Muscle Cell

CHAPTER I: INTRODUCTION

Mitochondria

In the 1850's scientists examining muscle cells under a microscope began describing previously unidentified organelles that looked like grains of wheat (Scheffler, 2008). Further investigation revealed that the morphology of these membrane bound organelles varied in different tissues and could be described as either wheat grains (Chondros, Greek) or more threadlike structures (Mitos, Greek), from which the name mitochondrion is derived. Over the next 30-40 years, biochemical characterization revealed that cellular energy production through oxidative phosphorylation originated at the mitochondria. With the new role of mitochondria as the "powerhouse of the cell," came the hotly debated question; did mitochondria evolve within a single cell through internal compartmentalization, or rather did a prokaryote capable of energy production form a symbiotic relationship with an early eukaryotic cell. While never firmly concluded, the identification of mitochondrial DNA (mtDNA) solidified the endosymbiotic theory thereby clarifying the evolution of the eukaryotic cell (Margulis, 1981).

Mitochondrial Fission and Fusion

Early descriptions of mitochondria as either small granules or longer threadlike structures highlight the dynamic nature of the organelle (Scheffler, 2008). Indeed mitochondria are not static organelles but rather undergo rapid fission and fusion events regulated by a group of large GTPases. Mitochondrial fusion is regulated by two outer mitochondrial membrane (OMM) localized proteins Mitofusin 1 (Mfn1) and Mitofusin 2 (Mfn2) (Figure 1.1A) (Chen, et al, 2003, Eura, et al, 2003, Hales & Fuller, 1997, Ishihara, et al, 2004, Legros, et al, 2002, Santel & Fuller, 2001, Santel, et al, 2003), and Optic Atrophy 1 (Opa1),

localized to the inner mitochondrial membrane (IMM) (Cipolat, et al, 2004). Fusion of the OMM occurs through the C-terminal coiled-coil domains of Mfn1/2 interacting with like proteins on adjacent mitochondria (Koshiba, et al, 2004). While it is not known how Mfn1/2 mediates mitochondrial fusion, a recently proposed model suggests once the adjacent mitochondria are bound by Mfn1/2, GTP hydrolysis induces a conformational change, folding the protein in half, allowing for fusion to occur (Knott, et al, 2008). Fusion of the IMM is proposed to occur through the interaction of Opa1 with itself in *trans* allowing for inner membrane tethering and fusion (Knott, et al, 2008, Meeusen, et al, 2006).

Mitochondrial fission is regulated by the dynamin homologue Dynamin related protein 1 (Drp1) (also called Dynamin like protein 1 (Dlp1)) (Smirnova, et al, 2001, Smirnova, et al, 1998). Drp1 localizes in the cytosol until signaling events mediate its translocation to the mitochondria where it interacts with the OMM localized Fis1 (Figure 1.1B) (James, et al, 2003, Smirnova, et al, 2001, Smirnova, et al, 1998, Stojanovski, et al, 2004, Yoon, et al, 2003). There are conflicting views as to how Drp1 mediates mitochondrial scission once at the mitochondrion. The first view suggests that Drp1 forms concentric rings around the mitochondria that constrict, dividing one mitochondrion into two (Knott, et al, 2008, Praefcke & McMahon, 2004, Urrutia, et al, 1997, Youle & Karbowski, 2005). The alternative theory is that Drp1 acts as a pinchase, pinching off small amounts of the OMM through GTP hydrolysis. When a critical amount of the OMM has been depleted, fission occurs through the snapping of the once fused mitochondrion into two (Youle & Karbowski, 2005).

The importance of balanced mitochondrial fission and fusion is highlighted by the fact that mutations in many fission and fusion proteins lead to hereditary neurodegenerative diseases, or early death. Mutations in Opa1 cause the most common type of hereditary blindness, Dominant Optic Atrophy (DOA), which in

rare cases presents with additional symptoms such as deafness or other neurological or neuromuscular abnormalities (Amati-Bonneau, et al, 2009, Lenaers, et al, 2009, Liesa, et al, 2009). Two different variants of the neurodegenerative disease Charcot Marie Tooth (CMT) disease are caused by mutations in mitochondrial fission and fusion proteins (Liesa, et al, 2009). Mutations clustered in the N-terminal Ras like domain, the GTPase domain and the first coiled-coil domain of Mfn2 are responsible for about 20% of CMT type 2A (CMT2A), making it the most common cause of hereditary neuropathy (Chung, et al, 2006, College, 2006, Engelfried, et al, 2006, Palau, et al, 2009, Verhoeven, et al, 2006, Zhu, et al, 2005, Zuchner, et al, 2004). Mutations in GDAP1, a proposed mitochondrial fission protein, have been shown to cause the demyelinating form of CMT, type 4A, a recessive variant of the disease (Palau, et al, 2009, Vallat, et al, 2008). Lastly, a *de novo* mutation of Ala395Asp in Drp1 was found in an infant born with microencephaly, who died shortly after birth (Waterham, et al, 2007). Microscopic examination of patient fibroblasts revealed abnormal mitochondrial fission due to impaired oligomerization and decreased mitochondrial localization (Chang, et al, 2010, Waterham, et al, 2007). Overall, the occurrence of pathology related to mitochondrial dysfunction signifies the importance of maintaining a balance between mitochondrial fission and fusion.

The role of fission and fusion in promoting mitochondrial function

Though the mitochondria were originally identified as power producing organelles, their known functions are numerous, quite diverse and require balanced fission and fusion. Fusion is important for many functions including cellular respiration, where decreased fusion impairs oxidative phosphorylation and decreases membrane potential possibly due to an inability to repair

damaged mtDNA (Benard & Rossignol, 2008, Chen & Chan, 2005, Seo, et al, 2010).

The relationship between mitochondria and calcium has been intimately explored over the past sixty years. Not only are mitochondria able to buffer large calcium efflux within the neuronal synapse (MacAskill & Kittler, 2010), but also store Ca^{2+} until it is needed elsewhere by the cell (Walsh, et al, 2009). Additionally, Ca^{2+} influx is tightly regulated by membrane potential and is both important for and dependent on cellular respiration.

The ability of mitochondria to undergo regulated fission is important not only for apoptosis, but also for the selective degradation of damaged mitochondria through autophagy. One of the initial steps in apoptosis is Drp1 mediated mitochondrial fragmentation preceding cytochrome c release and activation of caspase cascades (Karbowski, et al, 2002, Suen, et al, 2008, Youle & Karbowski, 2005). Inhibition of Drp1 activity delays but doesn't abolish cell death (Knott, et al, 2008). Similarly, mitochondrial quality control is dependent on the selective targeting of damaged or dysfunctional mitochondria for autophagy (Chen & Chan, 2009). Impairing the ability of mitochondria to undergo autophagy, due to loss of Drp1 function, leads to an increased presence of damaged mitochondria (Twig, et al, 2008).

The brain is the most power hungry tissue in the body utilizing 1/5 of the energy produced for maintaining synaptic transmission and the promotion of action potential (MacAskill & Kittler, 2010). Most of the energy produced in the brain is derived from mitochondria localized in the neurons at sites of high-energy demand, such as the pre and post synapse. Therefore mitochondria need a reliable method of transportation from the soma to the synapse. Anterograde transport of mitochondria to the synapse occurs along the microtubules and is mediated by the kinesin motor proteins KIF5 and KIF1B (Hirokawa & Takemura,

2005, Nangaku, et al, 1994). TRAK1/2 (human homologues of the *Drosophila* protein Milton) and Miro act as adaptors anchoring the mitochondria to the motor proteins (MacAskill & Kittler, 2010). Damaged mitochondria are transported retrogradely along the axon to the soma by dynein motor proteins and currently unknown anchor complexes. Recent evidence has shown that Mfn1/2 interact with the Milton/Miro complex responsible for mitochondrial anterograde transport (Misko, et al, 2010). Loss of Mfn2 specifically, results in delayed axonal movement due to decreased attachment to the transport complex.

In conclusion, regulation of mitochondrial fission by Drp1 and Fis1, or fusion, by Mfn1, Mfn2, and Opa1 is required not only for proper localization within neurons, but also for the myriad of mitochondrial functions where inhibition of fission or fusion can lead to delayed apoptosis, loss of autophagy, decreased oxidative phosphorylation and a decrease in membrane potential. Recent acknowledgement of the contribution of mitochondrial dysfunction to neurological disease and cancer further highlights the importance of regulated fission and fusion activity.

PKA signaling activity at the mitochondria

Protein Kinase A

The cAMP/Protein Kinase A (PKA) signaling pathway is a complex network involving the activation of a cascade of proteins resulting in the direct phosphorylation of target substrates. Initiation of the cAMP/PKA signaling cascade begins when ligand binds to the G-protein coupled receptor (GPCR), activating the α subunit by exchanging GDP for GTP allowing it to dissociate from the $\beta\gamma$ subunits. The signal is terminated when the α subunit hydrolyses GTP to GDP. The $G\alpha_s$ subunit of GPCR specifically activates adenylate cyclase, which converts ATP to cAMP and releases it into the cytosol. The released cAMP

can activate a diverse group of substrates including phosphodiesterases (Houslay & Adams, 2003), guanine nucleotide exchange proteins activated by cAMP (EPACs) (Bos, 2003, Cheng, et al, 2008) and Protein Kinase A (PKA) (Wong & Scott, 2004). PKA is a tetramer consisting of two regulatory (R) monomers that hold in place two inactive catalytic (C) monomers creating the holoenzyme. The structure of the R subunits consists of a N-terminal dimerization/docking domain (D/D), a linker region that contains an inhibitor site, followed by two cAMP binding domains (Sarma, et al, 2010). The presence of either RI (subtype I) or RII (subtype II) within the holoenzyme dictates PKA subtype. While both PKA subtypes respond to cAMP by releasing the C subunits to phosphorylate target substrates, they differ in their ability to be post-translationally modified by autophosphorylation (Erlichman, et al, 1974, Francis & Corbin, 1994, Taylor, et al, 1990) or nitrosylation (Burgoyne & Eaton, 2009), their sensitivity to substrate mediated PKA activation through facilitation of holoenzyme dissociation (Viste, et al, 2005), and their affinity for binding AKAPs (Banky, et al, 1998). The binding of PKA RI and RII to AKAP1 is mediated through their N-terminal D/D domain that forms a docking site for AKAPs through the formation of X-type antiparellel four-helix bundles (Banky, et al, 1998, Sarma, et al, 2010). Within the D/D domain of RI are two cysteines, Cys16 and Cys37, which form disulfide bonds across the antiparellel bundles (Leon, et al, 1997). Mutation of Cys37His disrupts disulfide bond formation (Leon, et al, 1997), but further mutations of Phe47Ala and Phe52Ala are required to prevent RI dimerization (Banky, et al, 1998).

A-Kinase Anchoring Protein 1

A kinase anchoring proteins (AKAPs) are a diverse family of proteins whose shared function is to serve as scaffolds anchoring PKA and other

signaling molecules in distinct locations providing substrate specificity (Skroblin, et al, 2010, Wong & Scott, 2004). The N-terminal portion of AKAP1 (alternatively called D-AKAP1, AKAP121 or AKAP149) is responsible for targeting the protein to the mitochondria, while alternative splicing of the C-terminus mediates protein interaction and dimerization (Chen, et al, 1997, Huang, et al, 1997, Huang, et al, 1999, Ma & Taylor, 2008, Wong & Scott, 2004). Unique among its family members, AKAP1 is able to interact with both type I and type II regulatory subunits of PKA (Huang, et al, 1997) as well as Protein Phosphatase 1 (Steen, et al, 2000). The region of AKAP1 important for binding PKA is found in the core domain of the protein and is present in all splice variants (Huang, et al, 1997).

Formation of the Protein Phosphatase 2A holoenzyme complex

Protein Phosphatase 2A (PP2A) is one of four major serine/threonine phosphatases that is highly conserved throughout evolution (Janssens, et al, 2008, Lechward, et al, 2001, Shi, 2009). PP2A plays a crucial role in many cellular processes including cell cycle regulation, cell growth, development and death, cell mobility, cytoskeletal dynamics, and participates in many cell signaling pathways (Shi, 2009). The core region of PP2A consists of a scaffolding A subunit and a catalytic C subunit, while the inclusion of a variable regulatory B subunit completes the holoenzyme. The A and C subunits are encoded by two highly similar genes, while the B subunits are encoded by three unrelated gene families, B (B55), B’ (B56) and B”” (McCright, et al, 1996). Though some of the subunits show tissue specific expression, most cells contain multiple PP2A holoenzyme complexes that differ in subcellular localization, substrate specificity and protein regulation, predominantly determined by the inclusion of the B subunit.

The core enzyme

The core of the PP2A enzyme consists of the A and C subunits. Structurally, the A subunit contains 15 tandem Huntington, elongation, A subunit, TOR (HEAT) repeats that form an elongated horseshoe structure (Hemmings, et al, 1990, Shi, 2009, Walter, et al, 1989). HEAT repeats 11-15 have been found to interact directly with the C subunit (Xing, et al, 2006). The core enzyme is differentially regulated through interactions with tumor inducing toxins Okadaic Acid (OA) and microcystin-LR (MCLR) (Shi, 2009, Xing, et al, 2006), which bind in a hydrophobic pocket and interact with residues within the active site of the C subunit inhibiting PP2A activity (Xing, et al, 2006).

The regulatory subunit

The regulatory subunits are grouped into families based on sequence and structural similarity. The B family is encoded by four genes (α, β, γ, δ), which structurally form a β propeller consisting of seven WD40 repeats (Shi, 2009). While Bα and Bδ are expressed in a variety of tissues (Strack, et al, 1999), Bβ and Bγ are neuron specific (Strack, et al, 1998). Characterization of Bβ localization has found that alternative splicing of an N-terminal tail targets the subunit to the mitochondria, where is it proposed to dephosphorylate resident proteins (Dagda, et al, 2003, Dagda, et al, 2005, Dagda, et al, 2008). One of the most well characterized substrates of the B family is tau. Hyperphosphorylation of tau has been linked to Alzheimer's disease, suggesting a possible role of decreased PP2A B family activity in pathology (Qian, et al, 2010). Recent work in the Strack lab found that PP2A Bα and Bδ regulate the Mitogen Activated Protein Kinase (MAPK) signaling cascade through dephosphorylation of Erk (Van Kanegan, et al, 2005).

The B' family is encoded by five genes (α, β, γ, δ, ε) that structurally consist of eight HEAT repeats forming a crescent shape (Xu, et al, 2006). The B' family plays an important role in cellular development and neuronal outgrowth through regulation of signaling cascades. B'α interacts with and destabilizes β-catenin leading to a overall decrease in wnt signaling (Eichhorn, et al, 2009, Seeling, et al, 1999, Yamamoto, et al, 2001). B'δ dephosphorylates the TrkA receptor producing sustained signaling and neuronal differentiation (Van Kanegan & Strack, 2009). While B'β is responsible for dephosphorylating tyrosine hydroxylase (TH) causing a decrease in catecholamine production (Saraf, et al, 2007, Saraf, et al, 2010).

The third family of regulatory subunits is B'', which is encoded by one gene that yields two proteins through alternative splicing (Janssens & Goris, 2001). B" family subunits are mainly localized to the nucleus and are thought to be calcium dependent phosphatases with a role in the regulation of the G_1/S cell cycle transition (Janssens, et al, 2003, Voorhoeve, et al, 1999).

Overall, the role of PP2A in dephosphorylating target substrates either in the cytosol or mitochondria is regulated not only by the inclusion of a specific regulatory subunits, but also through the inactivation of the core enzyme by pharmacological inhibitors.

Cell Systems

The selection of an appropriate cell culture model for my thesis work was based on two criteria; 1) Microscopic analysis of mitochondria morphology required the use of larger, flat cells that were responsive to pharmacological treatment; 2) Biochemical approaches required the production of large quantities of over-expressed protein in order to examine interactions or modifications that occurred in only a small fraction of the protein population. Based on these

requirements, CV1, NT2 and Long Hela cells were used for the immunofluorescence studies and the FRAP assays performed by the Youle lab while Cos 1 and Cos M6 were used for the biochemical assays.

CV1 cells are kidney epithelial cells from *Cercopithecus aethiops* (Jensen, et al, 1964). While these cells grow flat and have abundant mitochondria, they are unresponsive to forskolin induced mitochondrial elongation (data not shown). N-tera 2 (NT2) cells are a human embryonic testicular carcinoma cell line (Andrews, 1988) that differentiate following neuroectodermal lineages in the presence of retinoic acid (Andrews, 1984). These cells provided an excellent way of studying the effects of phospho-mutations in Mfn2 on protein function by monitoring changes in mitochondrial morphology under both basal and forskolin stimulated conditions (Chapter 2). The last cell line used for immunofluorescence was Long Hela cells, a human cervical carcinoma cell line (Scherer, et al, 1953). We began using these cells in order to determine whether the variation in the ability of Mfn2 phospho-mutants to regulate function in Fluorescence Recover After Photobleaching (FRAP) assays and immunofluorescent experiments was due to differences in cell culture models or technique (Chapter 2).

For biochemical assays I used Cos 1 cells, which are kidney epithelial cells from *Cercopithecus aethiops* (Gluzman, 1981) in Chapters 3 and 4, while I used a clonal cell line Cos M6 for experiments in Chapter 2. These cell lines have high transfection efficiency with very little associated cell death, allowing for the production of large quantities of expressed proteins.

Additionally various tissue extracts from rat where used to look at expression of Mfn2, while primary hippocampal neurons (PHN) were used to examine the neuroprotective role of Mfn2 in Chapter 2.

Dissertation Research Focus

Mitochondria are required for a diverse array of functions, from energy production through oxidative phosphorylation, to buffering and storing Ca^{2+} in the neuronal synapse, to control of autophagy and apoptosis. The maintenance of proper function is dependent on the ability of the mitochondria to balance dynamic fission and fusion events, regulated by Drp1 and Mfn1/2 respectively. Recently mitochondrial fission and fusion proteins have been identified as substrates of kinases and phosphatases localized both at the mitochondria as well as in the cytosol. I will present data herein addressing the question whether the regulation of phosphorylation events profoundly effects the function of target substrates. I will address this question by testing three separate and distinct hypotheses (Figure 1.2); 1) Phosphorylation of Mfn2 on Ser442 mediates the mitochondrial morphology and cell survival actions of PKA at the outer mitochondrial membrane; 2) Nitrosylation of Drp1 Cys663 inhibits phosphorylation of Drp1 Ser656 to mediate mitochondrial fission and cell death; 3) The E3 ubiquitin ligase Cul3 along with the novel adaptor protein KLHL15 specifically target PP2A B'β for degradation. The conclusions of this research provide important insight in the identification of novel sites of PKA phosphorylation of Mfn2, determination of whether posttranslational modifications of neighboring residues act dependently or independently in the modulation of protein function, and the characterization of a novel Cul3::KLHL15 complex that regulates the stability of PP2A B'β.

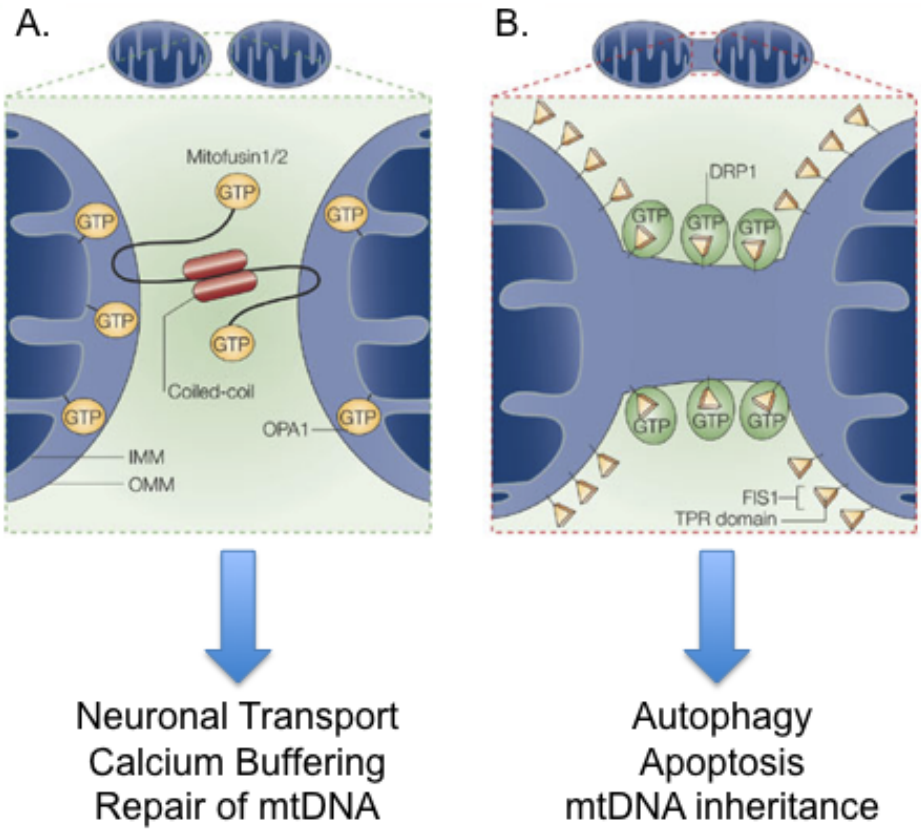

Figure 1.1 Placement of mitochondrial fission and fusion proteins, and their role in mitochondrial function.
A. Mitofusin1/2 are localized to the outer mitochondrial membrane, where they interact with like proteins to promote mitochondrial fusion. Opa1 serves a similar purpose on the inner mitochondrial membrane. Fusion, specifically the function of the Mfns, promotes mitochondrial transport within neurons, and is important for Calcium buffering and repair of mtDNA. ***B.*** Drp1 translocates to the mitochondria, where it interacts with Fis1 constitutively localized to the outer mitochondrial membrane. Once at the mitochondria, Drp1 promotes fission and proper function is required for autophagy and apoptosis. (Figure modified from Youle and Karbowski, 2006).

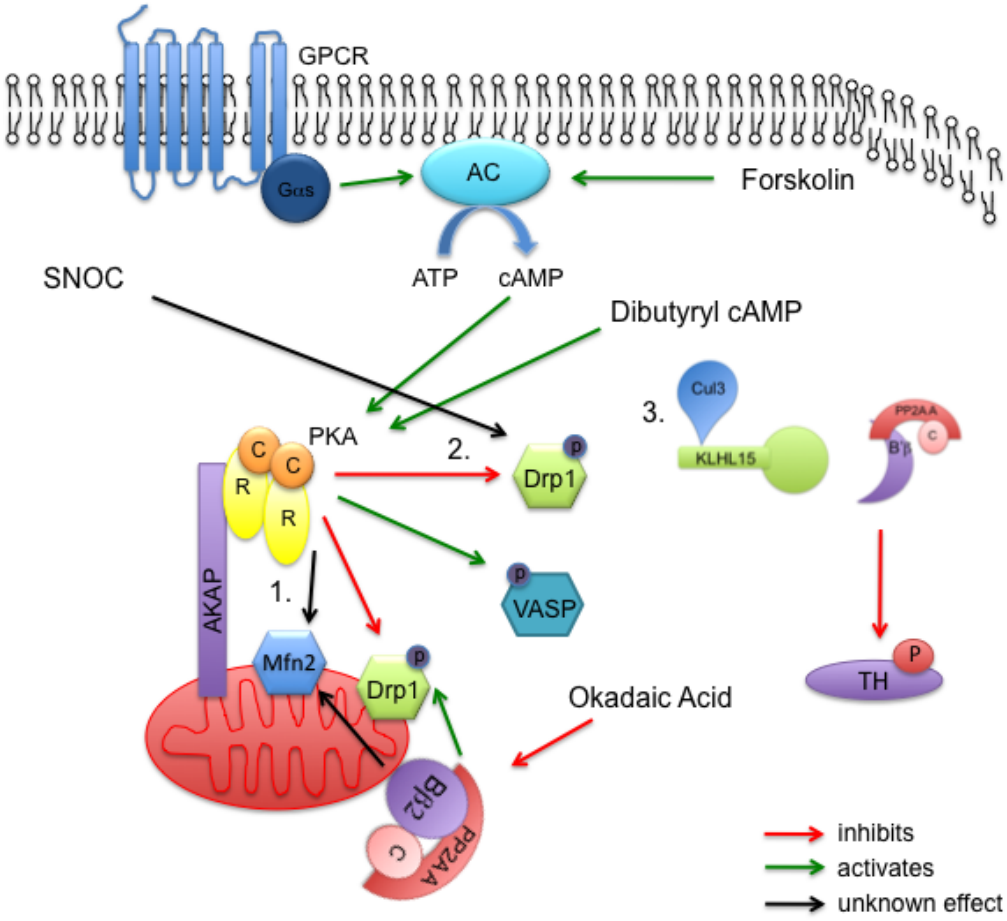

Figure 1.2 Model outlining the questions posed by this thesis.
This thesis is broken down into three distinct areas of research. 1) Determine how phosphorylation of Mfn2 by PKA regulates protein function at the mitochondria; 2) Investigate whether nitrosylation of Drp1 modulates the ability of Ser656 to be phosphorylated, and the role of Ser656 and Cys663 in mediating nitric oxide (NO) induced mitochondrial fragmentation; 3) Characterize a novel E3 ubiquitin ligase complex and its role in regulating PP2A B'β protein stability. Highlighted in the model are the pharmacological treatments utilized in Chapter 2 and 3 to modulated the activities of PKA and PP2A.

CHAPTER II: REGULATION OF MITOFUSIN 2 BY PHOSPHORYLATION

Introduction

Mfn1 and Mfn2 share similar domain structures, a N-terminal GTPase domain, two coiled-coil domains and two C-terminal transmembrane domains (Figure 2.1A,B) though they are functionally distinct and non-redundant (Chen & Chan, 2005, Chen, et al, 2003, Eura, et al, 2003, Ishihara, et al, 2004). Mfn1's primary function is to tether mitochondrial membranes in a GTP dependent manner, and to work in concert with Opa1 to promote mitochondrial fusion (Dimmer & Scorrano, 2006, Ishihara, et al, 2004). In addition to interacting with Mfn1 (Ishihara, et al, 2004, Koshiba, et al, 2004), Mfn2 is thought to function as a signaling GTPase with a role in the assembly of mitochondrial complexes (Benhar, et al, 2009). The focus of this chapter is on Mfn2 and its role in not only promoting mitochondrial fusion, but also in maintaining a diversity of mitochondrial functions.

Mfn2 in development, disease and death

Mfn2 is ubiquitously expressed in most organs (Figure 2.1C), though it has a critical role in the nervous system and in the heart. Initial characterization of the role of Mfn2 in development found that while heterozygous loss of Mfn2 produced viable mice, homozygous deletion resulted in embryonic lethality due to disruption in placental development (Chen, et al, 2003). In the cerebellum, Mfn2 is required not only for dendrite outgrowth, and spine formation in Purkinje cells (Chen, et al, 2007), but also protects granule cells against DNA damage and oxidative stress induced cell death (Jahani-Asl, et al, 2007).

Missense mutations in Mfn2 are the most common cause of the hereditary and sensory motor neuropathy Charcot Marie Tooth Disease type 2A (CMT2A)

(Chung, et al, 2006, Engelfried, et al, 2006, Palau, et al, 2009, Reilly, 2005, Verhoeven, et al, 2006, Zhu, et al, 2005, Zuchner, et al, 2004). It is thought that loss of Mfn2 function disrupts mitochondrial transport down the long neurons resulting in axonal degeneration (Cartoni & Martinou, 2009, Misko, et al, 2010, Palau, et al, 2009).

In the vascular system Mfn2 acts in an anti-proliferative manner by inhibiting the MAPK signaling cascades resulting in subsequent cell cycle arrest at G_0 (Chen, et al, 2004). Further evidence shows that following oxidative stress, PKA activation or serum deprivation, Mfn2 is upregulated triggering vascular smooth muscle cell (VSMC) apoptosis (Guo, et al, 2007). More recently it was found that Mfn2 expression is reduced in the skeletal muscle of patients who are obese or have type 2 diabetes (Zorzano, et al, 2009). This loss of Mfn2 results in decreased respiration exemplified by a decrease in mitochondrial membrane potential and reduced cellular oxygen consumption.

Work by the Youle lab has helped clarify the role of Mfn2 in both apoptosis and autophagy. In healthy cells the Bcl-2 family members Bax and Bak promote mitochondrial fusion by interacting with Mfn2 and promoting the formation of large GTPase complexes (Karbowski, et al, 2006). Following apoptotic induction, however, Bax and Bak form distinct foci on the OMM at fission sites that contain both Mfn2 and Drp1 (Karbowski, et al, 2002). Additional work has shown that following apoptotic stimuli Endophilin B1, a regulator of autophagosome biogenesis (Pierrat, et al, 2001, Takahashi, et al, 2005, Takahashi, et al, 2008), translocates to the OMM where it plays a role in mitochondrial remodeling during cell death (Karbowski, et al, 2004). While it is currently unknown how Endophilin B1 anchors at the mitochondria preliminary evidence shows Endophilin B1 interacts directly with Mfn2 (data not shown), further supporting a role for Mfn2 in OMM complex formation following cell death signaling.

Posttranslational regulation of Mfn2

The regulation of mitochondrial function by the posttranslational modifications of fission and fusion proteins has recently become an important field of study. The function of the fission protein Drp1 is tightly regulated by a variety of modifications including phosphorylation, nitrosylation and SUMOylation (Chang & Blackstone, 2010). However, the regulation of mitochondrial fusion proteins remains largely uncharacterized. Downregulation of the yeast Mfn2 homologue, Fzo1 by ubiquitin dependent proteasomal degradation, is an important step in maintaining mitochondrial homeostasis, as many OMM proteins are susceptible to oxidative damage (Neutzner, et al, 2007). Yet in mammalian cells, while Mfn2 has been shown to interact with the E3 ubiquitin ligase March V (Karbowski, et al, 2007, Nakamura, et al, 2006), and display increased expression following inhibition of proteasomal degradation (Karbowski, et al, 2007), no evidence for direct ubiquitination has not been found. Similarly, while many groups have suggested that Mfn2 is PKA phosphorylated, based on *in silico* consensus sequence analysis, no direct evidence has been shown (Chen, et al, 2004, Dimmer & Scorrano, 2006, Zhou, et al, 2010). These results suggest the possibility that Mfn2 function is posttranslationally regulated, allowing for the identification of targeted residues.

Kinase signaling at the mitochondria

Reversible phosphorylation is one method of communication within the cell. Long thought to be isolated organelles, recent evidence has suggested a startlingly complex signaling network located at the mitochondria. Erk localizes to the mitochondria where it modulates apoptosis by phosphorylating and inactivating Bcl-2 and Bad, as well as promotes mitochondrial turnover through autophagy (Dagda, et al, 2009, Horbinski & Chu, 2005). AKAP1 is constitutively

localized to the OMM where it acts as a scaffold for PKA (Carlucci, et al, 2008, Dagda, et al, 2009, Horbinski & Chu, 2005, Huang, et al, 1999), resulting in increased mitochondrial fusion and neuroprotection mediated by the phosphorylation and inactivation of Drp1, and possibly other resident OMM proteins (Chang & Blackstone, 2007a, Cribbs & Strack, 2007, Merrill, et al, 2010).

PP2A Bβ2 dephosphorylation at the mitochondria

Recent evidence has found that the divergent N-terminal extension of PP2A Bβ2 is both necessary and sufficient for targeting PP2A to the mitochondria (Dagda, et al, 2003). At the mitochondria PP2A Bβ2 enhances serum-starvation induced apoptosis (Dagda, et al, 2003) by promoting mitochondrial fragmentation (Dagda, et al, 2008). Ongoing work in the lab has recently found that PP2A Bβ2 specifically dephosphorylates Drp1, activating protein function and mitochondrial fragmentation (unpublished data).

The role of kinases and phosphatases to modulate mitochondrial morphology through the phospho-regulation of mitochondrial fission/fusion proteins has previously been established by the identification of the PKA mediated Drp1 Ser656 phosphorylation causing protein inactivation and increased mitochondrial fusion (Cribbs & Strack, 2007). These results suggest that in order to maintain the fission/fusion balance, PKA may phosphorylate and activate Mfn2. My original hypothesis predicted phosphorylation of Mnf2 Ser442 mediates the actions of PKA at the mitochondria. Here I provide evidence suggesting that PKA does not phosphorylate Mfn2 on Ser442 in the brain.

Materials and Methods

Cell Culture and Constructs

Cos M6 (Gluzman, 1981), CV1 (Jensen, et al, 1964), N-tera 2 (NT2) (Andrews, 1988) and Long Hela cells (a generous gift from Richard Youle, NIH) (Scherer, et al, 1953) cells were cultured (37^{o}C, 5% CO_2) in RPMI 1640 (Gibco) containing 10% fetal bovine serum (heat inactivated). Dissociated primary hippocampal neurons were prepared fresh as previously described (Lim, et al, 2003) and maintained in serum free Neurobasal media (Invitrogen) containing B27 (Invitrogen) and 0.5 mM glutamine (Chen, et al, 2008).

The cDNA of Mfn2 in the pEGFP N1, pEGFP C1 or pcDNA 3.1 myc vector were generous gifts from Ansgar Santel (Santel & Fuller, 2001, Santel, et al, 2003). Site directed mutagenesis was carried out using the pEGFP N1 Mfn2 cDNA as a template. The mutations were made to either mimic pathogenic Mfn2 mutations (Arg94Gln, Thr206Ile, Arg384Trp or Trp740Ser (Chung, et al, 2006, Verhoeven, et al, 2006, Zhu, et al, 2005, Zuchner, et al, 2004)), disrupt potential phosphorylation sites (Tyr269Phe, ThrSer283AlaAla, Ser431Ala/Asp, Ser442Ala/Asp, Ser511Ala, Thr580Ala, Ser615Ala/Asp), or to disrupt GTPase activity (Lys109Thr (Santel & Fuller, 2001, Santel, et al, 2003)).

Five short hairpin RNAs (Table 2) were designed based on algorithms predicting the 5' end stability, ability to bind target mRNA, and consensus targeting across species (Reynolds, et al, 2004). The p-Super H1 vector (Brummelkamp, et al, 2002) was used as a template to amplify the sequence of interest from oligos containing flanking PciI and BspEI enzyme sites. The PCR product was then placed into the complimentary sites in pCOX8 3HA mCherry vector (Shu, et al, 2006), a vector that will target the hairpins to the mitochondrial matrix, and express red fluorescence to mark transfected cells.

In order to simultaneously knockdown endogenous Mfn2 while over-expressing the mutant Mfn2 construct for analysis in a one-plasmid transfection protocol (Strack, et al, 2004), the sh3 hairpin was subcloned into the vector already containing the Mfn2-GFP construct. Site-directed, PCR-based mutagenesis was then used to render the Mfn2 construct resistant to the hairpin by introducing four silent base changes.

Antibodies

Antibodies commercially available are as follows: GFP (ab290 (Abcam)), EZ view FLAG conjugated beads purchased from Invitrogen, myc (9E10) (Santa Cruz), FLAG (Cell Signaling), Mfn2 and Mfn1 (Sigma). We also received an aliquot of a chicken anti-Mfn2 antibody made by the Youle lab (NIH). The phospho-specific Mfn2 Ser442 antibody was made by injecting rabbits (Hybridoma facility at Iowa State University) with a peptide containing the region of interest (Cys-Ala-Glu-Glu-Ile-Arg-Arg-Leu-Ser (PO_3H_2)-Val-Leu-NH_2) coupled to maleimide activated KLH. Bleeds from two rabbits were tested for protein specificity, and phospho-specificity before the antibody was purified. Secondary antibodies include goat αRabbit IR800, goat αMouse IR800, goat αRabbit IR680, and goat αMouse IR680 (Licor, Lincoln, NE).

Other Reagents

Forskolin was purchased from Fisher and a 50 mM stock solution was prepared and aliquoted and stored at -20^{o} C for dilution in media prior to use. Okadaic Acid was purchased from Alexis (Lausanne, Switzerland) and stored at -80^{o} C. Rolipram (Sigma) was prepared as a 20 mM stock solution and stored at -20^{o} C. A stock solution of 100 mM Glutamate (Sigma) was kept at -20^{o} C prior to dilution in media.

shRNA

Cos M6 cells, plated at a density of 150,000 cells/mL media on a 24 well plate, were transiently transfected with the shRNA constructs targeting Mfn2 or scrambled sequence, and co-expressing pEGFP Mfn2. The cells were allowed to grow for 72 hours post transfection to allow for efficient knockdown of the target sequence, then washed one time with PBS and lysed in 1X sample buffer. Samples were sonicated for 10 seconds each, boiled, and subjected to SDS-PAGE, transferred to nitrocellulose membrane, and western blotted. Images were generated using the Kodak Phospho Imager, and quantification of protein expression was performed using ImageJ analysis.

Once the most efficient hairpins were identified, 30,000 CV-1 cells were plated on collagen coated, glass bottom chamber slides, and transiently transfected with the selected hairpins (sh1, sh2, and sh3). 72 hours post transfection cells were washed one time with PBS, and fixed for 20 minutes in the incubator with 4% paraformaldehyde (PFA). Following fixation, cells were washed two times with PBS, blocked for 30 minutes at room temperature with 4% normal donkey serum (Invitrogen) in Tris buffered saline containing 0.1% Triton X 100 (TTBS). Cells were stained with a 1:500 dilution of mitochondrial cytochrome oxidase in TTBS for 16 hours at 4^{o} C. Following washing 5x for 5 minutes with PBS cells were incubated with Alexa Flour-543 in PBS for 2 hours at room temperature. After secondary incubation cells were washed 5x for 5 minutes in PBS. Cells from each condition were imaged in the green channel (shRNA) and the red channel (all mitochondria) using a Zeiss 200M inverted microscope equipped with a Hamamatsu ER camera.

Generation of GST fragments and protein purification

Glutathione S-transferase (GST) fragments of Mfn2 were generated in order to identify regions of Mfn2 that were targeted for *in vitro* phosphorylation. The pEGFPN1 Mfn2 was used as a template for primers containing flanking BamHI and EcoRI restriction enzyme sites targeting the regions of interest for each of the fragments. The PCR product was then cut with the above enzymes and ligated into the same sites in the previously cut pGEX2T vector. The ligated product was then transformed into BL21* cells and the proteins were purified from E. coli using the following protocol. Starter culture (5 mL of SOB media containing Ampicillin) was grown for 7-8 hours shaking in a 37^{o} C incubator. Then 5 mL was transferred into a fresh 100 mL volume of SOB + Ampicillin so that the OD was 0.2-0.3, and grown for about 5 hours or until it was at an OD reading of 0.6-0.8. After reaching log growth phase, 1 mM IPTG was used to induce protein expression, and the cultures were incubated for 5-6 hours shaking in the 37^{o} C incubator. The next morning cells were pelleted by centrifuging the culture at 1000 x g. Pellets were resuspended in bacterial lysis buffer (154 mM NaCl, 50 mM Tris, pH 7.5, 1% Triton X-100, 1mM EDTA, 2 mM benzamidine with fresh 1 mg/mL lysozyme and 1 mM PMSF) and then rocked for 30 minutes at 4^{o} C. Lysates were then probe-tip sonicated for 5 minutes before pelleting at 40,000 x g for 20 minutes at 4^{o}. The supernatants were collected and incubated with 300 uL of glutathione-agarose beads at room temperature for 2-3 hours. Beads were washed three times in 1 mL bacterial lysis buffer with one tube change. GST-Mfn2 was then run on SDS-PAGE along with Bovine Serum Albumin (BSA) standards followed by coomassie staining and image quantification using ImageJ analysis to determine the protein concentration of the various fragments for standardization for subsequent assays.

In vitro phosphorylation

GST-Mfn2 fragments (0.1-1 μg/ml) were suspended in 1X kinase buffer (0.01% Triton X-100, 50 mM Tris HCl, pH 7.5, 10 mM $MgCl_2$, 2 mM DTT, 1 mM EDTA) and then incubated for 10-30 minutes at 30° C with 0.5 U/μl PKA catalytic subunit or a similar amount of Erk (Upstate Biotech), 200 μM ATP, 0.2 μCi [γ-^{32}P]ATP, and10 mM $MgCl_2$ in the presence of phosphatase and protease inhibitors. To stop the reaction, SDS-sample buffer with 25 mM EDTA was added to each sample, followed by separation on SDS-PAGE. Proteins were analyzed by densitometry from the Coomassie blue-stain, and ^{32}P incorporation via a PhosphoImager.

Metabolic labeling

COS M6 cells were transfected with Lipofectamine 2000 one day after plating 200,000 cells/well on a 6 well plate to express the different Mfn2 constructs. Cells were incubated with phosphate-free media containing 1% dialyzed FBS for 30 minutes in a CO_2 incubator at 37° C and then metabolically labeled with $^{32}PO_4$ (0.5 mCi/ml) in the same media for 4-6 hours in the incubator. Cells were lysed in buffer containing 1% Triton X 100, 0.5% deoxycholate and 0.1% SDS along with protease and phosphatase inhibitors, after which the Mfn2 fusion protein was immunoprecipitated (IP'd) using the polyclonal GFP (ab290) antibody and Protein A/G beads for 4-6 hours to isolate the transfected Mfn2 constructs only. IPs were run along with input samples on a 10% SDS gel, transferred to nitrocellulose and immunoblotted for GFP in order to gage Mfn2 expression before being analyzed for ^{32}P incorporation using a PhosphoImager. NIH ImageJ was used to quantify relative phosphorylation of each band as a ratio of ^{32}P to immunoblot signal.

To identify the kinase and phosphatase involved in Mfn2 phosphorylation, cells were metabolically labeled as above prior to treatment with either 10-50 μM forskolin (an adenlyate cyclase agonist that increases production of cAMP leading to the activation of PKA) for 30 minutes, or 300 nM okadaic acid (a PP2A specific inhibitor at this concentration) for 2 hours.

Use of phospho-specific antibodies

Initial characterization of the phospho-specific antibody involved phosphorylation of over-expressed pEGFP N1 Mfn2. Cos M6 cells were plated at 100,000 cells/mL media and then transiently transfected 18 hours later with wild type, Ser442Ala or Ser442Asp Mfn2 using Lipofectamine 2000 (Invitrogen). 48 hours post transfection cells were treated with 20-25 μM forskolin plus 0.1 μM rolipram for 1 hour. Cells were then washed one time with PBS and then lysed in Radio immunoprecipitation assay (RIPA) buffer (20 mM Tris HCl, pH 7.5, 150 mM NaCl, 1% Triton X-100, 1 mM EDTA, 1 mM EGTA, 2.5 mM $Na_4P_2O_7$, 1 mM Na_3VO_4, 1 mM beta-glycerolphosphate, 1 ug/mL leupeptin 1 mM benzamidine, 0.5% Deoxycholate (DOC), 0.1% sodium dodecyl sulfate (SDS) and fresh 1 mM PMSF and 1mM DTT). Lysates were centrifuged at 13,000 rpm for 10 minutes followed by removal of 30 uL of the supernatant as the input sample. The remaining supernatant was incubated with 10 uL Protein A/G beads and 7 uL GFP or myc (9E10) antibody for 2-3 hours rotating at 4^{o} C. Beads were washed three times with RIPA buffer before resuspension in 1X sample buffer, followed by protein separation by SDS-PAGE and transfer to nitrocellulose membrane for western blotting. Images were generated using the Odyssey Imaging System (Licor, Lincoln, NE).

In some instances following the immunoprecipitation, beads were subjected to an *in vitro* PKA kinase assay to further activate potential Ser442

phosphorylation. Briefly, beads were suspended in 1X kinase buffer and then incubated with 0.5 U/uL PKA catalytic subunit, 200 μM ATP, and 10 mM $MgCl_2$ for 30 minutes at 30°. 1X sample buffer was then added to stop the reaction, and the beads were then run on SDS-PAGE, and transferred to nitrocellulose membrane for western blotting. Images were generated using the Odyssey Imaging System (Licor, Lincoln, NE).

To address the phosphorylation state of endogenous Mfn2 we examined the protein from rested or stressed rats, (10 minute forced swim in room temperature water). Tissues were harvested, weighed, and finely diced with a razor blade before being placed in 1X kinase buffer containing microcystin LR (Alexis, Lausanne, Switzerland) and 1 mM Na_3VO_4 to a volume that was 5x the weight of the brain (mg to μL). The tissues were further homogenized with a plastic pestle in a 1.5 mL eppendorf tube, sonicated for 5 seconds and rotated for 10 minutes at 4° C before centrifugation at 13,000 rpm for 10 minutes. To ensure that the same amount of protein was being compared from each tissue, 2 uL of each supernatant was dotted onto nitrocellulose paper followed by ponceau staining of the membrane. Relative protein concentration was determined by scanning the membrane followed by ImageJ analysis. The collected supernatant, adjusted for protein concentration, was then pre-cleared with Protein A/G beads for 1 hour at 4° C. The beads were pelleted by centrifugation at 3000 rpm for 2 minutes. The supernatant was then incubated for 2 hours at 4° C with the Mfn2 antibody and Protein A/G beads. The beads were washed two times in kinase buffer, followed by resuspension in 1X sample buffer. The beads were then subjected to SDS-PAGE, transferred to nitrocellulose membrane and western blotted. Images were generated using the Odyssey Imaging System (Licor, Lincoln, NE).

Immunofluorescence

N-tera 2 (NT2) cells were plated at 30,000 cells/well on glass bottomed 4 well chamber slides, and were transiently transfected with plasmids that co-express Mfn2-targeted shRNA to knockdown endogenous Mfn2 and RNAi-resistant, phosphorylation site mutant Mfn2 cDNAs, specifically wild type, Ser442Ala, Ser442Asp, and mGFP (GFP targeted to the inner mitochondrial membrane) as a control, using Lipofectamine 2000 (Invitrogen). 48 hours post transfection cells were left untreated, or treated with 25 μM forskolin plus 0.1 μM rolipram for 1 hour. Following treatment cells were washed one time with PBS and fixed with 4% PFA for 20 minutes in the cell culture incubator. Cells were then washed two times with PBS and blocked with 4% normal donkey serum (Invitrogen) in TTBS for 30 minutes rocking at room temperature. Staining was performed using a 1:3000 dilution of GFP and 1:200 mitochondrial cytochrome oxidase in TTBS for 16 hours at 4^{o} C. Following washing 5x for 5 minutes with PBS cells were incubated with Alexa Flour-488 and -543 in PBS for 2 hours at room temperature. After secondary incubation cells were washed 5x for 5 minutes in PBS. To detect the nucleus Hoechst DNA dye was diluted 1:1000 in PBS and incubated on the cells for 5 minutes at room temperature. Cells from each condition were imaged on the green channel (transfected cells) and the red channel (all mitochondria).

Image Analysis

Computational analysis of mitochondrial morphology was performed in Image J using an iterative deconvolution plugin (Dougherty, 2005) and a custom macro (Cribbs & Strack, 2009). The macro performs background subtraction and binary thresholding followed by calculation of several metrics of size including area, perimeter, length of mitochondria, major and minor axis, form factor

($p^2/a \bullet \pi \bullet 4$) (a measure of mitochondrial shape complexity), and aspect ratio (a measure of mitochondrial length versus width), for the mitochondria from each cell.

Fluorescence recovery after photobleaching (FRAP)

Fluorescence recovery after photobleaching (FRAP) of the Mfn2 constructs were performed by Megan Cleland in the Youle lab (NIH) using Long Hela cells. The following protocol is from the Youle lab. Long Hela cells were transfected with mutant Mfn2-YFP constructs using Lipofectamine 2000 and incubated for 24 – 36 hours before the microscopy procedure (Karbowski, et al, 2006, Szabadkai, et al, 2004). The fluorescent photobleaching occurred in a 1 μm^2 randomly selected perinuclear region, and the recovery of fluorescence into that area was measured for up to 1 minute. All values were normalized to the fluorescent intensity both before and after bleaching. Recovery rate constants and mobile fractions were calculated by curve fitting.

Neuronal survival assays

Primary hippocampal neurons (PHN) (Chen, et al, 2008) were transfected at days *in vivo* (DIV) 10-14 (Dagda, et al, 2003) with Lipofectamine 2000 and the shRNA/cDNA plasmids to replace endogenous Mfn2 with Mfn2 phosphorylation site mutants, in the presence or absence of co-expressed AKAP1. 48-72 hours post transfection the cells were treated with ± 40μM glutamate for 10 minutes then washed and kept in neurobasal media for the remaining 48 hours. Prior to fixation, cells were incubated with 5 μg/mL propidium iodide (PI) in neurobasal media for 5 minutes in the 37^o C incubator, washed two times in PBS and then fixed in 4% paraformaldehyde for 15 minutes in the incubator. Neurons were then washed two times with PBS and blocked with 4% normal donkey serum (Invitrogen) in TTBS for 30 minutes rocking at room temperature. Staining was

performed using a 1:500 dilution of GFP in TTBS for 16 hours at 4^{o} C. Following washing 5x for 5 minutes with PBS cells were incubated with Alexa Flour-488 in PBS for 2 hours at room temperature. Neuronal survival was calculated by visualizing the GFP positive neurons (mark of transfected neurons) using the 40X objective on the microscope, and then determining if the nuclei were PI stained on the red channel. A percent survival was then calculated for all constructs.

GTP binding assays

Cos M6 cells were plated at a density of 300,000 cells/mL media and then transiently transfected using plasmids that co-expressed the Mfn2 shRNA/cDNA constructs, wild type, Ser442Ala, Ser442Asp, Thr580Ala, and Lys109Thr using Lipofectamine 2000 (Invitrogen). 72 hours post transfection cells were washed one time, lysed in kinase buffer, then centrifuged at 13,000 rpm for 10 minutes. After input samples were removed, the supernatant was incubated with 10 uL of GTP agarose (Ishihara, et al, 2004) for 2 hours at 4^{o} C. Following incubation, beads were washed two times in kinase buffer, resuspended in 1X sample buffer, run on SDS-PAGE gels, transferred to nitrocellulose membrane and subjected to western blotting. Images were generated using the Odyssey Imaging System (Licor, Lincoln, NE).

Results

Targeted knockdown of Mfn2 produces mitochondrial fragmentation

In order to determine which of the five designed short hairpin RNAs was the most efficient at targeting Mfn2 specifically all five were co-expressed with GFP tagged Mfn2 in Cos M6 cells. Western blot analysis of shRNA mediated knockdown showed three (sh1, sh2, sh3) of the five hairpins produce a greater

than 80% decrease in Mfn2-GFP expression (Figure 2.2A). Of these three shRNAs, sh3 appeared to be the most potent in experiments where a lower ratio of shRNA/target was transfected (data not shown).

It has previously been shown that loss of Mfn2 leads to mitochondrial fragmentation (Eura, et al, 2003, Santel & Fuller, 2001). I next looked at the efficiency of the three most efficacious hairpins to cause mitochondrial fragmentation in CV1 cells. 72 hours after transfection cells were fixed and stained with GFP antibody to mark transfected cells, and mitochondria antibody MTC02 (NeoMarker) to label all mitochondria. Mitochondrial morphology was calculated using ImageJ macro analysis of the images. From the calculations of form factor and aspect ratio it is apparent that hairpin sh3 causes fragmentation (Figure 2.2B,C), while sh1 and sh2 are indistinguishable from control (data not shown).

Analysis of Mfn2 phosphorylation *in vitro*

Mitochondria are highly dynamic organelles whose morphology can be modified by the action of kinases and phosphatases acting on fission and fusion proteins at the outer mitochondrial membrane (Dagda, et al, 2009, Dagda, et al, 2003, Dagda, et al, 2005, Huang, et al, 1999, Merrill, et al, 2010). To begin to address the question of whether Mfn2 is phosphorylated I generated GST Mfn2 fragments encompassing the entirety of the protein and then performed *in vitro* kinase assays using PKA or Erk. *In vitro* PKA phosphorylation assays showed some degree of ^{32}P incorporation on all six fragments, though fragments 3 (261-407), 4 (407-558) and 6 (657-757) showed the highest degree of phosphorylation (Figure 2.3A). In contrast to PKA, only fragments 3 (261-407) and 5 (558-617) showed Erk phosphorylation (Figure 2.6A).

Two web-based phosphorylation site identification algorithms, NetPhos 2.0 (Blom, et al, 1999) and KinasePhos (Huang, et al, 2005) were then used to analyze the Mfn2 sequence and predict which serine, threonine, or tyrosine residues had the highest probability of being phosphorylated. The identified residues were Ser211, Tyr269, Ser431, Ser442, Thr580 and Ser615. Ser442 had also been identified in the literature as a potential phosphorylation site (Chen, et al, 2004, Dimmer & Scorrano, 2006).

To try to identify potential PKA phosphorylation sites, mutations were made to residues highlighted by the *in silico* approach on the various GST fragments shown in Figure 2.3A to be phosphorylated (summarized in Table 1). Of the mutants evaluated, only Ser442Ala showed complete ablation of ^{32}P incorporation following *in vitro* PKA phosphorylation (Figure 2.3B).

Evaluation of the Erk phosphorylation site was much easier, as one fragment showed the predominant Erk phosphorylation, and within that fragment only one residue was highlighted *in silico* as having a high probability of MAPK phosphorylation. Mutation of Thr580Ala resulted in the complete ablation of ^{32}P incorporation following Erk phosphorylation (Figure 2.6B).

Determination of Mfn2 phosphorylation state in whole cells

Once I had the *in vitro* data demonstrating that Ser442 was PKA phosphorylated, it was important to follow up on those results *in vivo* using wild type Mfn2-GFP or a Ser442Ala mutation that blocks phosphorylation. To overcome the issue of low basal PKA phosphorylation (Cribbs & Strack, 2007), cells expressing wild type Mfn2 were left untreated, or treated with 25μM forskolin plus 0.1μM rolipram (F/R) or 100nM okadaic acid (OA). Analysis of the ^{32}P incorporation showed no significant change in total phosphorylation of

Ser442Ala compared to wild type, with only a 15% decrease overall when multiple experiments were pooled (Figure 2.3C,D). These results indicate that either a) Ser442 is not phosphorylated, b) Ser442 is one of many phosphorylation sites, or c) loss of Ser442 phosphorylation promotes phosphorylation at a different site. Additionally, there was no significant change in wild type Mfn2 phosphorylation levels following treatment with either F/R or OA. Taken together, the metabolic data is inconclusive as to whether Mfn2 is PKA phosphorylated.

Phosphorylation state of endogenous Mfn2

To verify PKA phosphorylates Mfn2 Ser442 *in vivo* a phospho-specific antibody was generated. The serum from two rabbits injected with the maleimide activated KLH peptide was evaluated using GST Mfn2 fusion proteins phosphorylated *in vitro*. Data from these tests showed that antibody 4046 was the stronger of the two and showed the greater specificity towards the phosphorylated wild type fragment over the Ser442Ala fragment (data not shown and Figure 2.3F).

Based on these results I started to characterize the PKA phosphorylation of Mfn2 in whole cells. Initially, Cos M6 cells expressing GFP Mfn2, wild type or Ser442Ala/Asp, were treated +/- 25 μM forskolin plus 0.1 μM rolipram for 1 hour. Whole lysates probed with both Mfn2 and Mfn2 phospho-Ser442 generated no detectable phospho signal (data not shown). Next, Mfn2 was immunoprecipitated out of the lysates using either the Mfn2 or the GFP antibody with Protein A/G beads, followed by immunoblotting with the phospho-Ser442 antibody. These experiments generated similar results where there was no detection of phosphorylated Mfn2 (data not shown). In order to detect a specific band with the phospho Ser442 antibody, Cos M6 cells expressing myc Mfn2 were treated +/-

25 μM forskolin plus 0.1 μM rolipram for 1 hour, subjected to IP using the myc antibody and Protein A/G beads, and finally *in vitro* phosphorylated with PKA. Wild type Mfn2 is specifically phosphorylated by PKA *in vitro* following IP, independent of prior F/R treatment as neither the lane containing Mfn2 Ser442Ala, nor the empty vector lane show any phospho Ser442 band (Figure 2.3E). Unfortunately these results could not be duplicated.

It is possible to imagine that Mfn2 is only PKA phosphorylated under very specific circumstances, and the methods I was using to detect the potential phosphorylation were not physiologically relevant. Previous work in the lab has demonstrated that mice subjected to a stress and exercise regiment of a 15 minute forced swim produced a detectable increase in PKA mediated Drp1 phosphorylation in the heart (Cribbs & Strack, 2007). I therefore subjected an adult male rat to a 10 minute forced swim in room temperature water. The forebrain, cerebellum, midbrain and heart were all evaluated for Ser442 phosphorylation following Mfn2 IP, and in all cases there was no detectable phospho-specific band in either the stressed or unstressed tissues (data not shown). Finally, I tried *in vitro* PKA phosphorylating Mfn2 IP'd from midbrain homogenates, using the 407-558 fusion proteins as a positive control. Results from this experiment showed that the PKA was able to efficiently phosphorylate the GST Mfn2 fusion protein in a specific manner, as the Ser442Ala fragment was undetected by the phospho Ser442 antibody (lanes 5 & 6), but there was no detectable phosphorylation of the brain IP'd Mfn2 (lanes 1 & 2) under these conditions (Figure2.3F).

One possible explanation for the above results is that the Mfn2 phospho-Ser442 antibody is not very strong, and is therefore unable to detect any small amount of Ser442 phosphorylation that might be occurring. To test this possibility, I performed an Elisa assay using the original Mfn2 Ser 442 or Drp1

Ser656 peptides to test the strength and specificity of the two phospho-specific antibodies generated by the lab. Later experiments utilized whole cell lysates expressing Mfn2 GFP to compare the Mfn2 phospho-Ser442 to the commercially available Mfn2 and GFP antibodies. In each case, the lowest concentration of Mfn2 phospho Ser442 antibody was able to detect its peptide in a more sensitive and specific manner than the other antibodies tested (data not shown). These results suggest that the inability of the phospho Ser442 antibody to detect Mfn2 phosphorylation is not due to the weakness of the antibody, but rather the lack of phosphorylation of full length Mfn2 under the conditions tested.

Modulation of mitochondrial morphology by Mfn2 phospho-site mutations

The dynamic balance between mitochondrial fission and fusion occurs through tight regulation of the actions of fission proteins Drp1 and Fis1 and the fusion proteins Mfns1/2 and Opa1 (Chen & Chan, 2009, Herzig & Martinou, 2008, Youle & Karbowski, 2005). Numerous groups have shown that the regulation of Drp1 activity by phosphorylation can either activate, in the case of CaMKIα and Cdk1 (Han, et al, 2008, Taguchi, et al, 2007), or inactivate, following PKA phosphorylation (Chang & Blackstone, 2007a, Cribbs & Strack, 2007) protein function. I therefore wanted to determine whether PKA phosphorylation of Mfn2 regulated protein function by analyzing whether phospho-site mutations modulated mitochondrial morphology.

Initial characterization of phospho-site mutants in NT2 cells showed that the Ser442Ala mutant caused significant fragmentation, and the Ser442Asp trended towards elongation, though was not significantly different from wild type expressing cells (Figure 2.4A,B). While these results were encouraging, evidence from FRAP assays (discussed later) suggested that the phospho-ablating

Ser442Ala mutant resulted in no functional change in mitochondrial motility. These results were puzzling based on the morphology in NT2 cells. I sought to determine whether the lack of functional consequence of the Ser442Ala from the FRAP assay was due to a difference in the cell type used, Long Hela versus NT2, or due to an inherent problem with the immunofluorescence assay. I therefore performed similar immunofluorescence experiments in Long Hela cells, while the FRAP assay was conducted in CV1 cells. Long Hela cells were transfected with the GFP Mfn2 constructs as was done previously in the NT2 cells. Unlike previous results, there was no significant difference between the Mfn2 wild type and either phospho-site mutant following three independent studies (data not shown). Further characterization of the fragmentation caused by the Ser442Ala mutant in NT2 cells showed the initial results to be non-reproducible in their significance (Figure 2A,B).

Next it was important to determine if the Mfn2 phospho-site mutants could block the elongation caused by pharmacological activation of PKA. Treatment of the NT2 cells with 50 μM forskolin plus 0.1 μM rolipram (F/R) caused significant and reproducible elongation of the wild type Mfn2 compared to untreated cells (Figure 2.4B and data not shown). When cells expressing the phospho-site mutants were treated with F/R both the Ser442Ala and the Ser442Asp mutant blocked the F/R induced mitochondrial elongation seen in wild type cells (Figure 2.4B). However, the absolute value of the form factor score in cells expressing Ser442Asp and treated with F/R was identical to WT treated cells. While the requirement of Ser442 in mediating mitochondrial elongation following F/R treatment was only performed one time in Hela cells, the results show a similar trend as that from similar experiments performed in NT2 cells. In NT2 cells Ser442Ala mutants clearly and significantly block F/R induced mitochondrial elongation, while the Ser442Asp mutants trend towards elongation, but are not

significantly different from wild type expressing cells (data not shown). These data suggest that the Ser442Ala mutant might be causing a disruption in Mfn2 function, as it blocks the actions of F/R, but this disruption does not seem to be related to PKA phosphorylation, as the two phospho-site mutants do not display opposing effects.

Mobility of Mfn2 in the outer mitochondrial membrane

Mfn2 is tethered to the outer mitochondrial membrane through two transmembrane domains in the C-terminal portion of the protein (Figure 2.1A). The majority of the protein is exposed to the cytosol, where it can interact with cytosolic proteins such as Bax (Karbowski, et al, 2002) or Endophilin B1 (data not shown) and more importantly, form hetero- and homodimeric complexes with Mfn1/2 on opposing mitochondria (Koshiba, et al, 2004). Fluorescence recovery after photobleaching (FRAP) quantifies network complexity by measuring the rate at which mitochondria matrix localized YFP migrates to a region irreversibly photobleached (Karbowski, et al, 2006, Szabadkai, et al, 2004). Previous work by Megan Cleland in the Youle lab (NIH) has demonstrated that a hyperactive Mfn2 containing the Ras_{G12V} mutation shows increased protein function (Jahani-Asl, et al, 2007) and increased mobility within the OMM (Figure 2.4C). Conversely the Lys109Thr mutation that disrupts Mfn2 GTPase activity (Santel & Fuller, 2001, Santel, et al, 2003), shows slower mobility within the OMM (Figure 2.4C). Therefore, Megan performed FRAP analysis to determine if the phospho-site mutants displayed a change in mobility, pointing to a disruption in protein function. Long Hela cells were analyzed after transfection with GFP Mfn2 wild type, Ser442Ala or Ser442Asp. The Ser442Asp mutants showed a significant increase in protein mobility compared to wild type Mfn2, while the Ser442Ala mutant showed no change (Figure 2.4D,E). The increase in mobility seen with

the Ser442Asp mutant, while significant when compared to wild type Mfn2, was not as dramatic as the increase seen with the Mfn2 Ras_{G12V} mutation, suggesting that the difference in mobility does not represent hyperactivity.

Mfn2 protects against glutamate induced neurotoxicity

Maintaining the balance between mitochondrial fission and fusion is important for cell function. While complete loss of Mfn2, or even point mutations can result in severely disturbed embryos (Chen, et al, 2003) and neuronal pathology (Chung, et al, 2006, Chung, et al, 2008, Engelfried, et al, 2006, Verhoeven, et al, 2006, Zuchner, et al, 2004) expression of the constitutively active Mfn2 Ras_{G12V} mutant is neuroprotective (Jahani-Asl, et al, 2007). Previous work in the lab has demonstrated the importance of phosphorylation in neuronal protection where overexpression of AKAP1 (Merrill, et al, 2010), or downregulation of PP2A Bβ2 promotes neuronal survival (Dagda, et al, 2003, Dagda, et al, 2005, Dagda, et al, 2008). In order to address the possibility that Mfn2 is able to protect hippocampal neurons, important for learning and memory, against insult, I used glutamate to induce neuronal death. Glutamate is an excitatory neurotransmitter that activates receptors important for learning, memory and synaptic plasticity (Matsuzaki, et al, 2001). However, excessive glutamate stimulation has been implicated in a number of neuropathies, including stroke, seizures and brain trauma (Matsuzaki, et al, 2001). If phospho-regulation modulates Mfn2 function, then the phospho-site mutants should either block (Ser442Ala) or enhance (Ser442Asp) the neuroprotective activity of Mfn2 against excitotoxic insult.

Primary hippocampal neurons (PHN) were transfected at DIV 10-14 with Mfn2 GFP wild type, Mfn2 Ser442Ala, Mfn2 Ser442Asp, or mGFP as a control and then treated with 40 μM glutamate to induce excitotoxic neuronal death. In

three independent experiments, overexpression of wild type Mfn2 was able to protect the neurons from glutamate-induced neurotoxicity compared to mGFP neurons. However, neither phospho site mutant showed any neuroprotection, but rather they both behaved similar to control neurons (Figure 2.5A). These results confirmed the findings of other groups, demonstrating the importance of Mfn2 in neuronal protection, and showed the requirement of Ser442 for this function.

Next I wanted to determine if the actions of AKAP1 to promote neuronal survival (Merrill, et al, 2010) required Mfn2 Ser442 phosphorylation. PHNs were co-transfected as described above +/- AKAP1. Neurons were treated with 50 μM glutamate, followed two days later by PI staining and fixation. In the absence of AKAP1, the Mfn2 provided neuronal protection against glutamate-induced death as seen previously (Figure 2.5A). When co-expressed with AKAP1 the mGFP and Mfn2 showed increased neuroprotection compared to when expressed alone while the Ser442Ala showed no change in percent survival independent of the presence of AKAP1 (Figure 2.5B). Taken together these results suggest that the neuroprotective effect of AKAP1 is dependent on the presence of Mfn2 Ser442.

Disruption of Mfn2 GTP binding by phospho-site mutants

Mfn2 is a large GTPase whose binding and hydrolysis of GTP are required for fusion activity (Ishihara, et al, 2004). In order to determine if any of the phospho-site mutants, Ser442Ala, Ser442Asp or Thr580Ala, disrupted the ability of Mfn2 to bind GTP, I performed a binding assay using GTP agarose beads. Cos M6 cells expressing either wild type, phospho mutants Ser442Ala, Ser442Asp, Thr580Ala or the GTPase defective mutant, Lys109Thr, Mfn2 were lysed in kinase buffer and precipitated with the GTP agarose. When normalized to input amount, there is a 25-30% increase in GTP binding with the Ser442Asp,

Thr580Ala and Lys109Thr mutants compared to wild type, which shows similar binding as the Ser442Ala (Figure 2.6C,D). It is interesting to note that while the Lys109Thr mutation disrupts GTPase activity (Santel & Fuller, 2001, Santel, et al, 2003), it does not seem to disrupt binding to GTP. These results are similar to how wild type Mfn2 has increased GTP binding but decreased GTP hydrolysis when compared to Mfn1 (Ishihara, et al, 2004). Results from these preliminary pull down experiments suggest that mutations in possible phosphorylation sites modulate the ability of Mfn2 to bind GTP.

Discussion

It has recently been reported in the literature that the Ser442Ala mutation in Mfn2 exerts anti-proliferative effects on VSMC due to a G1 cell cycle arrest (Zhou, et al, 2010). While Zhou and colleagues are able to demonstrate the opposing functions of the Ser442Ala and the Ser442Asp mutations in their mouse model of VSMC proliferation, they fail to directly demonstrate the phosphorylation of Mfn2 by PKA. The conclusions drawn from this paper bring in to question my own results, which suggest that Mfn2 may not be PKA phosphorylated on Ser442.

PKA phosphorylation of Mfn2 fragments *in vitro*

Perhaps the data that best supports the possibility of Mfn2 phosphorylation are the initial *in vitro* kinase assays that were performed shortly after this project began. In the case of both the PKA and Erk assays, multiple fragments showed strong ^{32}P incorporation (Figures 2.2A and 2.6A respectively). Following up on these findings I began to make and analyze a series of potential phospho-site mutants trying to identify the residue responsible for the of ^{32}P incorporation on each fragment (Table 1). The Mfn2 mutants of the two sites that showed complete loss of ^{32}P incorporation, Ser442 (Figure 2.2B) and Thr580

(Figure 2.6B), were then analyzed for GTP binding and changes in mitochondrial morphology. Based on extensive analysis of the Ser442 site, it was determined that under the conditions studied, Ser442 is not PKA phosphorylated. However, the initial examination of Thr580 suggests that Erk phosphorylation of this site may modulate Mfn2 function as the Thr580Ala mutant caused mitochondrial fragmentation (Table 1) and showed increased GTP binding (Figure 2.6C,D).

Characterization of the phospho-specific antibody

The data that initially suggested that Mfn2 might not be phosphorylated on Ser442 were the experiments characterizing the Ser442 phospho-specific antibody. After repeated attempts, using both the Cos M6 over-expressed GFP Mfn2 and brain precipitated Mfn2 as substrates, I could not detect any Ser442 phosphorylation (Figure 2.3F). I originally thought that the problem might be low basal levels of phosphorylated protein, yet neither stress induced phosphorylation (Cribbs & Strack, 2007), nor F/R treatment alone could produce a phospho-signal (Figure 2.3E and data not shown). In fact the only time I could detect full length Mfn2 phospho Ser442 was when the protein was phosphorylated *in vitro* following IP (Figure 2.3E). However, I know that the antibody is able to specifically detect the 407-558 fragment of Mfn2 following PKA phosphorylation, as it doesn't recognize the same fragment containing the Ser442Ala mutation (Figure 2.3F). It also appears that the antibody is very strong, as Elisa assays show recognition of its specific peptide at concentrations far lower than other antibodies currently used in the lab (data not shown). Taken together, these results suggest a couple of conclusions. First, that while the antibody is able to detect short fragments of Mfn2, and its peptide, the binding site for the antibody might be hidden by protein folding, and is therefore unable to recognize the phosphorylated substrate. This possibility seems unlikely, as

subjecting the protein to SDS PAGE should result in protein unfolding, allowing for the antibody to bind. Additionally, if the binding site was buried within protein secondary structure it's hard to believe that PKA would have access to the protein to phosphorylate Ser442. In fact, based on protein threading predictions it appears that Ser442 lies on the inside face of an alpha-helix (data not shown). If this structural prediction of Mfn2 is correct, it is hard to imaging how this site could be phosphorylated. The second, and seemingly more probable conclusion to be drawn is that Ser442 is not phosphorylated in the brain, under conditions similar to those tested here. I fully acknowledge that I did not examine the phosphorylation state following an exhaustive array of conditions, nor did I really focus on the heart, other than some initial studies. It is possible to imagine that Mfn2 is highly phosphorylated in the heart, as recent studies suggest (Zhou, et al, 2010), but is not phosphorylated in the brain.

Is Mfn2 phosphorylated?

While the initial *in vitro* data was exciting, I could not reproduce the Mfn2 Ser442 phosphorylation in whole cells. Previous work done in the lab has used similar *in vitro* phosphorylation assays as a starting point to identify phosphorylated residues that were then verified *in vivo* (Cribbs & Strack, 2007). In the case of Mfn2 I believe that PKA is a promiscuous kinase that interacts with many regions of the protein that contain some similarity to the consensus sequence, leading to false positive results. Based on the metabolic labeling experiments, it appears that Mfn2 is phosphorylated, though Ser442 does not appear to be the dominant site of phosphorylation (Figure 2.3C). I also believe that the interaction between Mfn2 and the MAPK pathway (Chen, et al, 2004, Zhou, et al, 2010) suggests that the Erk phosphorylation of Thr580 may prove to be important for Mfn2 function. Overall, there is clearly more work that needs to

be done in order to characterize the role of phosphorylation in regulating Mfn2 function, and to determine if the phosphorylation state of Mfn2 varies in different tissue types; ie whether Mfn2 Ser442 is phosphorylated in the heart (Zhou, et al, 2010) but not in the brain.

Modulation of mitochondrial morphology by phospho-site mutants

Mitofusin proteins are indispensable in the maintenance of mitochondrial morphology (Eura, et al, 2003, Hales & Fuller, 1997, Legros, et al, 2002, Santel & Fuller, 2001), where loss of either Mfn1 or Mfn2 results in mitochondrial fragmentation (Figure 2.2B,C) (Wang, et al, 2009). I therefore wanted to determine whether disruption in Mfn2 function through loss of the PKA phosphorylation site altered mitochondrial morphology.

Initial experiments conducted in NT2 cells showed that the Ser442Ala and Ser442Asp mutants altered mitochondrial morphology compared to wild type Mfn2. However, over a series of many independent experiments, the initial results showing opposite effects on mitochondrial morphology with the phospho-site mutants were not reproducible (Figure 2.4A,B). In preliminary experiments, the F/R induced mitochondrial elongation of wild type Mfn2 was blocked by either phospho-site mutation (Figure 2.4B). These results imply the PKA induced mitochondrial elongation is not mediated by Mfn2 Ser442.

Neuroprotective effects of AKAP1 require Mfn2 Ser442

We know that Mfn2 plays a critical role in the central nervous system based on its importance in neuronal development of the cerebellum (Chen, et al, 2007), its ability to protect neurons against insult (Jahani-Asl, et al, 2007) as well as its role in neuropathy (Chung, et al, 2006, Chung, et al, 2008, Engelfried, et al,

2006, Verhoeven, et al, 2006, Zuchner, et al, 2004). Here I demonstrate, for the first time, the role of Mfn2 in protecting hippocampal neurons against glutamate induced excitotoxicity.

Similar to its role in the cerebellum, (Jahani-Asl, et al, 2007), Mfn2 protects hippocampal neurons against glutamate-induced neurotoxicity (Figure 2.5A,B). Interestingly, mutation of Ser442 resulted in a complete loss of Mfn2 dependent neuroprotection (Figure 2.5A,B). If the neuroprotection caused by Mfn2 was dependent on PKA phosphorylation of Ser442, then it would be expected that the Ser442Ala mutation would result in neuronal death similar to control levels, while the Ser442Asp should behave similar to wild type, or show even greater neuroprotection. Since the results of the phospho-site mutants were identical, rather than opposite, this suggests that the Ser442 site is important for Mfn2 function, independent of PKA phosphorylation.

While previous work has shown that AKAP1 protects hippocampal neurons against glutamate induced death (Merrill, et al, 2010, Tanaka, 2001), I sought to take these findings a step further and determine whether the effects of AKAP1 on neuroprotection required the presence of Mfn2 Ser442. Hippocampal neurons co-expressing AKAP1 and mGFP showed a significant increase in neuronal survival compared to mGFP alone. There was a similar increase in neuronal survival in hippocampal neurons expressing both AKAP1 and Mfn2 compared to neurons expressing Mfn2 alone (Figure 2.5B). While these results are not significant, it is possible that the neuroprotective effects of Mfn2 under basal conditions are already at a maximum, and co-expression of AKAP1 does little to enhance the effects of Mfn2 alone. Interestingly, AKAP1 fails to protect neurons expressing Mfn2 Ser442Ala. These results suggest the ability of AKAP1 to exert neuroprotective effects requires the presence of Mfn2 Ser442.

In conclusion, the data provided herein demonstrate that Mfn2 is not PKA phosphorylated in the brain. However, evidence provided by the neuronal survival assay suggests that Ser442 is important for the fusion independent functions of Mfn2.

Table 1 Summary of analysis of Mfn2 CMT2A causing mutations or potential phosphorylation site mutants.

Mutation	Purpose	*In vitro* Phosphorylation	GTP Binding (compared to WT)	Mitochondrial Morphology
Lys109Thr	Disrupts GTPase activity	ND	increased	Fragmented
Arg94Glu	CMT2A	ND	increased	Aggregated
Thr206Ile	CMT2A	ND	completely ablated	Aggregated
Arg384Trp	CMT2A	ND	ND	Aggregated
Trp740Ser	CMT2A	ND	ND	Aggregated
Tyr269Phe	Src phosphorylation	unable to test	ND	inconclusive
ThrSer283AlaAla	PKA phosphorylation	no change	ND	ND
Ser431Ala/Asp	PKA phosphorylation	no change	ND	ND
Ser442Ala	PKA phosphorylation	ablates 32P incorporation	no change	inconclusive
Ser442Asp	PKA phosphorylation	ND	increased	inconclusive
Ser511Ala	PKA phosphorylation	no change	ND	Elongated
Thr580Ala	Erk phosphorylation	ablates 32P incorporation	increased	Fragmented
Ser615Ala/Asp	PKA phosphorylation	no change	ND	ND

Table 2 Summary of Mfn2 targeted shRNA sequence and analysis of function.

Name	Sequence	Species Targeted	Knockdown of Mfn2 Protein	Mitochondrial Fragmentation
5'	CGC ACA TGT CCG GAT TCC AAA AA	N/A	N/A	N/A
Loop	TCT CTT GAA	N/A	N/A	N/A
3'	GGG GAT CTG TGG TCT CAT ACA GAA	N/A	N/A	N/A
#1	ACA CAT GGC TGA GGT GAA T	human, rat, dog, bull	YES	NO
#2	GCA CTT TGT CAC TGC CAA G	human, rat, mouse	YES	NO
#3	TGA GGA TGT TTG AGT TTC A	human, rat, mouse, dog, bu	YES	YES
#4	TCC TCA AGG TTT ATA AGA A	human, rat, mouse	NO	ND
#5	AGA GGG CCT TCA AGC GCC A	human, rat, mouse, dog, bu	NO	ND

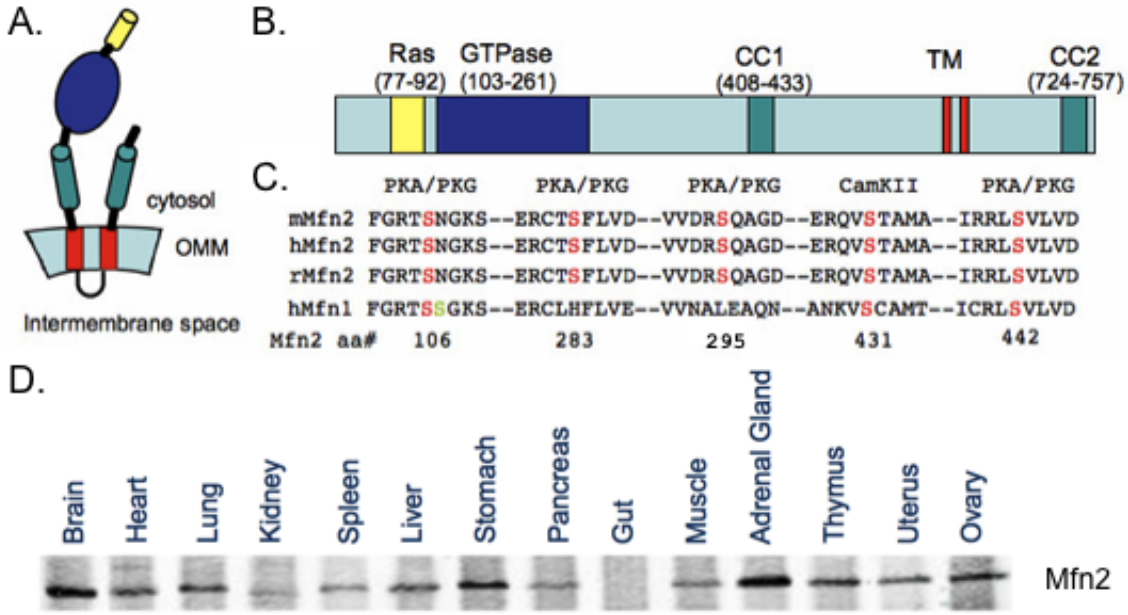

Figure 2.1 The cytosolic portions of Mitofusin 2 contain a GTPase domain, as well as multiple consensus phosphorylation sites.
A, B. Structural domains of Mfn2, and predicted topology of the protein. ***C.*** Consensus sequence of potential phosphorylation sites in human (h), mouse (m), and rat (r) Mfn2 and human Mfn1. ***D.*** Tissue distribution of Mfn2 in adult female rat.

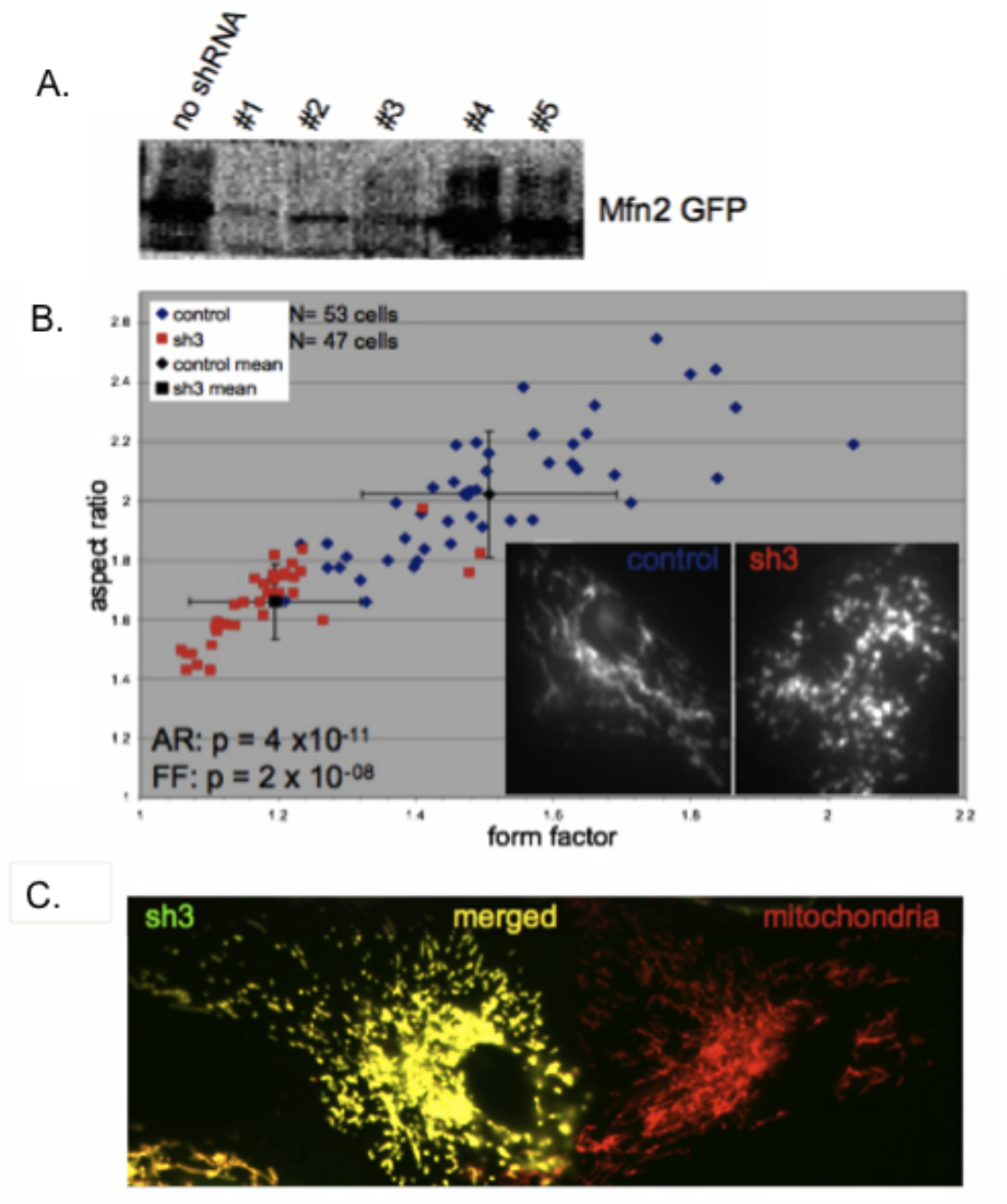

Figure 2.2 Knockdown of Mfn2 causes mitochondrial fragmentation. ***A.*** Testing of five Mfn2-directed shRNAs for knockdown of transiently expressed protein. Immunoblot analysis reveals shRNA #3 to be the most potent ***B.*** Analysis of sh3-mediated knockdown of Mfn2 revealed increased fragmentation that was significantly different from control. ***C.*** Cells transfected with sh3 (green) show mitochondrial fragmentation compared to untransfected cells (red).

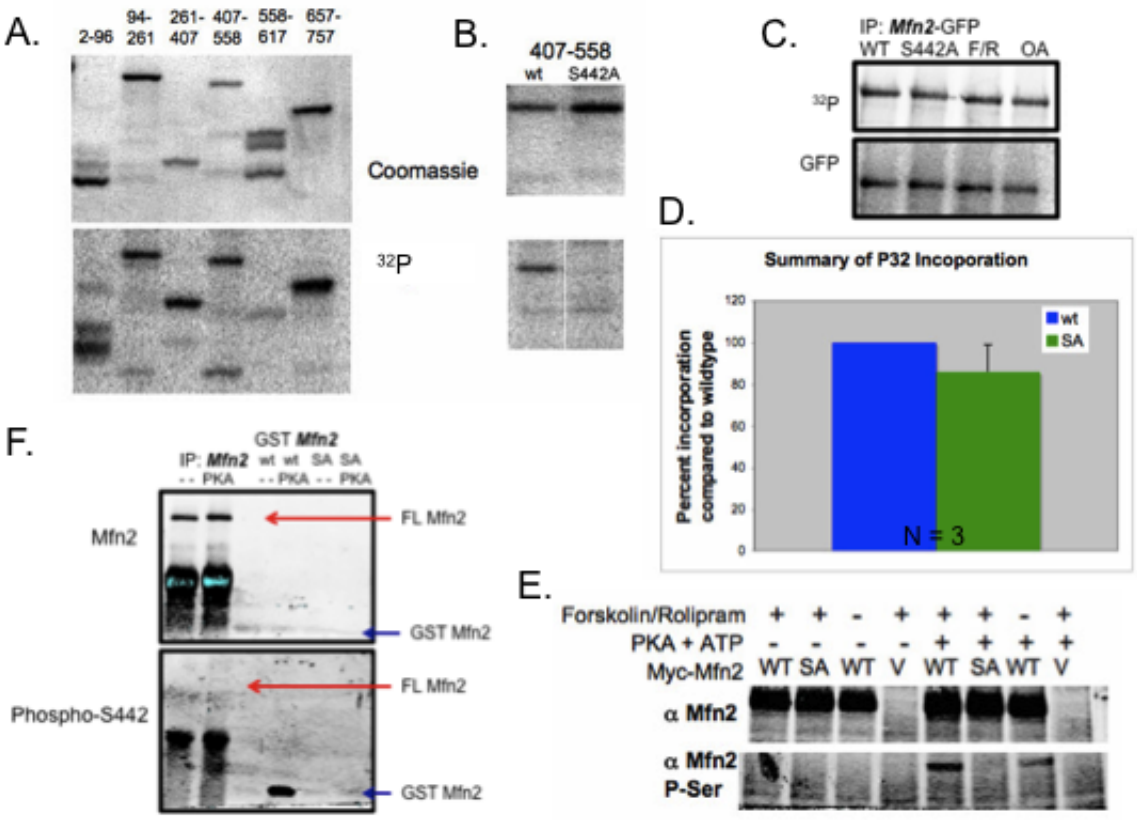

Figure 2.3 PKA induced phosphorylation of Mfn2 on Ser442.
A. GST fragments encompassing the entire Mfn2 protein, except the transmembrane domains were used for in vitro kinase assays. A PKA assay was performed, with each fragment containing some ^{32}P incorporation, signifying PKA phosphorylation. ***B.*** A mutation was made in the 407-558 fragment converting a potential PKA phosphorylated serine 442 to an alanine. This mutation completely ablates any ^{32}P incorporation. ***C.*** ^{32}P incorporation of wild type Mfn2 as well as Ser442Ala, a mutation meant to abrogate potential phosphorylation at this site, and wild type treated with 25 μM Forskolin plus 0.1 μM rolipram (F/R) or 100 nM Okadaic Acid (OA). From this experiment it appears that the Ser442Ala confers a slight loss of total Mfn2 phosphorylation, while F/R and OA have no effect. ***D.*** Quantification of ^{32}P incorporation in wild type or Ser442Ala Mfn2 GFP from three independent metabolic labeling experiments. ***E.*** Initial testing of Mfn2 P-Serine antibody shows the presence of a phospho-specific band in the lanes containing cells expressing wild type Mfn2, but not the SA mutation, or lanes containing cells expressing the empty vector alone (V). The appearance of the band is dependent on the presence of PKA and ATP in the IP conditions, and further enhanced by a 1 hour treatment with 25 μM Forskolin plus 0.1 μM rolipram prior to lysing. ***F.*** Rat forebrain homogenates and GST Mfn2 wild type or S442A were treated with PKA +/- ATP. The brain extracts were then subjected to Mfn2 IP. The blots were probed for both total Mfn2 and phospho-S442. Only the wild type GST fragment phosphorylated by PKA was detected by the phospho-specific antibody.

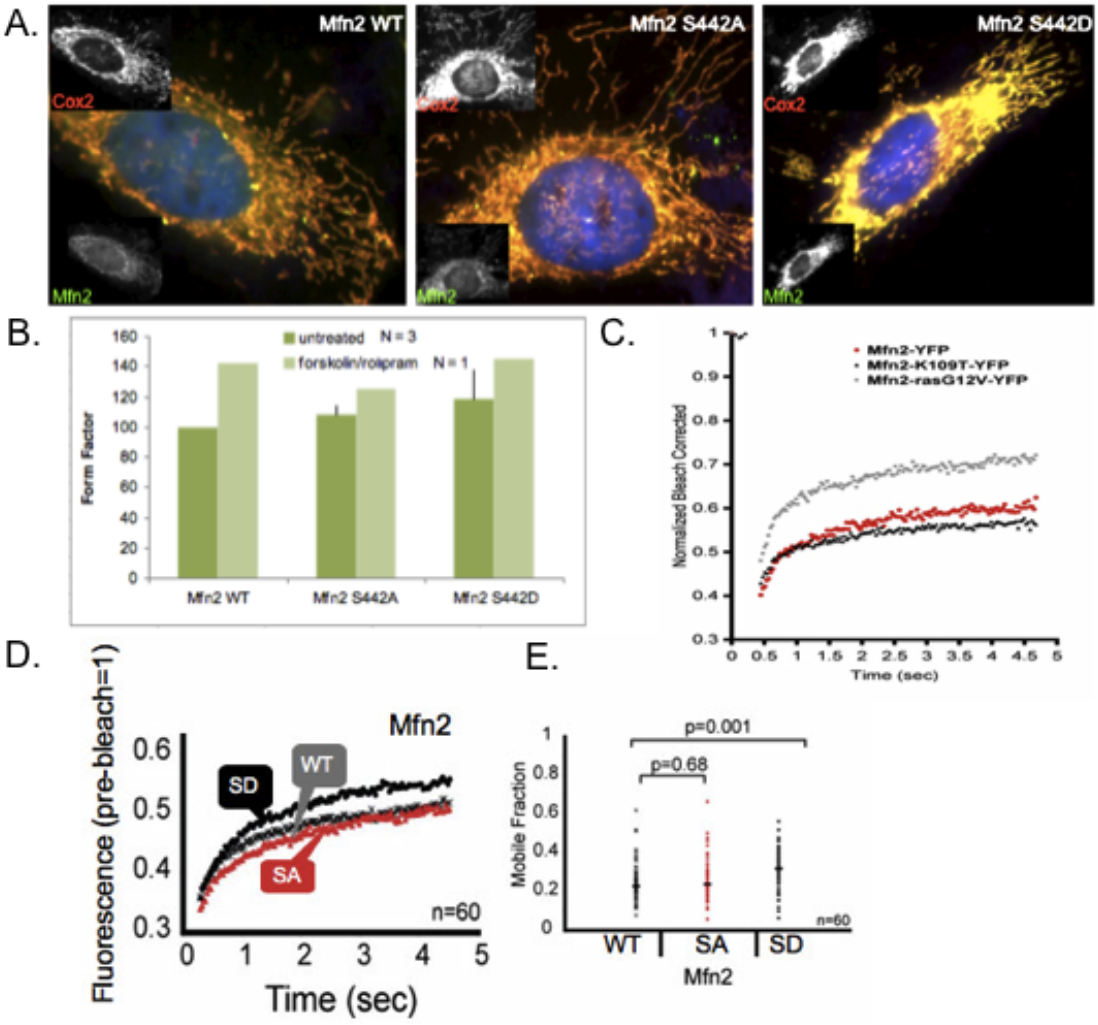

Figure 2.4 Modulation of mitochondrial morphology and Mfn2 mobility within the outer mitochondrial membrane by phospho-site mutants.
A. Immunofluorescence of N-tera 2 cells transfected with either wild type Mfn2 or the phospho-ablating Ser442Ala mutation or the phospho-mimicking Ser442Asp mutation. These cells were then left untreated, or treated for 1.5 hours with 25μM forskolin and 0.1μM rolipram. ***B.*** Mitochondrial morphometric analysis of untreated cells (left) shows the Ser442Ala and Ser442Asp mutations causes no significant change compared to WT. While cells treated with forskolin/rolipram (right) show significant elongation of WT cells compared to untreated WT, though the Ser442Ala and Ser442Asp mutations show similar behavior to untreated. ***C.D.E.*** FRAP analysis performed by Megan Cleland in the Youle lab (NIH). ***C.*** Analysis of the mobility of GTPase active (rasG12V) or GTPase inactive (Lys109Thr) Mfn2 by fluorescence-recovery after photobleaching (FRAP). Results show the rasG12V mutant enhances mobility while the Lys109Thr mutant is similar to WT. ***D.*** FRAP analysis of the mobility of the phosphorylation site mutants shows the pseudo-phosphorylated Ser442Asp mutant shows increased mobility, suggesting enhanced function. ***E.*** The quantification of the results in part D.

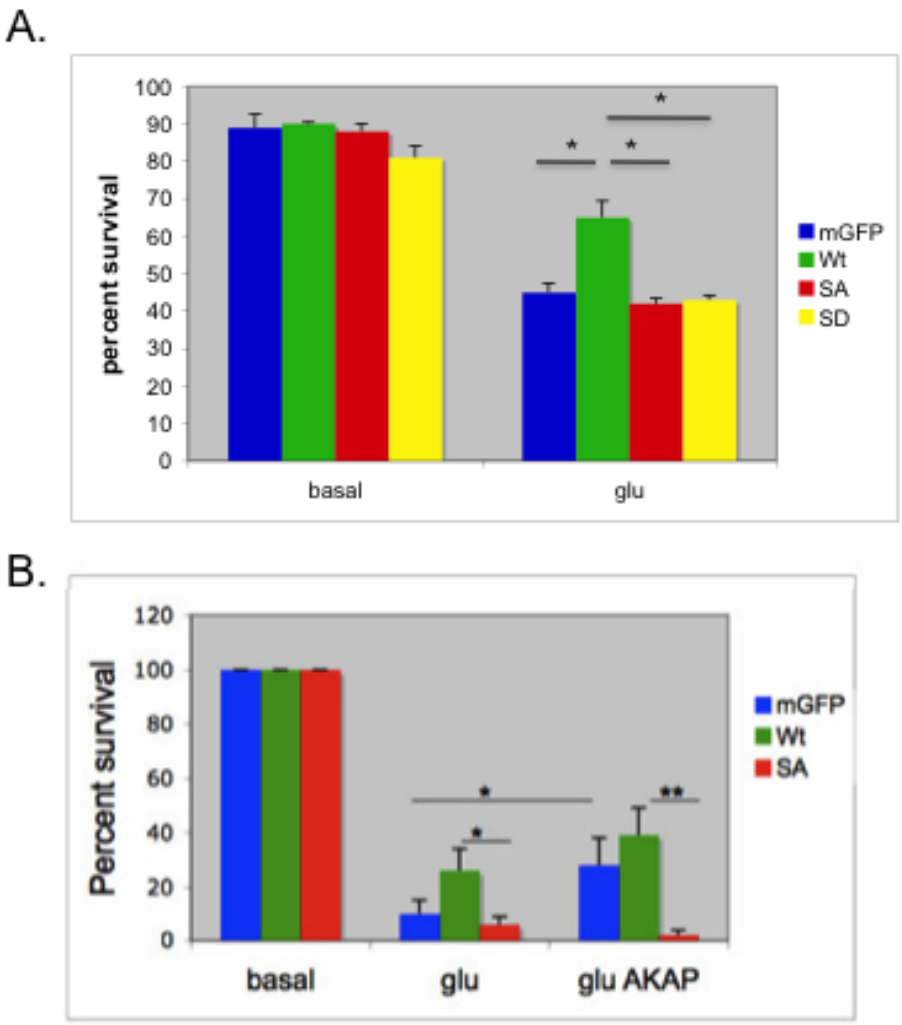

Figure 2.5 Neuroprotection imparted by Mfn2 requires Ser442.
A. Primary hippocampal neurons (PHNs) transfected with either mitochondrial GFP, or WT, Ser442Ala or Ser442Asp Mfn2 show similar basal survival levels (left) while only WT Mfn2 protects neurons against 40 μM glutamate treatment (right). Results are shown + the standard deviation of three wells, representative of three independent experiments. ***B.*** The expression of AKAP1 with the Mfn2 and control constructs provides additional protection against 50 μM glutamate not seen with the Ser442Ala Mfn2 mutation. These results suggest that Mfn2 mediated survival is dependent on the presence of Ser at residue 442. Results shown + standard deviation of three wells representative of one experiment.

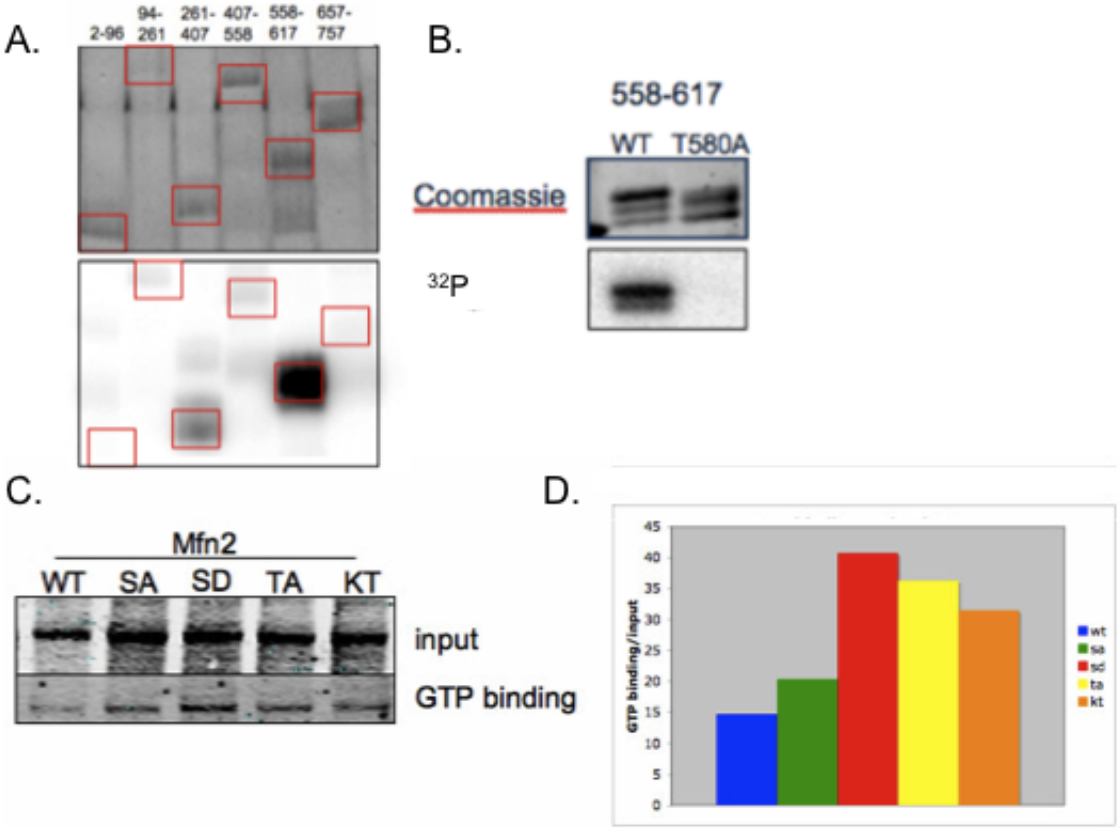

Figure 2.6 Analysis Erk induced phosphorylation of Mfn2 on Thr580. ***A.*** An *in vitro* Erk phosphorylation assay was performed, with GST fragments encompassing the entire Mfn2 sequence. Fragment 3 (261-407) and fragment 5 (558-617) were the only fragments to show any ^{32}P incorporation, with fragment 5 having a much greater degree of phosphorylation than fragment 3. ***B***. The Thr580Ala mutation was made in the 558-617 fragment, which completely ablated ^{32}P incorporation, signifying this site is Erk phosphorylated. ***C.*** The ability of PKA and Erk phosphorylation mutants to modify GTP binding was analyzed using GTP agarose beads in one preliminary experiment. The Ser442Ala mutation showed no difference in GTP binding compared to wild type, while the Ser442Asp, Thr580Ala and Lys109Thr mutants all showed increased binding. ***D.*** Quantification of the GTP binding seen in C.

CHAPTER III: MODULATION OF DRP1 SER656 PHOSPHORYLATION BY NITROSYLATION

Introduction

Proper mitochondrial function is dependent on maintaining the balance between mitochondrial fission and fusion. The large cytosolic GTPase Dynamin related protein 1 (Drp1) regulates mitochondrial fission by translocating to the mitochondria where it interacts with Fis1 and promotes scission (James, et al, 2003, Smirnova, et al, 2001, Smirnova, et al, 1998, Stojanovski, et al, 2004, Yoon, et al, 2003). The actions of Drp1 are tightly regulated by a variety of post-translational modifications that effect GTPase activity, localization, mobility and protein stability (Cereghetti, et al, 2008, Chang & Blackstone, 2007a, Cho, et al, 2009, Cribbs & Strack, 2007, Figueroa-Romero, et al, 2009, Han, et al, 2008, Karbowski, et al, 2007, Merrill, et al, 2010, Taguchi, et al, 2007).

The GED domain is the predominant site of Drp1 modifications

Dynamin related protein 1 (Drp1)

Drp1 is a member of the dynamin superfamily of proteins classified by their structural similarity and GTPase activity (Praefcke & McMahon, 2004, Smirnova, et al, 1998). Drp1 is similar to other dynamin family members in that it contains an N-terminal GTPase domain, a middle (MID) domain, the largely unconserved variable domain (VD) and a C-terminal GTPase effector domain (GED) (Figure 3.1). Alternative splicing of three exons, one in the GTPase domain and two in the VD, can yield up to eight alternatively spliced products (unpublished data from the Strack lab). While the function of the splice variants is largely unknown, work from the Strack lab has demonstrated that the presence of

the third exon, in the absence of the second exon, targets Drp1 to the microtubules, decreasing its actions on the mitochondria.

Drp1 is highly regulated by post-translation modifications to residues present in the core domain of the protein (Chang & Blackstone, 2007a, Cho, et al, 2009, Cribbs & Strack, 2007, Han, et al, 2008, Taguchi, et al, 2007). However, recent work has shown that four of the eight non-canonical SUMOylation sites of Drp1 are found in the variably spliced exons within the VD (Figueroa-Romero, et al, 2009), suggesting that some Drp1 protein regulation is splice form dependent.

Drp1 Phosphorylation

The most predominant form of Drp1 posttranslational modification is phosphorylation. There is bidirectional control of Drp1 activity by phosphorylation as multiple kinases and phosphatases act on different residues to modulate protein function. The most well characterized modification is the PKA phosphorylation of Ser656 (Cribbs & Strack, 2007) (in the longest splice variant or Ser637 in the splice variant missing the C-terminal splice (Chang & Blackstone, 2007b). From now on the PKA phosphorylation site will be referred to as Ser656). While it is unclear how Ser656 phosphorylation affects GTPase activity, it is clear that phosphorylation results in decreased Drp1 mediated mitochondrial fission (Chang & Blackstone, 2007b, Cribbs & Strack, 2007). The calcium dependent phosphatase Calcineurin dephosphorylates Ser656 (Cribbs & Strack, 2007) and mediates the translocation of Drp1 from the cytosol to the mitochondria where it functions to promote fragmentation (Cereghetti, et al, 2008) and initiate apoptosis (Cereghetti, et al, 2010). Increased Ca^{2+} influx in neurons has also been shown to activate CamKIα induced phosphorylation of Ser656, mediating the translocation of Drp1 to the mitochondria, resulting in increased mitochondrial fragmentation (Han, et al, 2008). Phosphorylation also

regulates the activity of Drp1 during mitosis, where Cdk1/cyclin B phosphorylation of Ser635 activates the protein, and is required for the mitochondrial fragmentation seen during mitosis (Taguchi, et al, 2007). However, outside of mitosis the phospho-blocking Ser635Ala mutation increases Drp1 dependent mitochondrial fragmentation (Cereghetti, et al, 2008), rather than the inactivation of function that occurs during mitosis (Taguchi, et al, 2007). Taken together, the contradictory phosphorylation of a single residue by multiple kinases, and the opposing actions of a phosphorylation site depending on cell cycle stage, demonstrate the complexity of Drp1 regulation that appears to be both cell type and cell cycle stage dependent.

SUMOylation and Ubiquitination of Drp1

The stability of Drp1 is regulated by both SUMO and ubiquitin modifications. SUMOylation is the conjugation of a SUMO moiety to a lysine of a target substrate mediated through an E3 SUMO-conjugating enzyme. MAPL, a SUMO-conjugating enzyme, mediates the addition of a SUMO group to Drp1 (Braschi, et al, 2009, Harder, et al, 2004), which occurs on eight non-canonical lysine residues (Figueroa-Romero, et al, 2009) and results in increased protein stability and mitochondrial fragmentation (Harder, et al, 2004).

The E3 ubiquitin conjugating enzyme March V interacts with and ubiquitinates Drp1 (Karbowski, et al, 2007, Nakamura, et al, 2006). Similar to SUMOylation, the ubiquitination of Drp1 appears to be required for Drp1 fission activity and serves to stabilize protein expression (Karbowski, et al, 2007, Nakamura, et al, 2006, Park, et al, 2010, Santel & Frank, 2008).

Drp1 Nitrosylation

In neurons, the presence of excessive nitric oxide (NO) leads to rapid mitochondrial fragmentation preceding neuronal death (Barsoum, et al, 2006).

Previous work demonstrated that nitrosylation of dynamin, the archetypal superfamily member, activates protein function, increasing both the rate and magnitude of endocytosis (Wang, et al, 2006). These findings lead to the hypothesis that nitrosylation of Drp1 might mediate the effects of NO treatment on mitochondrial morphology. Indeed, nitrosylation of Drp1 on Cys663 (Cys644 in the splice variant examined in the paper) increased Drp1 activity, mediating the mitochondrial fragmentation induced by NO (Cho, et al, 2009). Furthermore, overexpression of dominant negative Drp1 Lys38Ala or blocking nitrosylation with the Cys663Ala mutant, prevents NO induced mitochondrial fragmentation (Barsoum, et al, 2006, Cho, et al, 2009).

Nitrosylation/Denitrosylation as a signaling event

The use of nitric oxide (NO) as a signaling molecule in endothelial cells has long been recognized, but the pervasiveness of S-nitrosylation of diverse substrates has only more recently been examined. S-nitrosylation, or the addition of an NO group to any reactive cysteine, is a non-enzymatic process mediated by the presence of endogenous or exogenous NO, which reacts with glutathione or a free cysteine catalyzing the transnitrosylation of the target substrate (Benhar, et al, 2009, Hess, et al, 2005). The production of NO can occur through the actions of Nitric Oxide Synthase (NOS) to generate NO from arginine and O_2, or from the reduction of NO_x species (Hess, et al, 2005). The removal of NO groups from the substrate is just as complicated as the addition. While degradation by light, heat, reducing agents or nucleophilic compounds can catalyze the removal, there are two groups of denitrosylating agents that can act on specific substrates to remove the NO group (Benhar, et al, 2009). The denitrosylation of S-nitrosoglutathione (GSNO) by GSNO reductase (GSNOR) acts indirectly on proteins that are involved with GSNO, but not on substrates directly. Thioredoxin

(Trx) and Thioredoxin Reductase (TrxR) act together with NADPH to catalyze denitrosylation of specific substrates, many of which have been recently identified (Benhar, et al, 2010). Overall, the use of reversible nitrosylation to regulate protein activity is a complex field that has recently been the focus of more research.

Here I investigate whether the posttranslational modifications of Drp1, PKA mediated phosphorylation of Ser656 and NO mediated nitrosylation of Cys663 act dependently or independently to modulate Drp1 function. Our model (Figure 3.2) predicts that nitrosylation of Cys663 and phosphorylation of Ser656 are mutually exclusive events. Additionally, we believe the NO mediated Drp1 activation and mitochondrial fragmentation goes through modulation of the phosphorylation state of Ser656.

Materials and Methods

Cell Culture and Constructs

Cos 1 (Jensen, et al, 1964) and Long Hela cells (Scherer, et al, 1953) (a gift from Richard Youle) were cultured (37^{o}C, 5% CO_2) in RPMI 1640 (Gibco) containing 10% fetal bovine serum (heat inactivated).

The cDNA of Drp1 (Y Yoon, University of Rochester) was used as a template for generating the Ser656Ala/Asp (Cribbs & Strack, 2007), the Cys663Val, and the Ser656Asp plus Cys663Val double mutant using site directed mutagenesis as described elsewhere.

The cDNA of PKA RIα was cloned using RTPCR from rat tissue using the forward primer TGA CCT GGG ATC CGC CAC CAT GGC AGC CAG TGA GGA AGA GC and the reverse primer TCA GAT CGC GGC CGC CGA CGG ACA GTG ACA CAA AGC TG. The cDNA was then subcloned into the V5 vector using the BamHI and NotI restriction sites added during the RTPCR. Site directed

mutagenesis was then carried out using the V5 PKA RIα as a template to create the Cys39His mutation.

Antibodies

Antibodies commercially available are as follows: Total Drp1, PKA RIα and PKA RIIα (BD Transduction Laboratories), Drp1 phospho-Ser656, Total Vasp, Vasp phospho-S157, PKA substrate (Cell Signaling), V5 (Invitrogen), GFP (Abcam), Mitochondrial cytochrome oxidase 2 (NeoMarkers). Secondary antibodies include goat αRabbit IR800, goat αMouse IR800, goat αRabbit IR680, and goat αMouse IR680 (Licor, Lincoln, NE); Alexa conjugated donkey αRabbit-488 and Alexa conjugated donkey αMouse-543 (Invitrogen).

Other Reagents

Forskolin was purchased from (Fisher) and a 50 mM stock solution was prepared and aliquoted and stored at -20^{o} C for dilution in media prior to use. S-nitrosocysteine (SNOC) was prepared fresh before each use by mixing equal molar amounts of cysteine (Sigma) with sodium nitrite (Fisher) and then adding an equal amount of 1 M HCl bringing the solution to a final molarity of 100 mM. The mixture, which turns a burnt orange color if properly mixed, was incubated at room temperature for 5 minutes in the dark before dilution in media prior to use. Dibutyryl cAMP (Bt_2 cAMP) (CalBioChem) stock solution was prepared fresh prior to each use in Dimethylsulfoxide (DMSO) (Fisher) before diluting in media.

Immunofluorescence

Long Hela cells were plated at 40,000 cells/well on rat tail collagen (BD Biosciences) coated glass bottom four well chamber slides (Lab Tek) for same day transfection. Cells were transfected with plasmids replacing the endogenous Drp1 with wild type or mutant GFP Drp1. 24 hours following transfection cells

were either left untreated, or treated with 500 μM SNOC for 2 hours. After treatment cells were washed one time with PBS and fixed with 4% PFA for 20 minutes in the cell culture incubator. Cells were then washed two times with PBS and blocked with 4% normal donkey serum (Invitrogen) in TTBS for 30 minutes rocking at room temperature. Staining was performed using a 1:3000 dilution of anti rabbit GFP antibody and a 1:200 dilution of anti mouse mitochondrial cytochrome oxidase antibody in TTBS for 16 hours at 4^{o} C. Following washing 5x for 5 minutes with PBS cells were incubated with Alexa Flour-488 and -543 in PBS for 2 hours at room temperature. After secondary incubation cells were washed 5x for 5 minutes in PBS. To detect the nucleus Hoechst DNA dye was diluted 1:1000 in PBS and incubated on the cells for 5 minutes at room temperature. Finally the Hoechst dye was removed and replaced with fresh PBS. Cells were imaged at 63X on a Zeiss 200M inverted microscope equipped with a Hamamatsu ER camera.

Image Analysis

Mitochondrial morphology was analyzed either through subjective scoring of coded images, or by a custom macro written for Image J analysis software as discussed previously. Subjective scoring was performed by first coding all images using an Image J macro. The mitochondrial channel (red channel) of the images was then scored from 0.5 to 4, where 0.5 signifies 100% of the mitochondrial are fragmented into small shapes, similar to grains of pepper and 4 signifies 100% of the mitochondria are forming a unbroken network throughout the entire cell.

PKA phosphorylation assays

Cos1 cells were plated at 300,000 cells/mL media for same day transfection on a 24 well plate. Drp1 wild type or Cys663Val were transfected

using 0.06% Lipofectamine 2000. 40 hours post transfection cells were treated with 500 μM SNOC followed immediately by 10x dilutions of forskolin or Bt_2 cAMP. Prior to adding to the cells 10x serial dilutions of forskolin or Bt_2 cAMP were made so that once added to the cells I would have a final concentration of 0.64 μM, 1.6 μM, 4 μM, 10 μM and 25 μM or 125 μM, 250 μM, 500 μM or 1 mM respectively. 1.5 hours following treatment cells were washed in phosphate-buffered saline (PBS) and lysed in 75uL 1X Sample Buffer (for 24 well plate), sonicated and run on 10% SDS polyacrylamide gels followed by transfer to nitrocellulose membrane for western blotting. Images were generated using the Odyssey Imaging System (Licor, Lincoln, NE).

Quantitative immunoblotting using phospho-specific antibodies

Images were captured using the Odyssey Imaging System, and the quantification of band intensities was calculated using Image J software. To determine the relative phosphorylation of the bands, the phospho-specific antibody signal was divided by the total protein signal to control for loading differences. The values were then normalized to either the 25 μM forskolin concentration without SNOC for the forskolin dose curves, or the 10 μM forskolin concentration without SNOC for the Bt_2 cAMP dose curves. Statistical analysis was performed on data from at least three independent experiments using Excel to calculate either Student's t-test or two-way ANOVA.

cAMP Production Assays

Cos1 cells were plated at 150,000 cells/mL media in a 96 well plate and allowed to attach overnight. The next day the Bridge-It cAMP designer assay (Mediomics) was used based on manufacturers protocol. Specifically, 24 hours after plating the cells were washed in 100 μL PBS and then 50 μL 1X KRB-IBMX

buffer was placed on the cells, and incubated at room temperature for 15 minutes. During this initial incubation, serial dilutions of forskolin were made to 10X the desired concentration in KRB-IBMX buffer. SNOC was diluted to 5 mM in KRB-IBMX buffer containing forskolin. The 10X buffer containing forskolin and SNOC was added to the appropriate well to bring final concentration to 0.1 μM, 0.39 μM, 1.56 μM, 6.25 μM, and 25 μM or 500 μM respectively. Cells were incubated on a rocker at room temperature for 30 minutes covered in tin foil. Following treatment, the KRB-IBMX buffer was removed from the wells and 100 μL cAMP designer assay was added to each well. Cells were then incubated on the rocker for 30 minutes covered in tin foil. After incubation cells were scraped off and added to a black 96 well plate, to be read on a fluorescent plate reader at excitation of 480 and emission of 535. Once the raw fluorescent values were read, the background value of an empty cell was subtracted from each of the wells containing sample. Relative fluorescence was then calculated using the following formula RF = (R0 – R)/R0, where R0 is the blank well, or the cells containing no stimulation and R is the raw value for each well.

Disulfide Bond Formation Assays

Cos1 cells were plated at 300,000 cells/mL in a 12 well plate. The following day cells were treated with 1 mM Bt_2 cAMP along with the desired concentration of SNOC for 90 minutes. Prior to addition to the cells serial dilutions of the SNOC were made so that the final concentration added to the cells was 64 μM, 160 μM, 400 μM, 1 mM and 2.5 mM. Following treatment cells were washed one time in PBS and then lysed in 1X sample buffer without beta-mercaptoethanol, sonicated, run on 10% SDS polyacrylamide gels and transferred to nitrocellulose membrane for western blotting. Images were generated using the Odyssey Imaging System (Licor, Lincoln, NE).

Quantification of Disulfide Bond Formation

Images were captured using the Odyssey Imaging System, and the quantification of band intensities was calculated using Image J software. To determine the relative contribution of the dimer and monomer to the total PKA RIα signal the intensities of the two bands were added together and the percentage of each was calculated.

Results

Blocking nitrosylation with Drp1 Cys663Val enhances PKA induced mitochondrial elongation

Previous work has established that PKA induced mitochondrial elongation is dependent on its ability to phosphorylate and inactivate Drp1 on Ser656 (Chang & Blackstone, 2007a, Cribbs & Strack, 2007). I wanted to determine whether blocking nitrosylation, using the conserved Cys663Val mutation, affected PKA induced mitochondrial elongation. Hela cells were transfected with either wild type Drp1, Ser656Ala to block phosphorylation or the Cys663Val to block nitrosylation, along with outer mitochondrial targeted GFP (omGFP) as a control or outer mitochondrial targeted PKA (omPKA). Morphometric analysis of the various conditions found that in the cells co-expressing omGFP, the Ser656Ala mutant caused slight, though non-significant mitochondrial fragmentation while the Cys663Val mutant caused significant elongation (Figure 3.3A). In cells co-expressing omPKA, the wild type Drp1 showed significant elongation compared to control, that was completely ablated by the Ser656Ala mutant. The Cys663Val mutant significantly enhanced the omPKA induced mitochondrial elongation compared to wild type Drp1 containing cells (Figure 3.3A). These results suggest that blocking the ability of Drp1 to be nitrosylated, using a Cys663Val mutation, synergizes with PKA mediated phosphorylation of Ser656.

The Cys663Val and Ser656Asp independently block nitrosylation induced mitochondrial fragmentation.

The initial characterization of the regulation of Drp1 by nitrosylation found that NO treatment of Drp1 activates protein function resulting in Cys663 dependent mitochondrial fragmentation of neurons (Cho, et al, 2009). I sought to determine whether 1) nitrosylation modulated the phosphorylation state of Drp1 Ser656 causing mitochondrial fragmentation, and 2) whether the Ser656 and Cys663 sites acted dependently or independently to modulate the NO induced fragmentation. Prior to experimentation, I verified the previously reported NO induced mitochondrial fragmentation (Barsoum, et al, 2006) in Long Hela cells and determined that the NO donor S-nitrosocysteine (SNOC) resulted in the most significant fragmentation at the lowest concentration (data not shown). To examine the above posed questions Hela cells were transfected with wild type Drp1, Ser656Asp, Cys663Val, a double mutant containing both mutations, Ser656Asp, Cys663Val, and the Ser635Ala mutant, blocking Cdk1 induced phosphorylation, which was used as a control. Prior to fixation and staining, cells were either left untreated, or treated with 500 μM SNOC for 2 hours. Subjective scoring of the mitochondria revealed that under basal conditions the Ser656Asp, Cys663Val and the double mutant all showed similar significant mitochondrial elongation compared to wild type, while the Ser635Ala behaved similar to wild type (Figure 3.4B). Treatment of the cells with 500 μM SNOC caused mitochondrial fragmentation independent of the Drp1 construct. Specifically, the wild type and Ser635Ala Drp1 showed significant fragmentation compared to untreated cells, while the Ser656Asp, Cys663Val and the double mutant all provided some protection against nitrosylation induced fragmentation (Figure 3.4A,B). Analysis of three independent experiments showed that while the mitochondrial morphology of the double mutant construct was slightly longer than

either single mutant alone, there was no significant difference between the Ser656Asp and the double mutant constructs (Figure 3.4C). These results suggest that the Ser656Asp and the Cys663Val act independently to attenuate NO induced fragmentation. Yet the two mutations clearly have an additive effect as the double mutant is more protected from NO induced mitochondrial fragmentation than either mutation alone. One possible explanation is that the mitochondrial elongation caused by the Ser656Asp (Chang & Blackstone, 2007a, Cribbs & Strack, 2007) protects the cells against the nitrosylation-induced fragmentation. So rather than blocking the nitrosylation, the cells are buffered from the effects of the NO or just take longer to respond. I believe the Cys663Val mutant acts in much the same way. While the Val substitution is a conserved mutation, the mitochondrial elongation under basal conditions suggests the Cys663Val construct causes a non-specific conformational change leading to Drp1 inactivation, which again buffers the cell against the nitrosylation induced fragmentation.

Nitrosylation inhibits Adenylate Cyclase decreasing cAMP production.

Posttranslational modifications serve to regulate protein function, not only by turning the protein on or off, but also in initiating cascades of modifying events. With the identification of the nitrosylated cysteine (Cho, et al, 2009) in such close proximity to the Drp1 PKA phosphorylation site (Chang & Blackstone, 2007a, Cribbs & Strack, 2007) I wanted to determine whether nitrosylation affected the ability of Ser656 to be phosphorylated.

Cos 1 cells were transfected with HA Drp1 wild type or Cys663Val. Two days after transfection, cells were treated with 500 μM SNOC followed immediately by increasing concentrations of forskolin. In the absence of SNOC

treatment, wild type Drp1 showed a dose dependent increase in Ser656 phosphorylation following forskolin treatment, which was enhanced by the Cys663Val mutant at all forskolin doses, though it was only significant at the two highest doses (Figure 3.5A). The addition of SNOC lead to an overall decrease in Ser656 phosphorylation of wild type Drp1 that was significant at the highest forskolin concentrations (Figure3.5B) and was mirrored in the Cys663Val Drp1. The change in Drp1 phosphorylation following nitrosylation was specific to the PKA site, Ser656, as there was no change in the CDK1 phosphorylation site, Ser635 (Taguchi, et al, 2007), following either treatment (data not shown). To determine whether the decrease in Ser656 phosphorylation was a result of direct Drp1 nitrosylation, or an indirect effect on the signaling cascade, cell lysates were probed for phosphorylation of Vasp at Ser157, a specific substrate of PKA (Butt, et al, 1994, Eckert & Jones, 2007). The change in Vasp Ser157 phosphorylation mimicked Drp1 Ser656 phosphorylation, with a dose dependent increase in forskolin-induced activation that was significantly decreased in the presence of SNOC (data not shown). Taken together these results suggest SNOC is acting upstream of Drp1 to modulate PKA phosphorylation of target substrates, independent of the presence of Cys663.

Next a SNOC dose curve was carried out to determine which concentration produced an optimal block in Ser656 phosphorylation. When SNOC was added to the cells immediately following forskolin, there was no dose dependent change in Ser656 phosphorylation. Rather, initial activation of adenylate cyclase by forskolin produced the optimal substrate phosphorylation independent of the presence of SNOC (Figure 3.6A). These results suggested that the forskolin and SNOC are acting at the same point in the pathway, specifically adenylate cyclase, and whichever treatment is added first produces an irreversible activation or inactivation, respectively. However, the decrease in

Drp1 Ser656 phosphorylation at the highest concentration of SNOC (2.5 mM) suggests Drp1 is being directly nitrosylated, and resulting in decreased Ser656 phosphorylation.

Previous work has demonstrated that adenylate cyclase (AC) type 5 and type 6 are inactivated by nitrosylation (Hill, et al, 2000, McVey, et al, 1999). The predominant subtype of adenylate cyclase found in the adult kidneys is AC6, though AC4, 5, 7, and 9 are also expressed to a much lower degree (Defer, et al, 2000, Shen, et al, 1997). To examine the direct effects of nitrosylation on adenylate cyclase in Cos 1 cells a cAMP production assay was performed using the Bridge-It cAMP assay (Mediomics). When the assay was performed at concentrations similar to those used in the Ser656 phosphorylation assay (Figure 3.5), there was a significant decrease in the amount of cAMP produced at the highest forskolin concentrations in the presence of 500 μM SNOC (data not shown). When a more complete forskolin dose curve was undertaken, all but the lowest forskolin concentrations, (0.1 μM and 0.39 μM) showed a significant decrease in cAMP production in the presence of 500 μM SNOC (Figure 3.6B). These results suggest that SNOC inhibition of adenylate cyclase leads to an indirect decrease in PKA induced phosphorylation of Drp1 Ser656. However, these results do not address the role of direct Drp1 nitrosylation on Ser656 phosphorylation.

Nitrosylation induced activation of PKA RIα causes an increase in substrate phosphorylation

To overcome the inhibition of adenylate cyclase by nitrosylation, Dibutyryl cAMP (Bt_2 cAMP) was used to directly activate PKA. Cos 1 cells transfected with HA Drp1 wild type or Cys663Val were treated two days after transfection with 500 μM SNOC followed immediately by 10 μM forskolin (as a positive control) or

increasing concentrations of Bt_2 cAMP. Under basal conditions the wild type Drp1 showed a dose dependent increase in Ser656 phosphorylation that at the highest concentration (1 mM) was about three-fold lower than the phosphorylation seen with 10 μM forskolin (Figure 3.7 A,B). Similar to the forskolin curves, the Cys663Val mutant displayed enhanced Ser656 phosphorylation compared to wild type Drp1, under both basal and SNOC stimulated conditions. Addition of 500 μM SNOC to the cells resulted in a five-fold increase in Ser656 phosphorylation of both wild type and Cys663Val Drp1 (Figure 3.7A,B). Examination of Vasp phosphorylation revealed that addition of SNOC led to a four-fold increase in Ser157 phosphorylation compared to when treated with Bt_2 cAMP alone. These results suggest that SNOC is acting upstream of Drp1 mediating indirect effects on Ser656 phosphorylation.

To address the possibility that SNOC is activating PKA to increase substrate phosphorylation I looked at the disulfide bond formation of the PKA regulatory subunits. Untransfected Cos1 cells were treated with 500 μM SNOC in the presence or absence of 1 mM Bt_2 cAMP. Cells were lysed in the absence of β–mercaptoethanol to prevent disulfide bond reduction. Examination of the regulatory subunits revealed that PKA RIα shows a dose dependent increase in disulfide bond formation after the addition of SNOC that is independent by Bt_2 cAMP treatment (Figure 3.8A top and B). There was no detectable RIIα disulfide bond formation in the presence of either treatment (Figure 3.8A bottom), suggesting the actions of SNOC are PKA RI specific. To verify that the SNOC induced dimerization that I was seeing was due to disulfide bond formation I added back a reducing agent. Treating the cell lysates with β–mercaptoethanol resulted in a complete loss of the SNOC induced PKA RIα disulfide bond formation (Figure 3.8C). PKA RI contains two highly conserved cysteines Cys16 and Cys37 (human sequence), which are absent from PKA RII. Previous work

has found that Cys16 and Cys37 form disulfide bonds (Banky, et al, 1998, Burgoyne & Eaton, 2009, Leon, et al, 1997), which are enhanced by treatment of cells with H_2O_2 or NO donors (Brennan, et al, 2006, Burgoyne & Eaton, 2009). To address the role of the cysteines in mediating the NO induced disulfide bond formation of PKA RI, I made a Cys39His mutation (rat sequence), which has previously been demonstrated to block disulfide bond formation, but not disrupt PKA RI dimerization (Banky, et al, 1998). The Cys39His ablated the SNOC induced disulfide bond formation of PKA RIα (Figure 3.8D), further demonstrating the importance of disulfide bond formation, and specifically residue Cys39, in mediating the effects of NO on PKA.

Contrary to previous findings (Brennan, et al, 2006) SNOC induced disulfide bond formation of PKA RIα enhances the substrate phosphorylation only in the presence of Bt_2 cAMP (Figure 3.8E). Additionally, treatment of Cos1 cells with 500 μM SNOC does not induce PKA RI translocation out of the cytosol to a heavy membrane fraction (data not shown). These results are consistent with the idea that SNOC induced disulfide bond formation of RIα amplifies the responsiveness of PKA to levels of cAMP, promoting increased substrate phosphorylation.

Direct nitrosylation of Drp1 has no effect on the nearby PKA phosphorylation site S656

I next looked at the effects of Drp1 nitrosylation on Ser656 phosphorylation, using a constitutively active form of PKA (caPKA) targeted to the outer mitochondrial membrane (OMM). Cos 1 cells were transfected with wild type or Cys663Val Drp1 along with increasing amounts of caPKA. 24 hours post transfection cells were either left untreated, or treated with 500 μM SNOC for 1.5 hours. Under basal conditions the caPKA acted similarly to the forskolin

treatment, causing a dose dependent increase in substrate phosphorylation independent of the Drp1 construct expressed (Figure 3.9A,B). It is important to note here that the Cys663Val mutant causes slight, though non-significant enhancement of PKA mediated Ser656 phosphorylation. Upon treatment of the cells with the NO donor SNOC there is a slight, though non-significant decrease in Ser656 phosphorylation. Further analysis with the PKA substrate antibody showed a similar trend, where there was no change in overall phosphorylation levels after SNOC treatment (data not shown). While at this point I am unable to show that the SNOC is directly nitrosylating Drp1, it is evident that under the conditions tested here is no effect of nitrosylation on Ser656 phosphorylation.

Discussion

Drp1 Nitrosylation

Contrary to previous findings it is now clear that nitrosylation of Drp1 has no impact on Drp1 function. While NO donor treatment results in Drp1 nitrosylation, and evidence for Drp1 nitrosylation can be found in aged brains, including those from PD and AD patients, there is no consequence of Drp1 nitrosylation on GTPase activity (Bossy, et al, 2010). The initial report described SNOC induced Drp1 dimerization and NO mediated mitochondrial fragmentation that was dependent on Drp1 Cys663 (Cho, et al, 2009). Previous characterization of Drp1 demonstrated that oligomerization, not dimerization, is a hallmark of Drp1 activity (Shin, et al, 1999, Zhu, et al, 2004), and is unaffected by NO treatment (Bossy, et al, 2010). Furthermore, closer examination of GTPase activity of recombinant Drp1 reveals that SNOC treatment does not increase the GTPase activity of either wild type or the dominant negative Lys38Ala Drp1, as previously claimed (Cho, et al, 2009). The conclusions from this most recent paper, that the effects of nitrosylation on mitochondrial fragmentation do not go

through changes in Drp1 activity, but rather may modify the function of an as yet unidentified protein (Bossy, et al, 2010), are in agreement with my findings. Furthermore, as NO can have far reaching effects on any available cysteine, including kinases such as cdk2 (Kumar, et al, 2010), the increase in Drp1 activity following NO donor treatment may be due to the increased Ser635 phosphorylation (Ser616 in the splice variant examined in the paper) rather than directly to Drp1 nitrosylation (Bossy, et al, 2010) though my data does not support this conclusion (data not shown).

The results discussed above support the conclusions that I am able to draw from my studies. It is apparent that the Drp1 Cys663Val mutant consistently attenuates the PKA mediated Ser656 phosphorylation. While the difference between the Drp1 WT and the Cys63Val mutant are significantly different under basal conditions and when treated with forskolin, there is no significant enhancement of the caPKA phosphorylation of Ser656. I believe the discrepancy in these results is due to a difference in magnitude. If you compare the Ser656 phosphorylation caused by forskolin (Figure 3.5 A) versus caPKA (Figure 3.9A) it seems that the caPKA is more efficient at phosphorylating Drp1 than the forskolin. Additionally, the difference in the WT and Cys663Val constructs is subtle, requiring large numbers of experiments to become significant at even the highest doses of forskolin. Therefore, while the difference between the Drp1 WT and the Cys663Val in the presence of caPKA is not significantly different, the trend is towards enhanced PKA phosphorylation with the Cys663Val mutant that I believe would be significant if more experiments were performed. Furthermore, I believe the difference between the Ser656 phosphorylation levels of the two Drp1 constructs is not due to blocking nitrosylation but rather that the Val mutation somehow increases the availability of the Ser656 to be phosphorylated, either by changing the innate Drp1 structure to allow Ser656 to stick out more, or

by possibly widening a binding pocket allowing PKA better access. Evidence of this can be seen with the increase in Ser656 phosphorylation by western blot analysis (Figure 3.5A), as well as by an attenuation of the decreased Drp1 mobility seen with PKA activation (data not shown), or the elongation of mitochondrial following omPKA expression (Figure 3.3). However, treatment of cells with an NO donor has no effect on the ability of Ser656 to be phosphorylated (Figure 3.5B,C), suggesting the effects seen with the mutant are due to a structural change rather than loss of a modification.

The role of Drp1 in mediating NO induced mitochondrial fragmentation

One key point in my findings, is that contrary to previous reports (Cho, et al, 2009) the Cys663Val mutant is not able to block SNOC induced mitochondrial fragmentation (Figure 3.4), though there is a decrease in the percentage of fragmented mitochondria (data not shown). The discrepancy between the results of the Lipton lab and my own could be explained in many ways. First, the difference could be due to the use of a Cys663Val mutation rather than the Cys663Ala mutation used in the paper. While this is a possibility, the use of a conserved mutation (position 663 is a valine in *C. elegans*) (Figure 3.1) would not be expected to cause nonspecific conformational changes that result in disrupted function. A second possibility is the use of different cell culture models. The Lipton lab used primary cortical neurons for their immunofluorescent work, while I used Hela cells. Since I first optimized the concentration of NO donor used to induce mitochondrial fragmentation (data not shown), the cell culture model should not result in such dramatic differences. Finally, I believe the variation could be due to the use of selective publishing. The data from the Lipton lab showed only control cells both treated and untreated, along with the Drp1

constructs following SNOC treatment. Without knowing the percentage of fragmentation caused by the Drp1 constructs under basal conditions it is hard to draw complete conclusions. Similar to my data, the Lipton lab showed that the Cys663Val blocked nitrosylation induced fragmentation when compared to treated wild type Drp1. However, they make no comparison between treated and untreated Cys663Val, leaving the possibility that in neurons, there is also nitrosylation induced fragmentation of the Cys663Val construct, that is significantly less than that seen in wild type expressing neurons. While I am not saying that the data from the Lipton lab is wrong, I am simply stating that I believe that the conclusions drawn from their work are not complete based on the lack of proper controls presented in the paper. The conclusions that I draw from my results are that the Ser656Asp and the Cys663Val are able to attenuate the SNOC induced fragmentation, while the Ser635Ala and wild type Drp1 are not, possibly due to the protective effects of mitochondrial elongation on delaying apoptosis (Jahani-Asl & Slack, 2007, Lee, et al, 2004, Sugioka, et al, 2004).

Nitrosylation of the cAMP-PKA signaling cascade

Recently the nitrosylation of kinases and phosphatases have been found to play a key role in modulating signaling cascades. Specifically, Park et al (Park, et al, 2000) demonstrated S-nitrosylation of Cys116 inhibits JNK-mediated phosphorylation and activation of Jun, its downstream signaling substrate. Conversely S-nitrosylation of Src is associated with the formation of disulfide bonds across Src multimers, leading to activation through autophosphorylation of Tyr416 (Akhand, et al, 1999). Similarly the cAMP-PKA signaling cascade is diametrically regulated by S-nitrosylation of key components. cAMP production occurs following activation of adenylate cyclase (AC) by either $G\alpha_s$ or through pharmacological induction by forskolin. McVey et al (McVey, et al, 1999) found

that pre-incubation of cell membranes from N18TG2 cells with NO donors (SNP or SNAP) results in a dose dependent decrease in forskolin-induced cAMP production from AC6. The inhibition of AC activity by NO is specific to isoforms 5 and 6, as AC1 and AC2 show no change in forskolin-induced cAMP production following NO donor pre-incubation (Hill, et al, 2000). Looking downstream of AC in the pathway, PKA RI is directly activated by NO (Burgoyne & Eaton, 2009). When perfused rat hearts are exposed to increasing concentrations of SNOC there is a dose dependent increase in PKA RI nitrosylation and in disulfide bond formation (Burgoyne & Eaton, 2009). Previous work by Brennan et al (Brennan, et al, 2006) showed that oxidant-induced dimerization/disulfide bond formation lead to activation of RI resulting in translocation and increased substrate phosphorylation.

Evidence presented herein verifies the previous findings of others. Specifically, treatment of untransfected cells with the NO donor SNOC leads to a significant decrease in cAMP production (Figure 3.6B), suggesting that NO is acting to directly inactivate adenylate cyclase. Adenylate cyclase was identified as a possible target of NO modifications when it became clear that the sequence of the addition of SNOC and forskolin mediated the outcome of substrate phosphorylation. When cells were treated with SNOC followed immediately by increasing concentrations of forskolin, substrate phosphorylation was significantly decreased in the presence of SNOC compared to forskolin treatment alone (Figure 3.5B,C). Conversely, when cells were treated with forskolin prior to the addition of increasing concentrations of SNOC, the NO treatment resulted in no change in substrate phosphorylation (Figure 3.6A). Taken together these results suggest that both forskolin and NO are acting on the same target, namely AC5/6. It is possible to envision that conformation changes induced by forskolin masks the NO targeted cysteine, making it unavailable for modification. In the inactive

conformation, the targeted cysteine is available for modification by NO, possibly locking the enzyme in its inactive state, thereby ablating the effects of forskolin. Why then, is the decrease in substrate phosphorylation following SNOC treatment so minimal? Why is there still any phosphorylation at all? The answer to this is twofold. First, NO treatment has been found to specifically inhibit AC5/6 (Beazely & Watts, 2006, Hill, et al, 2000, McVey, et al, 1999) but not the other subtypes found in kidney epithelial cells (Defer, et al, 2000, Shen, et al, 1997). Therefore, following inactivation of a majority of the AC in the cells, there are still some AC subtypes available for activation by forskolin, producing a small, but important amount of cAMP (Figure 3.6B). Second, NO treatment increases PKA RI disulfide bond formation (Figure 3.8A,B) enhancing the PKA mediated substrate phosphorylation following cAMP (Figure 3.7A,B). Taken together, this means that the substrate phosphorylation seen in the presence of both forskolin and SNOC could be due to the moderate amount of cAMP produced from AC subtypes not effected by NO induced inhibition, acting on the PKA, whose activity is enhanced by NO modifications of PKA RI. Overall, these results highlight the complexity of NO signaling and its role in regulating phosphorylation signal cascades.

In conclusion it appears based on evidence presented herein, and recent published work, that direct nitrosylation of Drp1 Cys663 has no functional consequence, either through modulating Drp1 Ser656 phosphorylation, or through direct activation of protein function.

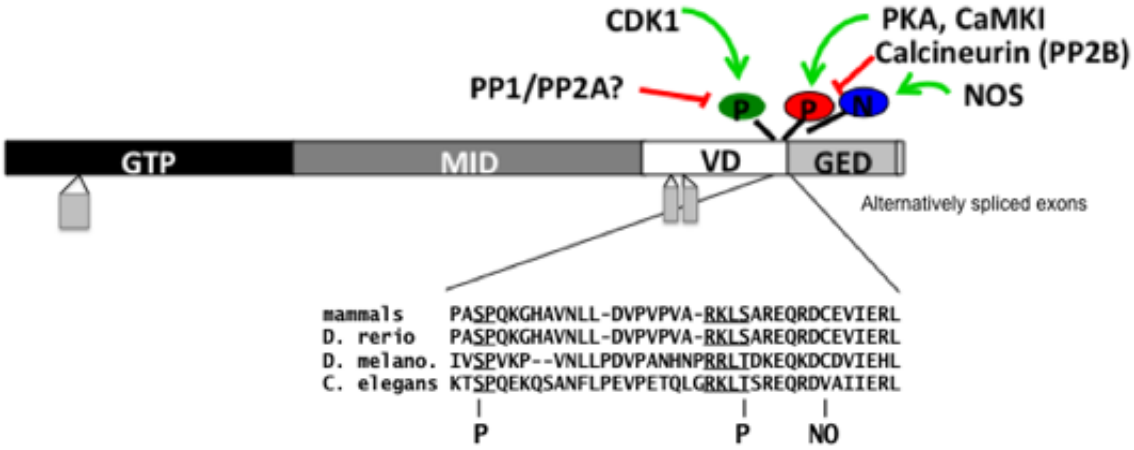

Figure 3.1 Schematic of Drp1 highlighting the highly conserved C-terminal posttranslational modifications and the three alternatively spliced exons. Figure modified from Cribbs JT and Strack S 2009.

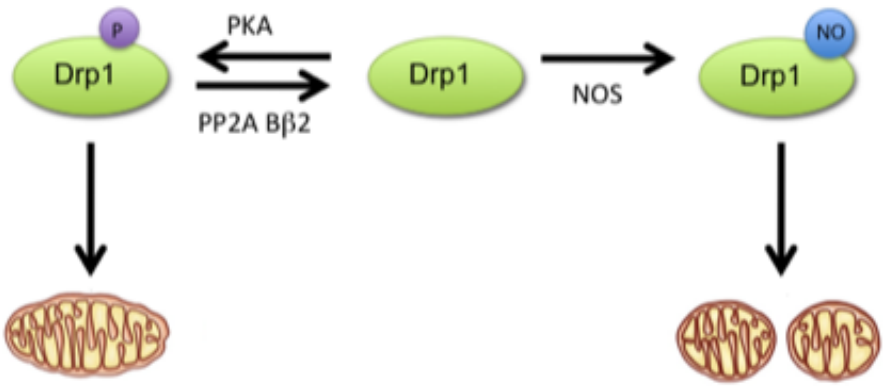

Figure 3.2 Model predicting the regulation of Drp1 by posttranslational modifications.
Our model proposes that Drp1 posttranslational modifications are mutually exclusive events. The nitrosylation of Cys663 prevents/inhibits the phosphorylation of Ser656, while blocking nitrosylation with the Cys663Val mutation, allows for PKA induced phosphorylation of Ser656.

A.

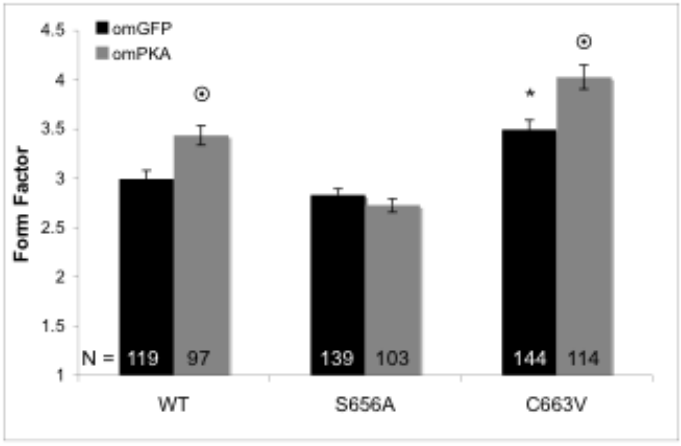

B.

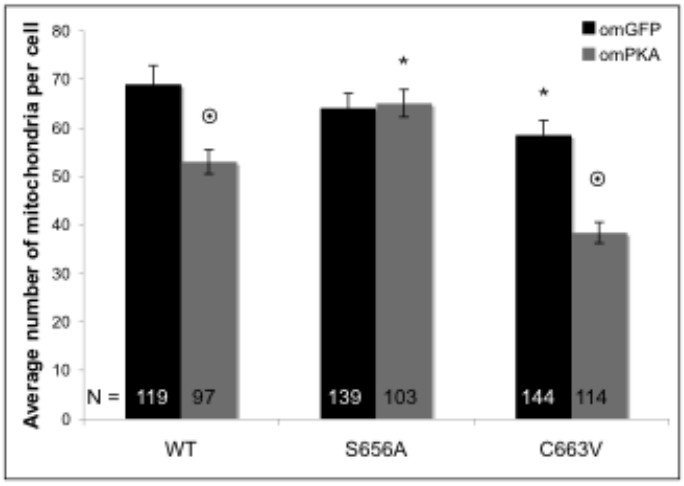

Figure 3.3 Blocking Drp1 nitrosylation with the Cys663Val mutant enhances PKA induced mitochondrial elongation.
Mitochondrial morphometric analysis of Long Hela cells transfected with GFP Drp1 wild type, Ser656Ala, or Cys663Val. ***A.*** Using form factor as a measure of mitochondrial length, a preliminary experiment shows that under basal conditions (omGFP), the Cys663Val causes mitochondrial elongation while the Ser656Ala causes slight mitochondrial fragmentation. Co-expression of omPKA induces mitochondrial elongation of wild type Drp1 that is blocked by the Ser656Ala mutant, and enhanced by the Cys663Val mutant. Results are shown + standard error where N = the number of cells per condition. ***B.*** Analysis of the average number of mitochondria per cell reveals that conditions that show significant mitochondrial elongation as described in A show significantly fewer mitochondria. Results are shown + standard error where N = the number of cells per condition.

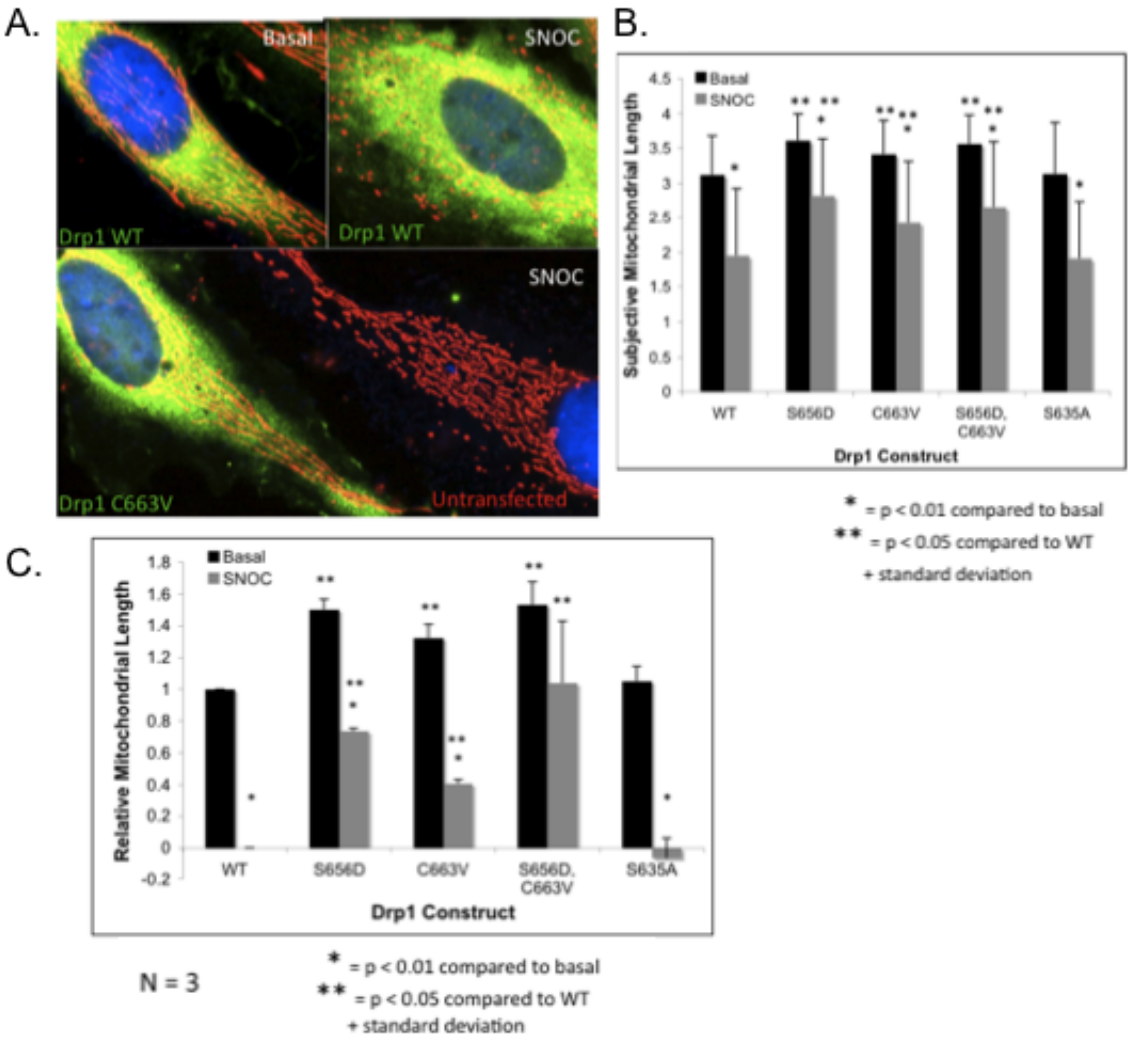

Figure 3.4 Cys663Val and Ser656Asp independently ablate nitrosylation induced mitochondrial fragmentation.
A. Immunofluorescence of Hela cells transfected with wild type (top) or Cys663Val (bottom) Drp1 either untreated (top left) or treated with 500μM SNOC (top right or bottom). ***B.*** Subjective scoring from one representative experiment. Under basal conditions the Ser656Asp, Cys663Val and the Ser656Asp, Cys663Val double mutant all cause significant mitochondrial elongation, while the Ser635Ala is indistinguishable from wild type. SNOC treatment results in mitochondrial fragmentation of all Drp1 constructs. ***C.*** Data from three subjectively scored experiments normalized to wild type basal and NO treated (1 and 0 respectively). Results show that the S635A is indistinguishable from wild type under both basal and NO treated conditions, while the other three constructs are significantly elongated. SNOC treatment results in significant fragmentation of all Drp1 constructs, though the Ser656Asp, Cys663Val and double mutant are all significantly longer than the wild type treated cells. The Ser656Asp and Cys663Val appear to independently block NO induced fragmentation as neither single mutant is significantly different from the double mutant.

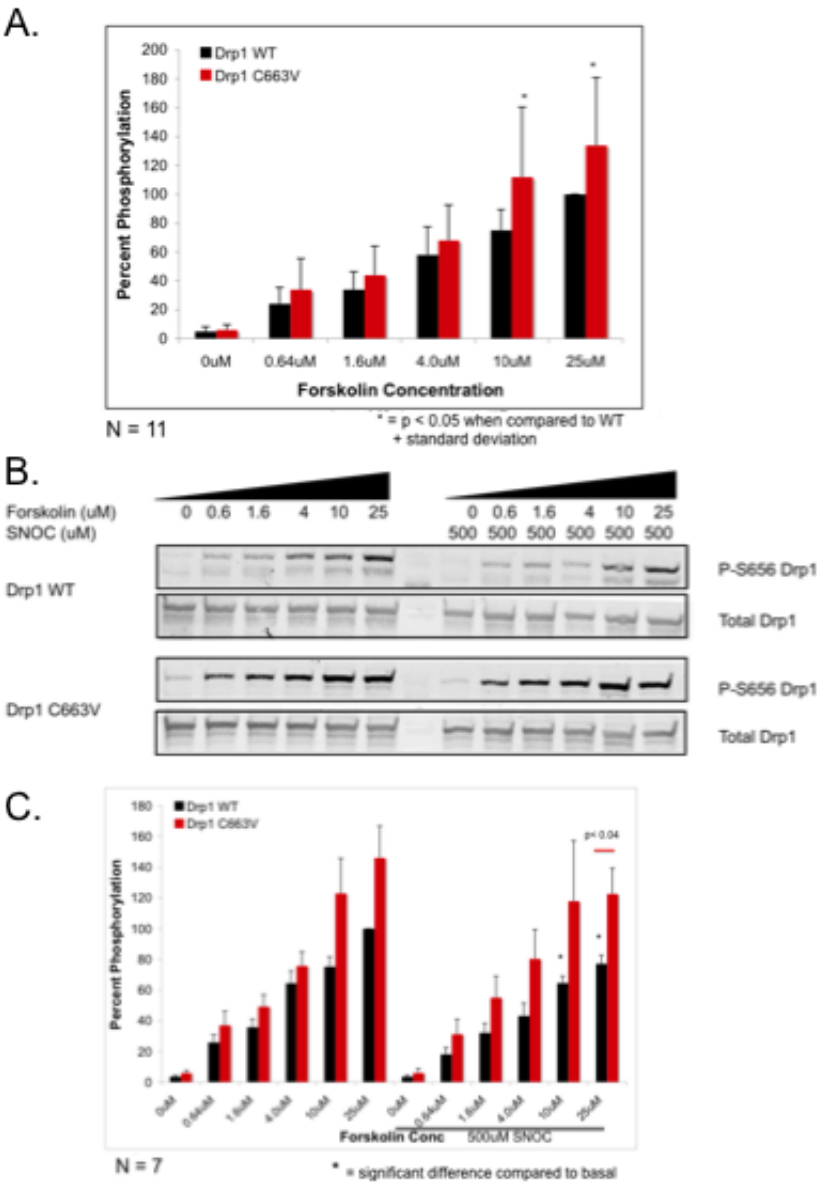

Figure 3.5 Treatment of cells with S-nitrosocysteine decreases forskolin induced Ser656 phosphorylation.
A. Quantification of Cos1 cells expressing either Drp1 wild type or Cys663Val treated with increasing concentrations of forskolin. Results show the Cys663Val enhanced PKA mediated phosphorylation compared to wild type. ***B.*** Representative blot showing cells expressing wild type or Cys663Val Drp1 with increasing concentrations of forskolin in the presence or absence of SNOC. ***C.*** Quantification of the results from seven independent experiments as shown in B. Results show treatment of the cells with SNOC causes decreased forskolin induced Ser656 phosphorylation independent of the availability of Cys663 for nitrosylation.

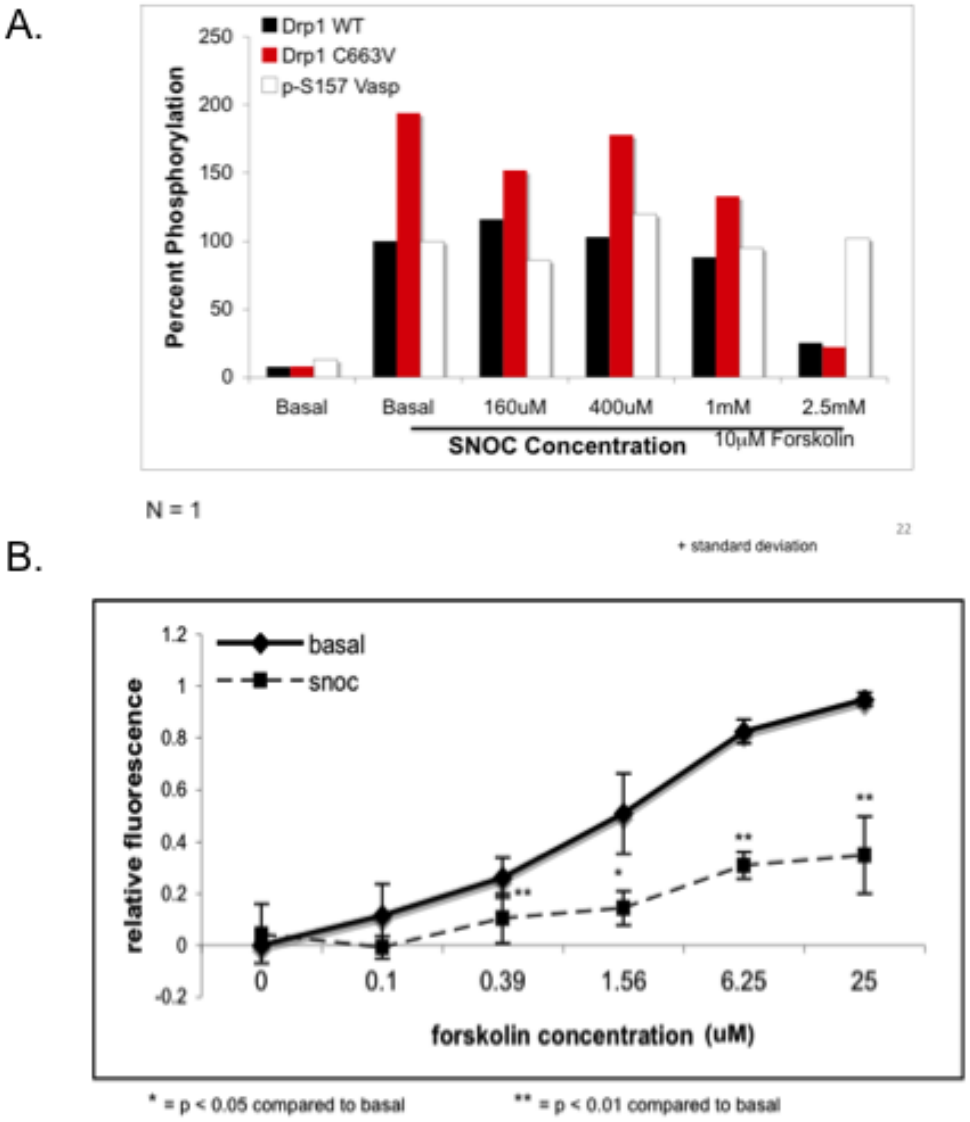

Figure 3.6 Nitrosylation decreases adenylate cyclase activity resulting in decreased cAMP production.
A. Quantification of Cos 1 cells expressing wild type or Cys663Val Drp1 that were treated with forskolin followed immediately by increasing concentrations of SNOC. Probing the cells for Ser656 phosphorylation revealed no change in levels at any concentration of SNOC independent of the availability of Cys663 to be nitrosylation. These results suggest forskolin and SNOC are acting in opposing manners on adenylate cyclase ***B.*** The Bridge-it cAMP production assay was used to monitor cAMP levels following treatment of untransfected cells with increasing concentrations of forskolin in the presence or absence of SNOC. Results show that treatment of the cells with SNOC prior to forskolin causes a significant decrease in cAMP production at almost all concentrations of forskolin.

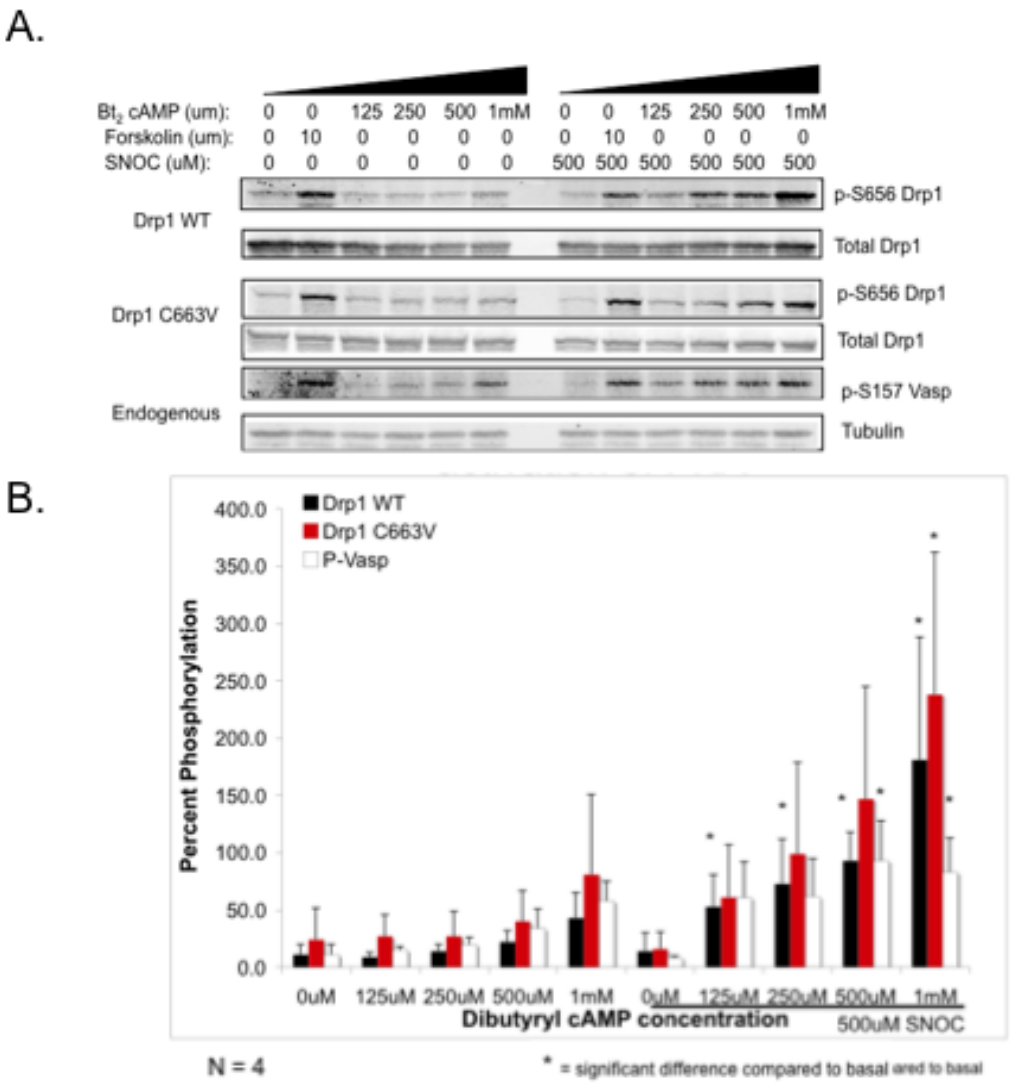

Figure 3.7 S-nitrosocysteine treatment of cells enhances Dibutyryl cAMP activation of PKA resulting in increased substrate phosphorylation.
A. Representative blot showing Cos 1 cells expressing wild type or Cys663Val Drp1 treated with Dibutyryl cAMP following SNOC treatment. ***B.*** Quantification of four independent experiments shows that SNOC treatment enhances the Dibutyryl cAMP mediated activation of PKA resulting in dose dependent phosphorylation of target substrates.

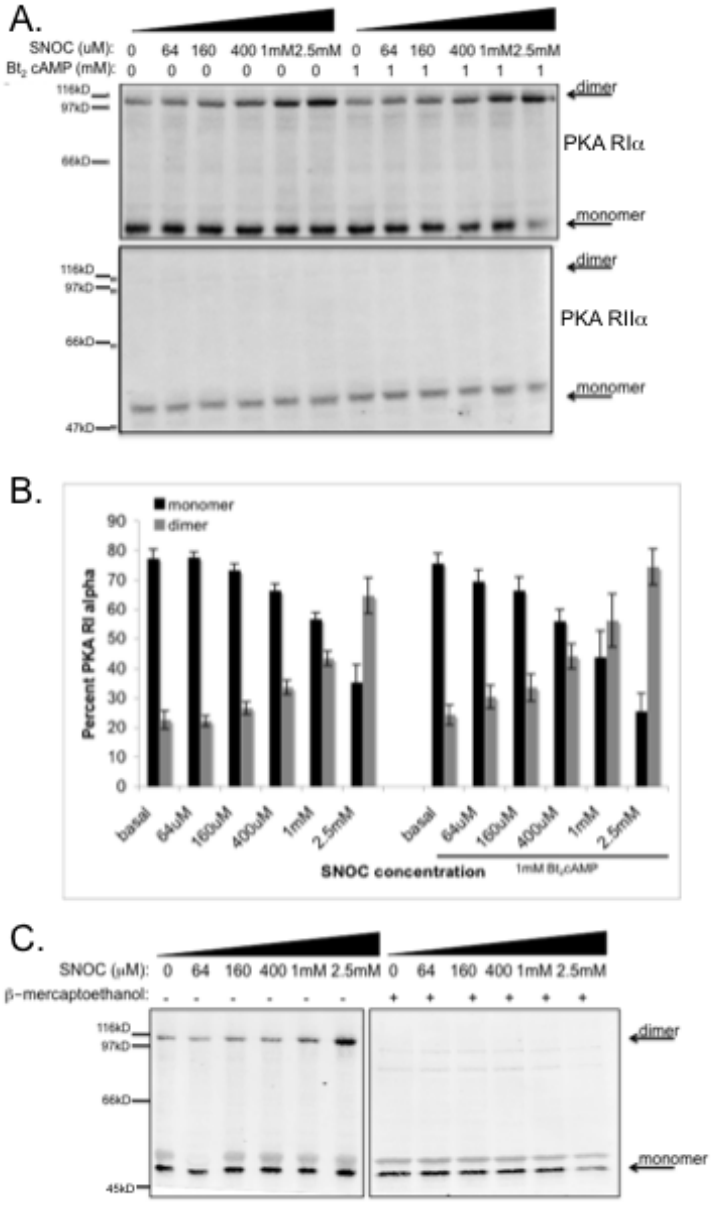

Figure 3.8 Nitrosylation increases PKA RIα disulfide bond formation leading to increased substrate phosphorylation following cAMP activation. ***A.*** Untransfected Cos 1 cells treated with increasing concentrations of SNOC show a dose dependent increase in disulfide bond formation of PKA RI, but not PKA RII, that is independent of cAMP activation. ***B.*** Quantification of three independent experiments demonstrates the dose dependent disulfide bond formation of PKA RI. ***C.*** Untransfected Cos 1 cells were treated with increasing concentrations of SNOC and lysed in the presence or absence of β-mercaptoethanol. Results show the NO induced PKA RI dimerization is due to disulfide bond formation, as the band is reduced following treatment with β-mercaptoethanol.

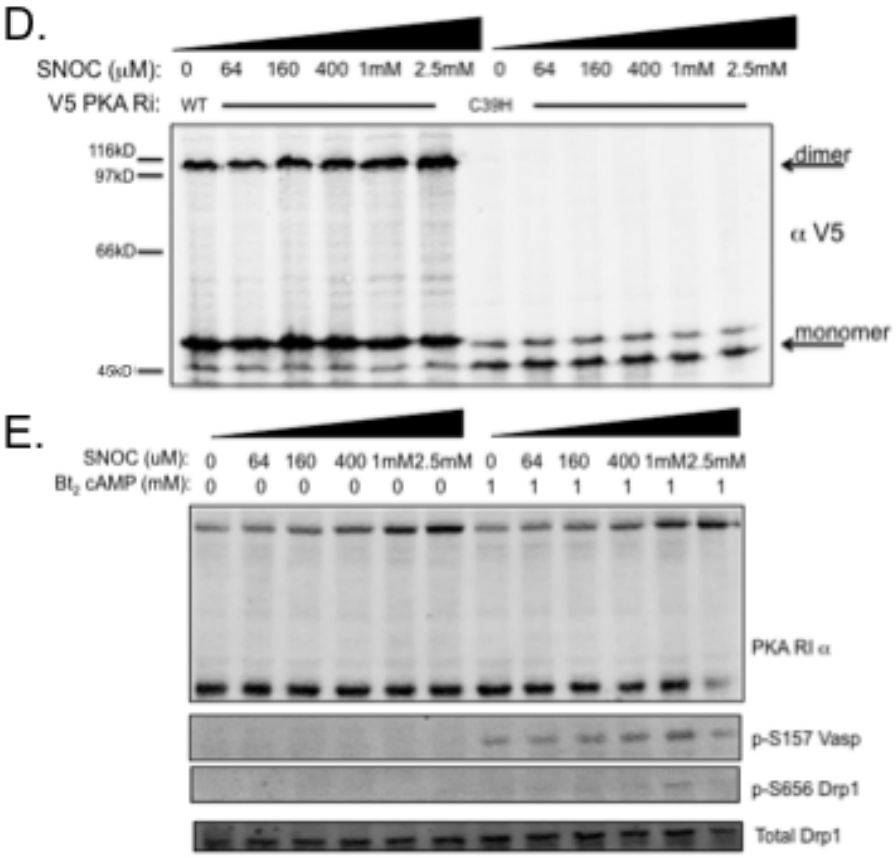

Figure 3.8 Continued
D. Cos 1 cells expressing wild type or Cys39His V5 PKA RI were treated with increasing concentrations of the NO donor SNOC. The presence of Cys39His blocked the NO induced PKA RI disulfide bond formation, suggesting this residue is important for mediating the effects NO on PKA. ***E.*** PKA induced substrate phosphorylation of untransfected Cos1 cells treated with increasing concentrations of SNOC in the presence or absence of Bt_2 cAMP. Results show PKA phosphorylation occurs only after Bt_2 cAMP treatment.

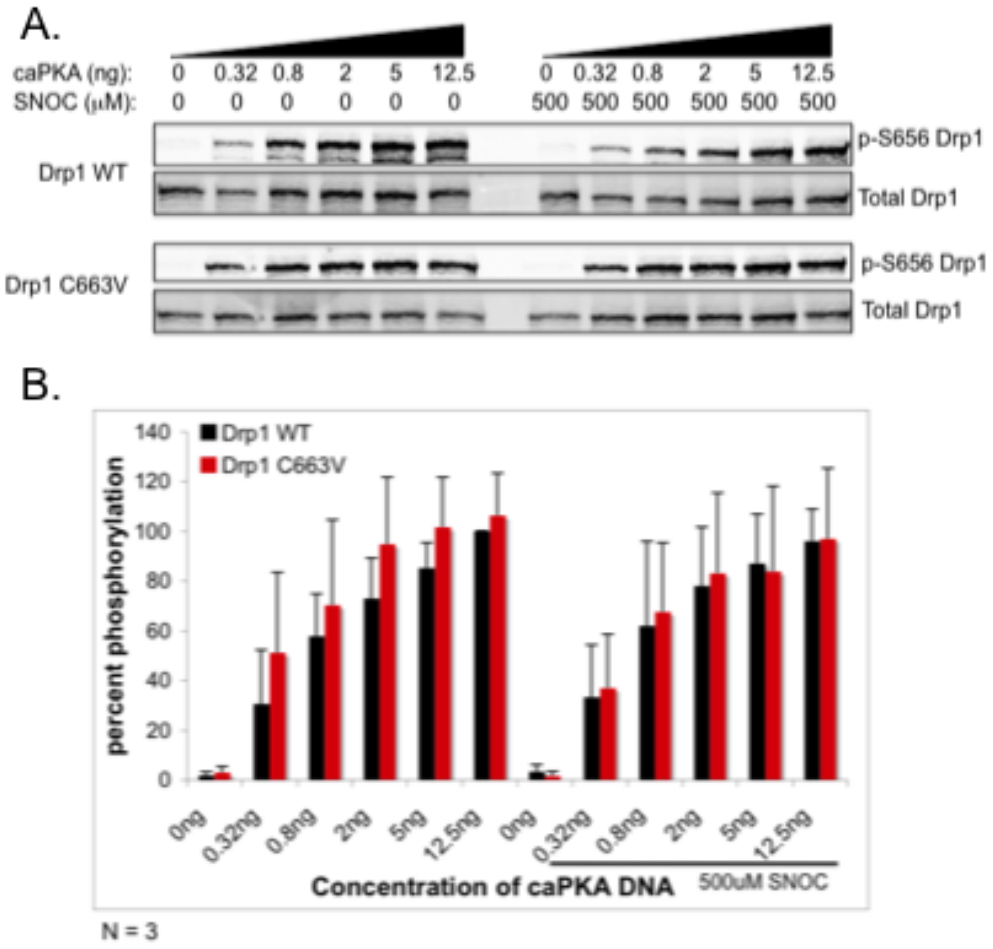

Figure 3.9 Direct nitrosylation of Drp1 has no effect on Ser656 phosphorylation by constitutively active PKA.
A. Representative blot showing Cos 1 cells expressing wild type or Cys663Val Drp1 along with constitutively active PKA (caPKA) in the presence or absence of SNOC. ***B.*** Quantification of three independent experiments shows that caPKA induces a dose dependent increase in Ser656 phosphorylation that is independent of the availability of Cys663 to be nitrosylated. Treatment of the cells with SNOC results in no change in Ser656 phosphorylation.

CHAPTER IV: CHARACTERIZATION OF A NOVEL E3 UBIQUITIN LIGASE COMPLEX THAT TARGETS PP2A B'β FOR DEGRADATION

Introduction

The regulation of protein function within the cell can take the form of many different types of posttranslational modifications. The most common and well studied is the on/off regulation of protein activity by direct (de)phosphorylation by kinases and phosphatases. The termination of protein activity often occurs through regulated protein degradation, where the substrate protein is tagged with mono or polyubiquitin and targeted for degradation by the proteasome. While previous work in the lab has focused on identification of target substrates, and determining downstream consequences of phosphatase activity, now the focus has shifted to understanding how PP2A itself is regulated. To this end, we performed a proteomic screen to identify novel interacting partners of PP2A B'β. HEK293 cells expressing Flag B'β were IP'd using FLAG conjugated beads and the lysates were subjected to liquid chromatography followed by tandem mass spectrometry (LC-MS/MS). This technique identified KLHL15 and Cul3 as specific interactors of B'β that did not interact with any other PP2A subunit.

Ubiquitination

Proteins are targeted for degradation through the addition of the 76 amino acid ubiquitin moiety onto lysine residues, which often directs the modified protein to the 26S proteasome. Ubiquitin molecules are added to the protein in a stepwise fashion by three classes of proteins; the E1 ligase activates the ubiquitin molecule, transferring it to the E2 ubiquitin-conjugating enzyme, which interacts with an E3 ubiquitin ligase. E3 ligases are either HECT domain proteins, which are able to directly ubiquitinate the substrate, or RING finger proteins,

which serve as a scaffold to bring the E2 in close proximity to the protein substrate (Petroski & Deshaies, 2005, Rotin & Kumar, 2009). The activity of the E3 ligase can serve to add one molecule of ubiquitin onto the substrate (monoubiquitination), one ubiquitin on multiple lysines of the substrate (multiubiquitination), or form ubiquitin chains through the conjugation of additional ubiquitins onto internal lysines of the original ubiquitin molecule (polyubiquitination) (Rotin & Kumar, 2009).

Cullins

One family of Ring domain E3 ligases is the Cullin family, composed of seven members (1, 2, 3, 4A, 4B 5, and 7) that act as scaffolds for various E2 enzymes and adaptor molecules. Each Cullin (Cul) contains a N-terminal adaptor binding domain, and a C-terminal Ring binding domain that interacts with the E2 ubiquitin conjugating enzyme, often called ROC1 or Hrt1 (Petroski & Deshaies, 2005). Adaptor molecules, which confer substrate specificity to the activity of Cullins, have been identified for many of the Cullins. Skp1 was identified as an adaptor connecting the substrate binding Fbox protein to the E3 ligase activity of Cul1/7. Cul2/5 bind Elongin C, which then interacts with SOCS proteins to convey substrate specificity. Unique among the family members are Cul3 and Cul4 that interact with BTB/Kelch and DDB1 proteins respectively, which are able to bind both the Cullin ligase and substrate through different domains within a single protein.

Kelch domain containing proteins

KLHL15 is a recently identified kelch protein containing a N-terminal BTB (broad-complex, tramtrack and bric a brac) domain a flexible linker BACK (BTB and C-terminal Kelch) domain, and a C-terminal kelch repeat domain (Yoshida, 2005). BTB domains are important for self-association of other BTB/Kelch

proteins, as well as interaction with Cul3 (Chen, et al, 1995, Perez-Torrado, et al, 2006, van den Heuvel, 2004). Previous groups have demonstrated the requirement of kelch domain protein dimerization for Cul3 mediated ubiquitination of the target substrate (McMahon, et al, 2006). The C-terminal kelch domain forms a seven blade β-propeller that conveys substrate specificity (Adams, et al, 2000, Rondou, et al, 2008). KLHL15 joins a family of kelch domain containing proteins that serve as adaptor molecules linking the Cul3/Hrt1 E3 ubiquitin ligase complex to the specific substrate (Pintard, et al, 2004).

Tyrosine Hydroxylase dephosphorylation by PP2A B'β

Tyrosine hydroxylase (TH), the rate-limiting enzyme in catecholamine synthesis, is activated by PKA induced phosphorylation of Ser40 (Haycock, 1990, Lew, et al, 1999). Previous work in the Strack lab showed that PP2A B'β specifically dephosphorylates TH on Ser40, leading to enzyme inactivation resulting in decreased dopamine synthesis (Saraf, et al, 2007, Saraf, et al, 2010).

The focus of this research was to characterize a novel E3 ubiquitin ligase complex through the identification of residues in the BTB domain of KLHL15 that are responsible for self association and interaction with Cul3, in the kelch domain that are required for substrate binding, and in PP2A B'β that mediate binding to the complex. The goal is to identify mutations that would enhance the interaction between PP2A B'β and the E3 complex, destabilizing the phosphatase, leading to enhanced activation of target substrates, specifically TH. Rational drug design could then be used to decrease PP2A B'β stability leading to increased dopamine synthesis.

Materials and Methods

Cell Culture and Constructs

Cos 1 (Gluzman, 1981) were cultured (37^{o}C, 5% CO_2) in RPMI 1640 (Gibco) containing 10% fetal bovine serum (heat inactivated).

The cDNA from KLHL15 was cloned using RTPCR from HEK 293T cells using the forward primer CAG CTC GAG CAG GGG ACG TGG AAG GAT TCT G and the reverse primer GTG CAA TTG TCA TTA GTT GCA ACG CCT GAC C. The cDNA was then cloned into the pEGFP C1 (Invitrogen) or pEGFP -3HA using the XhoI and MfeI restriction sites. The V5 tag was inserted between the KLHL15 DNA and the GFP tag at the BsrGI and XhoI sites using the oligo GTA CAA GTC TCG AGG AAA GCC AAT TCC TAA TCC TCT GCT CGG GCT CGA CAG CAC TGG AAG TGG TAA ACC GAT CCC AAA CCC GCT TCT AGG TCT GGA TTC TAC AGG. Site directed mutagenesis was carried out following the Quick Change (Stratagene) whole plasmid PCR protocol. pEGFP C1-KLHL15 was used as a template to generate the following mutations (Asp32Ala, His45Leu, IleLeuLys72AlaAlaAla, Arg318Glu, Glu335Arg + Leu337Ala, Glu371Arg, ArgAsp389AlaAla, and GluAsnLys567LysAspGlu) and the truncation mutant Δkelch. HA B'β (McCright & Virshup, 1995) (a gift from DM Virshup) and FLAG B'β (Van Kanegan, et al, 2005) were used as templates for generating point mutations (His45Gln, Tyr52Ser, 52SerGlnGlyLysProIle). Design of the FLAG B'β truncation mutants (Δ1-30, Δ1-65, Δ475-497 and Δ486-497) is described elsewhere (Saraf, et al, 2010). KLHL1 (Nemes, et al, 2000) was a generous gift from Michael Koob (University of Minnesota).

Antibodies

Antibodies commercially available are as follows: GFP (Abcam (rabbit) and NeuroMab (mouse), V5, EZ-View anti HA and anti FLAG conjugated beads

(Invitrogen), HA (Santa Cruz), FLAG (Cell Signaling). B'β and B'ε serum was a gift from DM Virshup. Secondary antibodies include goat αRabbit IR800, goat αMouse IR800, goat αRabbit IR680, and goat αMouse IR680 (Licor, Lincoln, NE).

Immunoprecipitation

Cos1 cells were plated at 300,000 cells/mL media in a 6 well plate and were transiently transfected the same day with either pEGFP C1 KLHL15 constructs or KLHL1 along with HA KLHL15 constructs, HA Cullin, or FLAG B' subunit constructs using 0.6% Lipofectamine 2000 (Invitrogen). 40 hours post-transfection cells were washed with PBS and harvested in Digitonin Buffer (50 mM Tris HCl, 150 mM NaCl, 1 mM EDTA, 1 mM EGTA, 1 mM benzamidine, 10 μg/mL (20 μM) leupeptin 250 μM PMSF and 1 mM DTT) containing 500 μg/mL digitonin. Soluble protein was IP'd with 10 μL conjugated beads (either HA or FLAG) in digitonin buffer to which 1% Triton X 100 was added for 2.5-3 hours. Beads were washed two times in IP Kinase Buffer (1% Triton X 100, 150 mM Tris HCl, 300 mM NaCl, 1 mM EDTA, 1 mM EGTA, 1 mM benzamidine, 10 μg/mL (20 μM) leupeptin, 1 mM β-glycerolphosphate, 2.5 mM sodium pyruvate, and 250 μM PMSF), extracted in SDS Sample Buffer, subjected on SDS PAGE and transferred to nitrocellulose membrane for western blotting. Images were generated using the Odyssey Imaging System (Licor, Lincoln, NE).

Co-expression Assays

Cos1 cells were plated at 300,000 cells/mL media in a 24 well plate and were transiently transfected the same day with HA or FLAG tagged B' subunits (α, β, γ, δ, ε), along with pEGFP KLHL15 or KLHL1 using 0.6% Lipofectamine 2000 (Invitrogen). In order to look at the requirement of Cul3 in the degradation of B'β HA Cullin constructs (Cul2, Cul3 or Cul3 ΔROC) were transiently

transfected with FLAG tagged B'β or B'ε along with pEGFP KLHL15 or KLHL1. 40 hours post transfection cells were washed one time with PBS and lysed in 1X Sample Buffer followed by sonication, and boiling. Samples were subjected to 10% SDS PAGE and transferred to nitrocellulose membranes for western blotting. Images were generated using the Odyssey Imaging System (Licor, Lincoln, NE).

Quantitative of protein expression

Images were captured using the Odyssey Imaging System, and the quantification of band intensities was calculated using Image J software. To determine the relative intensities of each subunit, the B' subunit band was divided by the KLHL band to control for loading differences. Then the ratio of B' subunit expressed in the presence of KLHL15:KLHL1 was calculated to determine the relative expression of each subunit in the presence of KLHL15.

Results

The BTB domain of KLHL15 is required for self-association

The N-terminal BTB domain is important for both kelch domain protein dimerization as well as interaction with the E3 ligase Cul3. Previous work has demonstrated that dimerization of Keap1, a kelch domain protein, is imperative for binding to Cul3, and targeting its substrate Nrf2 for ubiquitin mediated degradation (McMahon, et al, 2006). To examine the importance of the BTB domain of KLHL15 for both dimerization and Cul3 interaction, mutations were made in three highly conserved residues (Figure 4.1A), Asp32Ala and His45Leu that were previously shown to be important for BTB protein self association

(Chen, et al, 1995) or IleLeuLys72AlaAlaAla that was predicted to disrupt the interaction with Cul3.

Self-association was examined by co-expressing HA KLHL15 full length or kelch domain only with GFP KLHL15 wild type, the BTB domain mutants, or ΔKelch, which contains the BTB and Back domains. Precipitation of full length HA KLHL15, but not kelch only, was able to co-precipitate all the GFP KLHL15 constructs examined except Asp32Ala (Figure 4.1B). Importantly, the ΔKelch mutant still associated with full length HA KLHL15. These results suggest that the BTB domain of KLHL15 is both necessary and sufficient for self-association and requires residue Asp32, but not His45 or IleLeuLys72.

The KLHL15 BTB domain mediates the interaction with Cul3

Next I wanted to verify that the BTB domain is required for binding the E3 ubiquitin ligase. Specifically I wanted to show that Cul3, but not Cul2, is able to interact with KLHL15. Cos 1 cells co-expressing GFP KLHL15 or KLHL1 along with HA Cul2, Cul3 or Cul3 ΔROC (this mutant disrupts the interaction between Cul3 and E2 conjugating enzymes (Pintard, et al, 2004)) were IP'd using HA conjugated beads. Results show only Cul3 and Cul3 ΔROC are able to precipitate out both KLHL 15 and KLHL1 (Figure 4.2A). Not surprisingly, expression of the Cul3 ΔROC resulted in greater stability and IP of both the Cul3 and KLHL proteins, due to the loss of substrate ubiquitination. Taken together these results suggest that KLHL15 and Cul3 exist in a complex in cells.

In order to identify which BTB domain residues are required for the interaction between KLHL15 and Cul3 I used the BTB domain mutants described above, as well as a kelch domain mutant (Arg318Glu) described elsewhere. IP of HA Cul3 was able to specifically pull-down all the KLHL15 constructs examined,

though there was a 40% decrease of interaction with the His45Leu, IleLeuLys72AlaAlaAla, and Arg318Glu mutants (Figure 4.2B). The HA Cul3 ΔROC co-precipitated all the GFP KLHL15 constructs expressed except the IleLeuLys72AlaAlaAla mutant (Figure 4.2C). The inconsistency of these results could be due to variation in protein expression, or loss of a secondary interaction that further stabilizes complex formation. The disruption of KLHL15::Cul3 ΔROC complex with the IleLeuLys72AlaAlaAla mutant has been confirmed in multiple independent experiments leading to the conclusion that this residue is important for the direct interaction between Cul3 and KLHL15.

KLHL15 specifically targets B'β for degradation

KLHL15 was identified in large scale FLAG IPs of B'β, but not the A or C subunit (unpublished data). In order to determine whether the interaction of KLHL15 was specific for B'β, or universal for all B' subunits, we monitored the degradation of B' subunits following KLHL15 overexpression. Co-expression of KLHL15 and HA B' subunits resulted in a 60% decrease in B'β expression while other subunits showed no change in expression, when compared to co-expression with KLHL1 (Figure 4.3A). These results suggest KLHL15 induces degradation of B'β but not of other B' subunits (α,δ,γ,ε). To show that the degradation of B'β was due to an interaction with KLHL15, FLAG B'β or B'ε, were used to Co-IP GFP KLHL15 or KLHL1. The interaction between B'β and KLHL15 was shown to be specific as B'β was able to pulldown KLHL15 but not KLHL1 (Figure 4.3B), while B'ε did not pulldown either KLHL protein (Figure 4.3C). These results suggest that the degradation of B'β is due to the specific interaction between KLHL15 and B'β.

KLHL15 mediated degradation of B'β requires Cul3

To verify that the KLHL15 mediated degradation of B'β occurs through the formation of an E3 ubiquitin ligase complex with Cul3, co-expression tests were performed. FLAG B'β was co-expressed with GFP KLHL1 or 15 and HA Cul2, Cul3 or Cul3 ΔROC. Degradation of B'β occurred only when both KLHL15 and Cul3 were co-expressed, but not when expressed with Cul2 or Cul3ΔROC and not when KLHL15 was replaced with KLHL1 (Figure 4.3D). These results suggest that KLHL15 and Cul3 form an E3 ubiquitin ligase complex that specifically targets B'β for degradation.

KLHL15 binds to the N-terminal portion of B'β

Once it was determined that KLHL15 binds to and degrades B'β but not the other B' subunits, examination of the B' subunit sequence alignment showed low sequence conservation in the N-terminal and C-terminal portions of the B' subunits. Previously subcloned N and C-terminal truncation mutants (Saraf, et al, 2010) were used to narrow down possible binding regions (summarized in Figure 4.4B). Co-expression of KLHL15 with B'β wild type and B'β Δ1-30 showed a 75% decrease in protein expression compared to expression with KLHL1, while the B'β Δ1-65 showed no difference in expression (Figure 4.4A). In order to rule out additional binding sites in other portions of the protein, a pEGFP B'β C-terminal construct was co-expressed with either KLHL15 or KLHL1, which showed equal expression in the presence of both KLHL proteins (summarized in Figure 4.4B).

Next Co-IP assays were performed to determine which of the B'β truncation mutants were capable of specifically interacting with KLHL15. FLAG B'β constructs (wild type, Δ1-30, Δ1-65, and Δ475-497) were co-expressed with pEGFP KLHL15. Similar to the co-expression data, B'β wild type, Δ1-30 and Δ475-497 were able to specifically pullout KLHL15, while Δ1-65 was not (Figure

4.4C). These results suggest that the N-terminal portion, specifically residues 31-65, are necessary to bind KLHL15, leading to the degradation of B'β.

Scrutiny of the B'β sequence between residues 31-65 showed a high degree of sequence conservation not only among B'β homologs, but also amongst B' subunits (Figure 4.5A). In B'β His45 is conserved among homologs, but is replaced by a Gln in B'ε. Additionally, the YQSNQQ in rat B'β is SQGKPI in B'ε suggesting these residues might be important for mediating specific protein interactions. FLAG B'β His45Gln and Tyr52Ser were co-expressed with GFP KLHL15 and then IP'd using FLAG beads. The His45Gln interacted with KLHL15 in a manner similar to wild type B'β, while the Tyr52Ser mutation completely disrupted the interaction (Figure 4.5B). Taken together, the results from these co-expression and co-immunoprecipitation assays help to map the requirement of the N-terminal region of B'β, specifically residue Tyr52, for the interaction with KLHL15.

KLHL15 interacts with B'β in the holoenzyme

To identify all of the components of the KLHL15:Cul3 complex it is important to determine whether KLHL15 degrades the PP2A holoenzyme or just the B'β regulatory subunit. To address this question I focused on whether B'β can simultaneously interact with the PP2A core enzyme and KLHL15. Cos 1 cells transfected with KLHL15 along with FLAG B'β wild type or mutants that disrupt association of the regulatory subunit with the PP2A core enzyme, LysArg103AspGlu, and SerSer367AspAsp or the ArgLys232GluAsp mutation as a control (unpublished data). Analysis of FLAG IPs reveal that KLHL15 is able to bind to all the B'β constructs independent of its association with the PP2A core enzyme (Figure 4.6A). Reciprocal IPs were then performed to look at the ability of KLHL15 to precipitate out B'β as well as the PP2A/c subunit as a measure of

holoenzyme inclusion into the KLHL15::Cul3 complex. Cells were transfected as described above and IP'd using V5 conjugated beads. Initial results demonstrate that KLHL15 is able to interact with B'β independent of its association in the PP2A holoenzyme, as B'β mutants that disrupt PP2A/c subunit interaction (KR103DE and SS367DD) can still be precipitated out with V5/GFP KLHL15 (Figure 4.6B). Furthermore, KLHL15 appears to interact with the PP2A holoenzyme in a B'β dependent manner, as PP2A/c is only precipitated out in the presence of wild type B'β (Figure 4.6C). Taken together these results suggest that KLHL15 can interact with both the free B'β as well as the holoenzyme associated B'β. However, association of KLHL15 and the PP2A holoenzyme depends on the presence of wild type B'β, further verifying that KLHL15 only binds B'β, and not other PP2A subunits.

B'β binds to the top of the KLHL15 Kelch Domain

Now that I have identified the region of B'β responsible for interacting with KLHL15, it was important to identify which residues in the kelch domain were required for the interaction. Sequence alignment of multiple kelch domain containing proteins identified multiple non-conserved residues located on the top of the KLHL15 β-propeller structure (Figure 4.7B,C) marking them as possible substrate binding sites. Mutations of these sites (GluAsnLys567LysAspGlu, Arg318Glu, Glu335Arg Lys337Ala, and Glu371Arg) converted the KLHL15 residue into the equivalent residue from another family member. Cells expressing FLAG B'β and GFP KLHL15 wild type or kelch domain mutants were co-expressed and then IP'd using FLAG conjugated beads. Results show that all the kelch domain mutants disrupt binding to B'β (Figure 4.7A). These results suggest that the top of KLHL15 forms a binding surface, or possibly a pocket into which B'β binds.

KLHL15::Cul3::B'β exist as a complex *in vivo*

While we know that the degradation of B'β requires the presence of both KLHL15 and Cul3, it is important to determine if all three exist in a complex in intact cells. Since the purpose of the KLHL15:Cul3 complex, we believe, is to mediate ubiquitination and degradation of B'β I chose to use the Cul3 ΔROC mutant that should be able to form the proper complex, without ubiquitinating the substrate (Pintard, et al, 2004). Cos1 cells were transfected with HA Cul3 ΔROC, FLAG B'β, and GFP KLHL15 wild type, BTB domain mutants (Asp32Ala, His45Leu, IleLeuLys72AlaAlaAla), or kelch domain mutants (Arg318Glu and Glu371Arg). First I used HA conjugated beads to pullout HA Cul3 ΔROC, and looked for specific interactors. HA Cul3 ΔROC was able to precipitate B'β with wild type KLHL15, Asp32Ala and His45Leu, but not the Cul3 ΔROC binding disruption mutant (IleLeuLys72AlaAlaAla) or the kelch domain mutants (Arg318Glu and Glu371Arg) (Figure4.8A). Next I performed the reciprocal immunoprecipitation, pulling out FLAG B'β and looking for interacting partners. FLAG B'β is able to pull-down wild type GFP KLHL15 and the BTB mutants (Asp32Ala, His45Leu, IleLeuLys72AlaAlaAla), but not the kelch domain mutants (Arg318Glu and Glu371Arg) (Figure 4.8B). Cul3 ΔROC is only precipitated in the presence of wild type KLHL15 but not with any of the KLHL15 mutants (Figure 4.8B). Together these results suggest 1) that a complex consisting of KLHL15, B'β, and Cul3 exists in cells, and 2) unlike other BTB domain containing protein, KLHL15 dimerization is dispensable for proper protein function (Kim, et al, 2005, McMahon, et al, 2006, Zhuang, et al, 2009, Zipper & Mulcahy, 2002).

Discussion

Characterization of the KLHL15 BTB domain

The BTB domain was initially characterized as a protein self-association domain (Chen, et al, 1995, Robinson & Cooley, 1997). Indeed the self-association of substrate adaptors has long been thought to be required for the formation of the Cul3:kelch domain protein complex (McMahon, et al, 2006, Robinson & Cooley, 199, Kim, et al, 2005, Zhuang, et al, 2009, Zipper & Mulcahy, 2002). Using site-directed mutagenesis, based on dimerization disrupting mutations in other BTB domain containing proteins (Chen, et al, 1995) I was able to characterize the role of the KLHL15 BTB domain in self-association and its interaction with Cul3.

The BTB domain of KLHL15 was found to be both necessary and sufficient for protein self-association, with a specific requirement for the presence of Asp32 (Figure 4.1B). Analysis of the role of the BTB domain in mediating the interaction with Cul3 revealed that KLHL15 dimerization is dispensable for Cul3 interaction, as both Cul3 and Cul3 ΔROC were able to interaction with the KLHL15 Asp32Ala mutant. Interestingly, the presence of the ROC1 binding domain influenced the ability of Cul3 to interact with KLHL15. When KLHL15 was co-IP'd with HA Cul3, all KLHL15 mutations disrupted the interaction to some degree (Figure 4.2B). However, when KLHL15 was co-IP'd with Cul3 ΔROC, the IleLeuLys72AlaAlaAla specifically and completely, disrupted the interaction, while the other mutations had no affect (Figure 4.2C). These conflicting results can be explained in two ways; 1) co-expression of KLHL15 with wild type Cul3 leads to degradation of both proteins within the complex. Therefore, maybe the variation in interaction is due to a variation in protein stability, rather than a true reflection on complex formation. This explanation is

unlikely given the relatively similar levels of protein expression between the two transfections. 2) It is possible that there are secondary interactions between the E2 conjugating enzyme and KLHL15 that enhance complex formation. The results from the KLHL15 Cul3 ΔRoc IPs suggest a direct interaction between Cul3 and the BTB domain (Figure 4.2C). However, it appears that the E2 conjugating enzyme may interact with other portions of KLHL15 (Figure 4.2B) thereby explaining the discrepancy between the results. Either way, these results verify the role of the KLHL15 BTB domain in self-association and interaction with the E3 ubiquitin ligase Cul3.

The N-terminal portion of B'β interacts with the KLHL15 kelch domain

Once we were able to determine that KLHL15 mediates the degradation of only B'β it was fairly easy to narrow down the binding domain to the N-terminal portion of the protein. Mutagenesis of the residues that were highly conserved in B'β but were absent in other B' subunits lead to the identification of Tyr52 as the residue required for the interaction between B'β and KLHL15.

The identification of Tyr52 as being indispensable for KLHL15 leads to some intriguing possibilities as to the potential phospho-regulation of PP2A B'β stability. *In silico* analysis implicates Tyr52 as a potential Tyr phosphorylation site. One possible scenario is that phosphorylation of Tyr52 disrupts the interaction between B'β and KLHL15:Cul3 complex, causing increased B'β stability, an increase in substrate (TH) dephosphorylation, and an overall decrease in dopamine synthesis. If B'β stability is indeed regulated by Tyr phosphorylation, then treating Parkinson's disease patients with a tyrosine kinase inhibitor, or a tyrosine phosphatase activator, while there would be many off-target effects, might result in an overall increase in dopamine synthesis.

When examining the kelch domain of KLHL15 the picture is a little murkier. Mutation of multiple residues on the outer face of the kelch domain all disrupt binding to B'β (Figure 4.7A). Protein threading models predict that most of the mutations, Arg318Glu, Glu335Arg Lys337Ala, and Glu371Arg, are on the top of the β-propeller suggesting the possibility that these residues form a binding pocket or surface into which the substrate binds (Figure 4.7B). Taken together these results suggest that B'β Tyr52 fits into a binding pocket at the top of the kelch domain. Disruption of the binding pocket, by mutations in the kelch domain, or to B'β Tyr52, result in complete loss of the interaction, increasing B'β protein stability.

The intriguing aspect of the kelch domain mutagenesis is that the GluAsnLys567LysAspGlu, residues predicted to be on the opposite side of the β–propeller (Figure 4.7B,C), also disrupt binding to B'β (Figure 4.7A). It is possible, based on the crescent-like shape of the B' subunit family (Xu, et al, 2006), that multiple regions of the KLHL15 kelch domain are important for substrate binding. However, analysis of B'β truncation mutants revealed that only one region of B'β binds KLHL15 making the dual binding scenario less likely. A second explanation of these results, may be that while the top of the kelch domain interacts with B'β, the other side interacts with another part of the PP2A holoenzyme, which is indirectly responsible for binding B'β. This possibility is unlikely based on the original identification of KLHL15 and Cul3 as specific interactors of B'β that did not interact with other PP2A subunits. The third possibility is that all the kelch domain mutants non-specifically disrupt kelch domain structure or function. The evidence against this possibility is that the KLHL15 kelch domain residues were mutated to match residues found in the same position in other kelch domain containing proteins. Overall, while it is

difficult to imagine how the KLHL15 GluAsnLys567LysAspGlu mutants disrupts binding to B'β it is clear that the kelch domain is important for B'β binding.

Future work should characterize additional kelch domain mutants, finding some that do not disrupt binding to B'β, though the identification of the binding pocket on KLHL15 that mediates the interaction with B'β Tyr52 is very promising. Manipulation of these residues should allow for specific regulation of B'β protein stability, modulating the levels of dopamine synthesis.

The novel KLHL15:Cul3 ubiquitin ligase complex mediates the degradation of PP2A B'β.

Based on the mutational analysis and IP data it is clear that KLHL15 is acting as a substrate adaptor, bridging the E3 ubiquitin ligase Cul3 with the substrate B'β. Based on mutations within the BTB domain, it appears that unlike previously described kelch domain proteins (McMahon, et al, 2006) KLHL15 self-association is dispensable for Cul3 interaction (Figure 4.2 B,C) and substrate binding (Figure4.7A). While the KLHL15 kelch domain mutants all disrupt the interaction with B'β to some degree, evidence suggests that B'β Tyr52 (Figure 4.5) interacts with the binding pocket created by KLHL15 Arg318, Lys335, Glu337 and Glu371 (Figure4.7), on the top of the kelch domain β propeller. Since the N-terminal portion of B'β is responsible for binding KLHL15, this leaves the C-terminal portion available for binding the PP2A core enzyme (Figure 4.6). These results open up the possibility that KLHL15 mediates the degradation of the PP2A B'β holoenzyme, as the interaction of KLHL15 and B'β is independent of the ability of B'β to bind the PP2A C subunit (Figure 4.6A,B), though the inclusion of the PP2A holoenzyme in the KLHL15::Cul3 complex is B'β dependent (Figure 4.6C).

The focus of this work was to identify residues in B'β and KLHL15 that mediate direct interaction and substrate degradation. Once these residues are identified, work can then shift to determining how regulation of the stability of PP2A B'β affects downstream substrate activity. To this end, we believe that increasing the interaction between KLHL15 and B'β using pharmacological Tyr phosphatase activators or Tyr kinase inhibitors or a Tyr52Phe phospho-ablating mutation should decrease protein stability, resulting in a downstream increase in TH Ser40 phosphorylation and a measurable increase in dopamine synthesis. In conclusion future work directed at the regulation of PP2A B'β protein stability, by modulating its interaction with the Cul3:KLHL15 complex, is a viable target for research directed at increased dopamine synthesis.

Table 3 Summary of KLHL15 mutant binding to interaction partners.

KLHL 15 Mutant	Domain Location	Self Association	Cul3	B'β
WT	- - -	dimerizes	YES	YES
Asp32Ala	BTB	disrupts	YES	YES
His45Leu	BTB	dimerizes	YES	YES
Ile72Ala, Leu74Ala, Lys75Ala	BTB	dimerizes	NO	ND
Arg318Glu	KELCH	dimerizes	YES	NO
Glu335Arg, Leu337Ala	KELCH	ND	ND	NO
Glu371Arg	KELCH	ND	YES	NO
ArgAsp389AlaAla	KELCH	ND	ND	ND
Glu518Arg	KELCH	ND	ND	ND
GluAsnLys567LysAspGlu	KELCH	ND	YES	YES

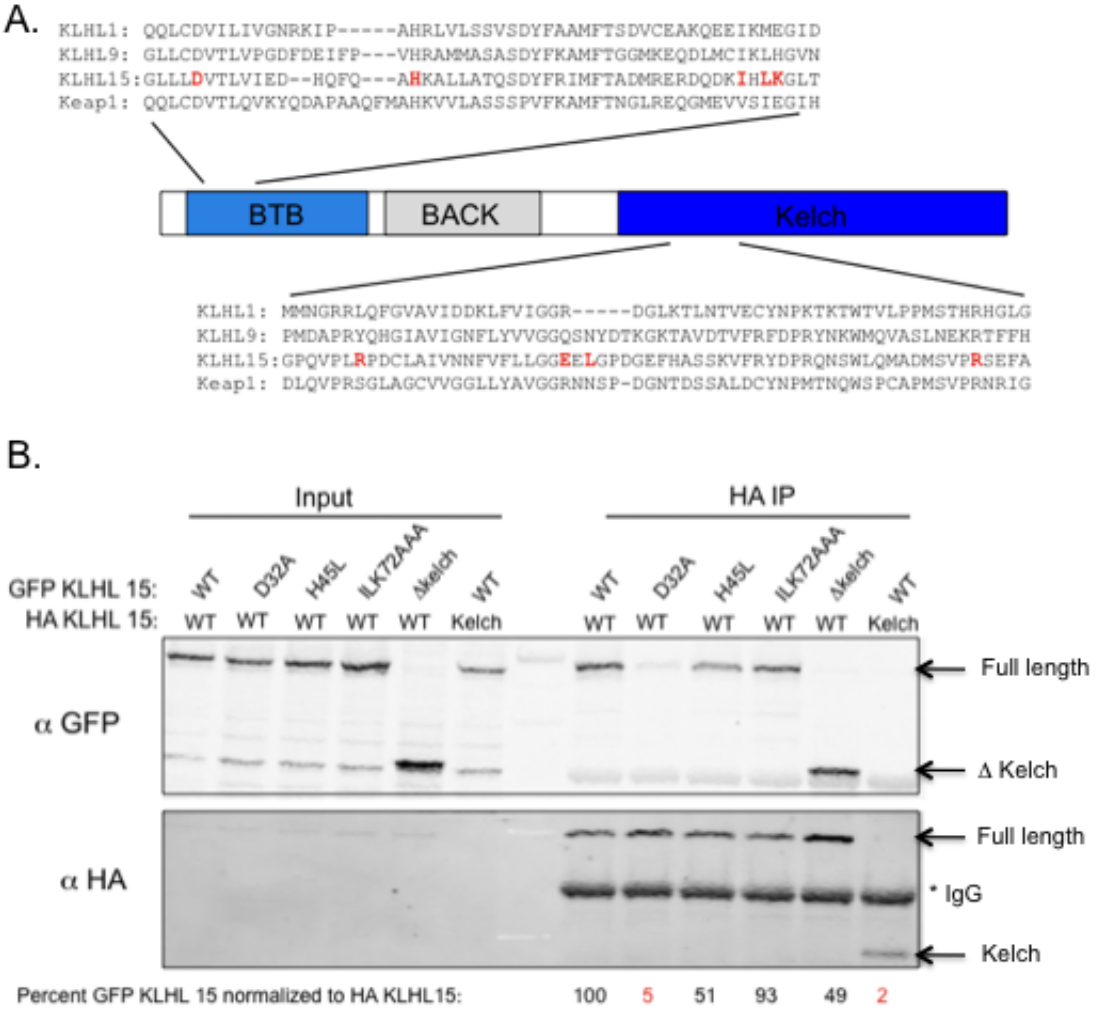

Figure 4.1 The N-terminal BTB domain of KLHL15 is both necessary and sufficient for protein self-association.
A. Structural domains of KLHL15 and the sequence alignment of the BTB and kelch domains of KLHL1, 9, 15 and Keap1. ***B.*** Residues previously identified to be important for BTB dimerization were mutated in the KLHL15 BTB domain. IP of HA full-length or Kelch domain only co-expressed with GFP KLHL15 wild type, BTB domain mutants, or the Δkelch domain. Results show that the BTB domain is necessary and sufficient for KLHL15 self-association and requires the Asp32 residue.

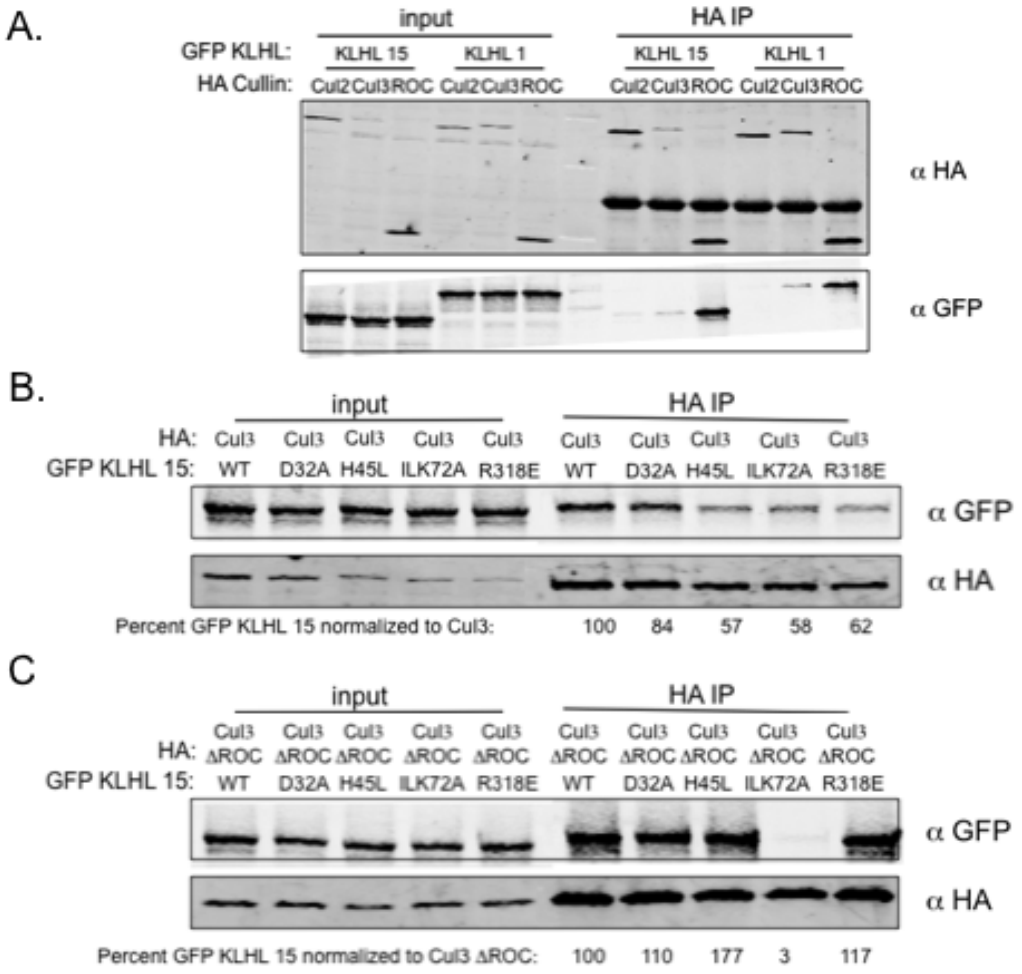

Figure 4.2 The BTB domain of KLHL15 interacts with the E3 ubiquitin ligase Cul3.
A. IP of HA Cul2, Cul3, or Cul3 ΔROC co-expressed with GFP KLHL15 or KLHL1 demonstrates that the N-terminal portion of Cul3 specifically interacts with both KLHL15 and KLHL1. ***B.C.*** IP of HA Cul3 (***B.***) or HA Cul3 ΔROC (***C.***) co-expressed with GFP KLHL15 wild type, BTB domain mutants (D32A, H45L, ILK72AAA) or Kelch domain mutant (R318E). Results reveal that KLHL 15 self-association is dispensable for Cul3. Cul3 is able to interact with all KLHL15 constructs, though there is a 40% decrease in binding with the H45L, ILK72AAA and R318E (***B.***). The Cul3 ΔROC construct is able to specifically interact with all the GFP KLHL15 constructs with the exception of ILK72AAA (***C.***).

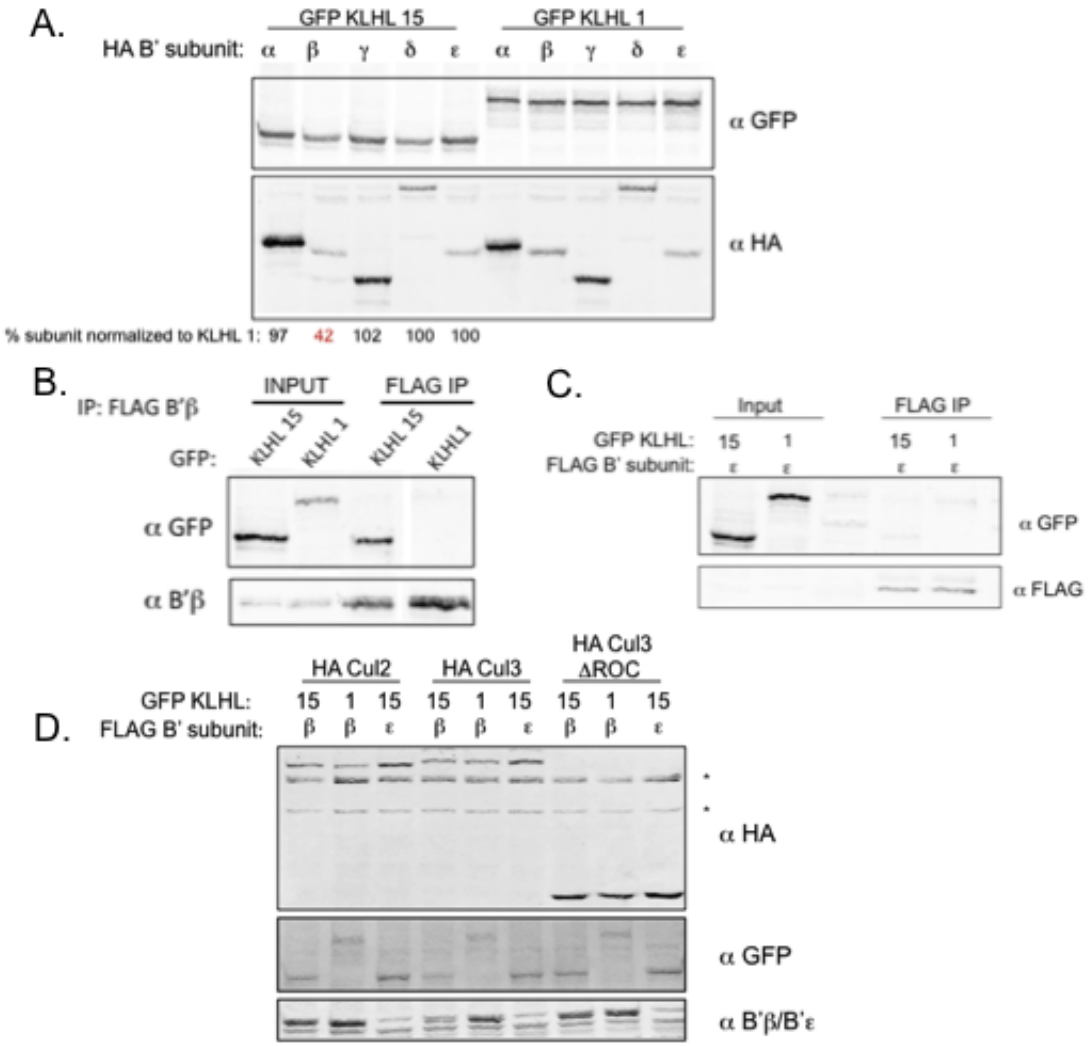

Figure 4.3 KLHL15 mediated degradation of B'β requires Cul3.
A. Co-expression of HA B' subunits with GFP KLHL15 or KLHL1 reveals that KLHL15 specifically degrades B'β, while having no affect on other B' subunits. ***B.C.*** IP of FLAG B'β (***B.***) or B'ε (***C.***) co-expressed with GFP KLHL15 or KLHL1 demonstrate that the KLHL15 mediated degradation of B'β is due to a specific interaction between KLHL15 and B'β. ***D.*** Co-expression of HA Cul2, Cul3, or Cul3 ΔROC with GFP KLHL15 or KLHL1 and FLAG B'β or B'ε shows that the KLHL15 specific degradation of B'b requires wild type Cul3.

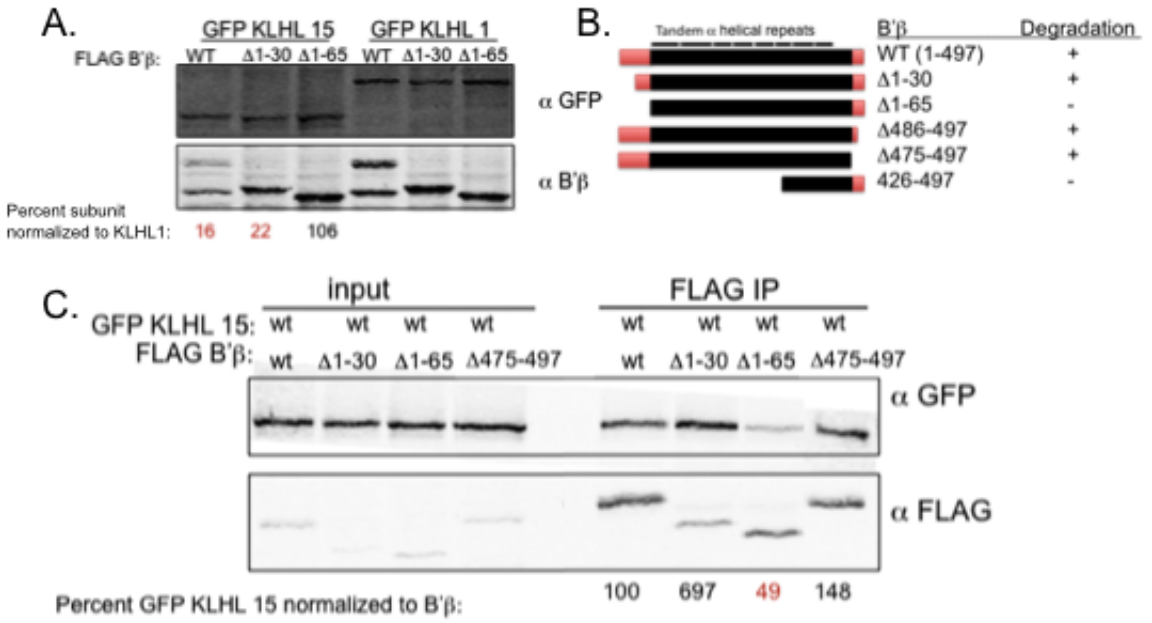

Figure 4.4 KLHL15 binds to the N-terminal portion of B'β to mediate degradation.
A. The region of B'β responsible for binding KLHL15 was examined by co-expressing B'β full length or N-terminal truncation mutants with GFP KLHL15. Analysis of B'β protein expression when co-expressed with KLHL15 revealed that both B'β full length and Δ1-30 are degraded while Δ1-65 remains unchanged. ***B.*** Summary of B'β N and C-terminal truncation mutant degradation when co-expressed with KLHL15. ***C.*** IP of FLAG B'β full length or truncation mutants co-expressed with GFP KLHL15. Results show KLHL15 interacts with full length, Δ1-30 and Δ475-497, but not the Δ1-65. Taken together these results suggest B'β residues 30-65 are required for interacting with KLHL15.

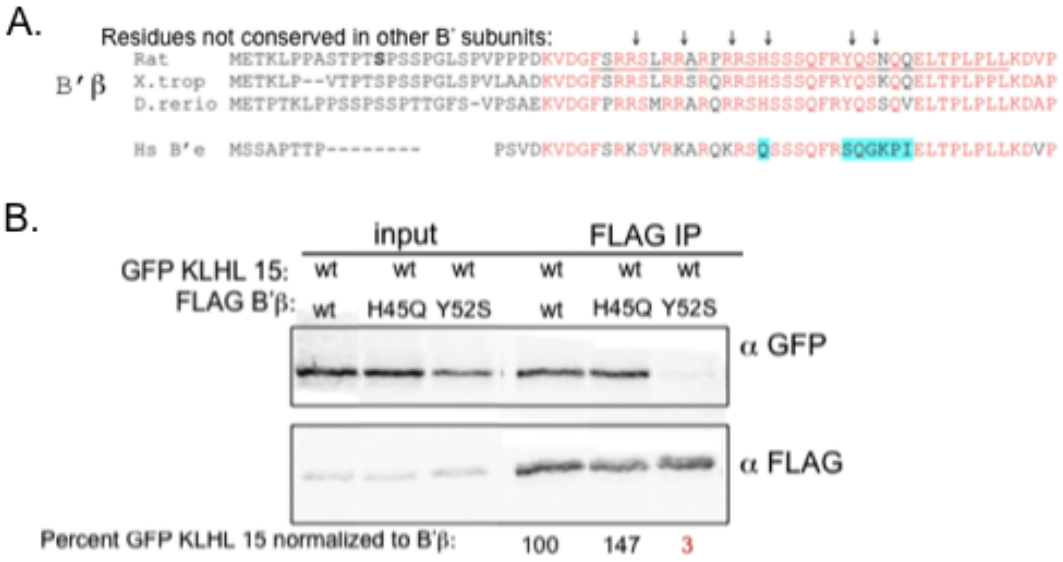

Figure 4.5 B'β Tyr52 is required for binding to KHLH15.
A. Analysis of the B'β orthologues reveals highly conserved residues that are absent in B'ε. These residues, His45 and Tyr52, were mutated to the equivalent residues in B'ε. ***B.*** IP of FLAG B'β wild type, His45Leu or Tyr52Ser co-expressed with KLHL15. Results show Tyr52 is required for binding KLHL15.

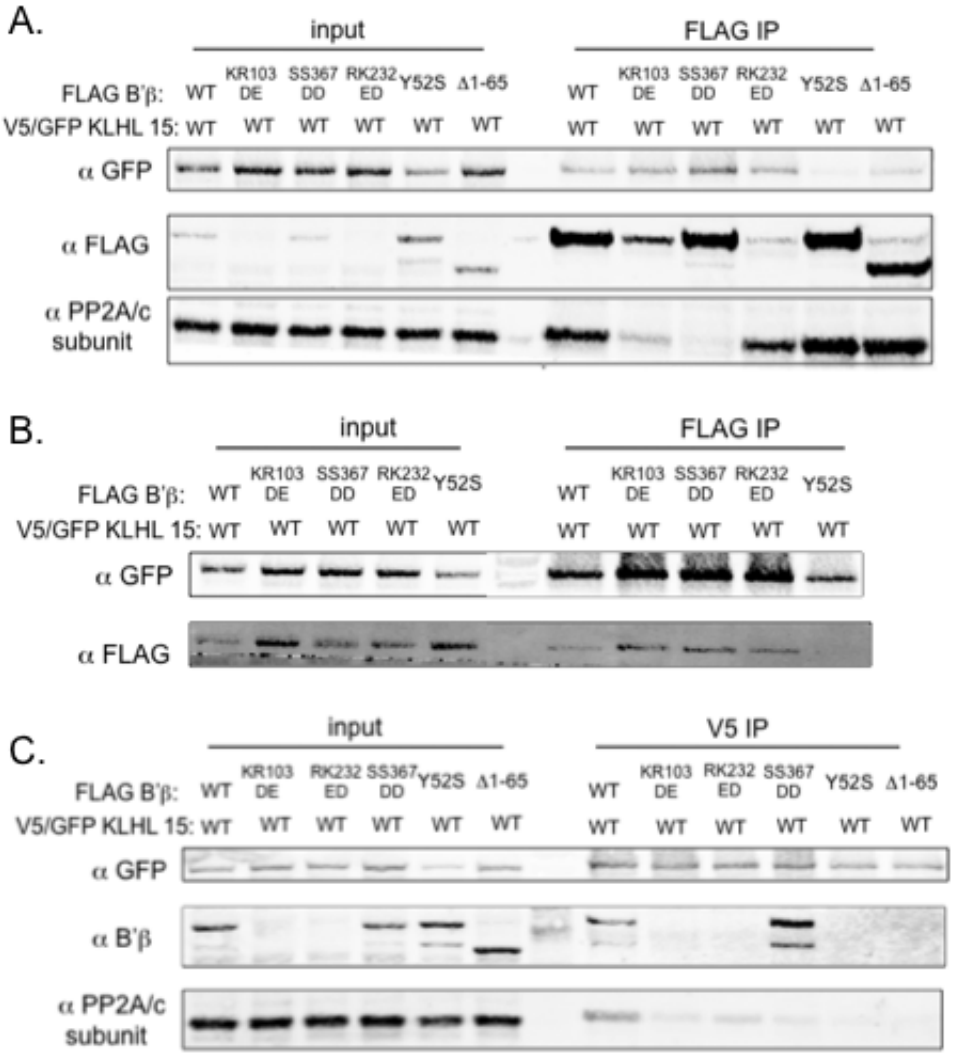

Figure 4.6 B'β in the PP2A holoenzyme binds to KLHL15.
Co-expression of V5/GFP KLHL15 with FLAG B'β wild type, holoenzyme disrupting mutants (LysArg103AspGlu, SerSer367AspAsp, and ArgLys232GluAsp as a control, (described elsewhere)) or the KLHL15 disrupting mutants Tyr52Ser and Δ1-65. ***A.*** FLAG IPs reveal that all B'β mutants still interact with KLHL15 independent of their inclusion in the PP2A holoenzyme. ***B.*** V5 IPs show that KLHL15 is able to interact with B'β independent of its inclusion in the holoenzyme. ***C.*** However, V5 IPs performed to examine the incusion of the PP2A holoenzyme show the C subunit is present in the complex in a B'β dependent manner as cells expressing B'β mutants that disrupt the association with the C subunit (SS367DD) fail to show interaction between KLHL15 and PP2A/c.

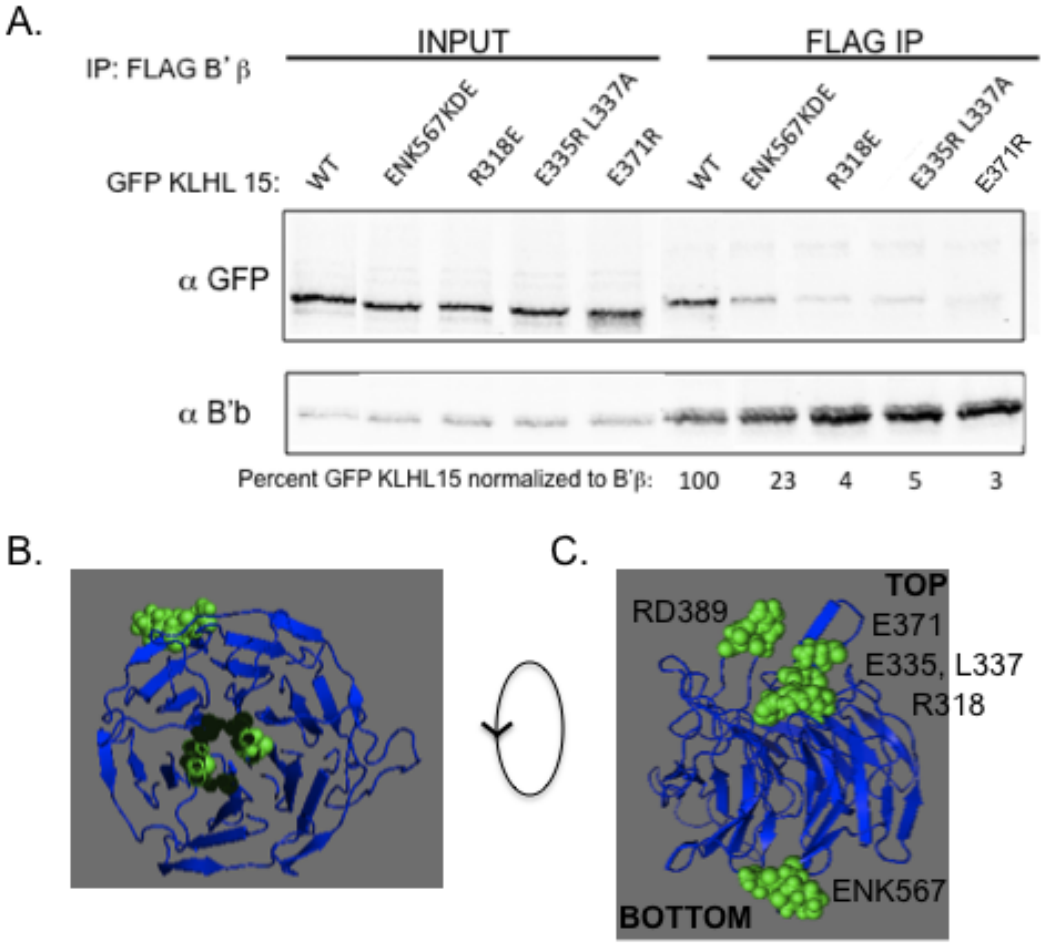

Figure 4.7 The top of the kelch domain of KLHL15 is responsible for binding B'β.
A. Mutations were made of residues that are present in the Kelch domain of KLHL15, but not other kelch domain proteins. IP of FLAG B'β co-expressed with GFP KLHL15 kelch domain mutants results in disrupted substrate binding with all mutants. These results suggest that the bottom face of the KLHL15 kelch domain is responsible for binding the substrate B'β. ***B.C.*** Model of the proposed structure of the KLHl15 kelch domain highlighting (in green) the residues that when mutated disrupt substrate binding. As all mutations lie on the bottom face of the β-propeller the results suggest these residues form a binding pocket or surface that interacts directly with B'β.

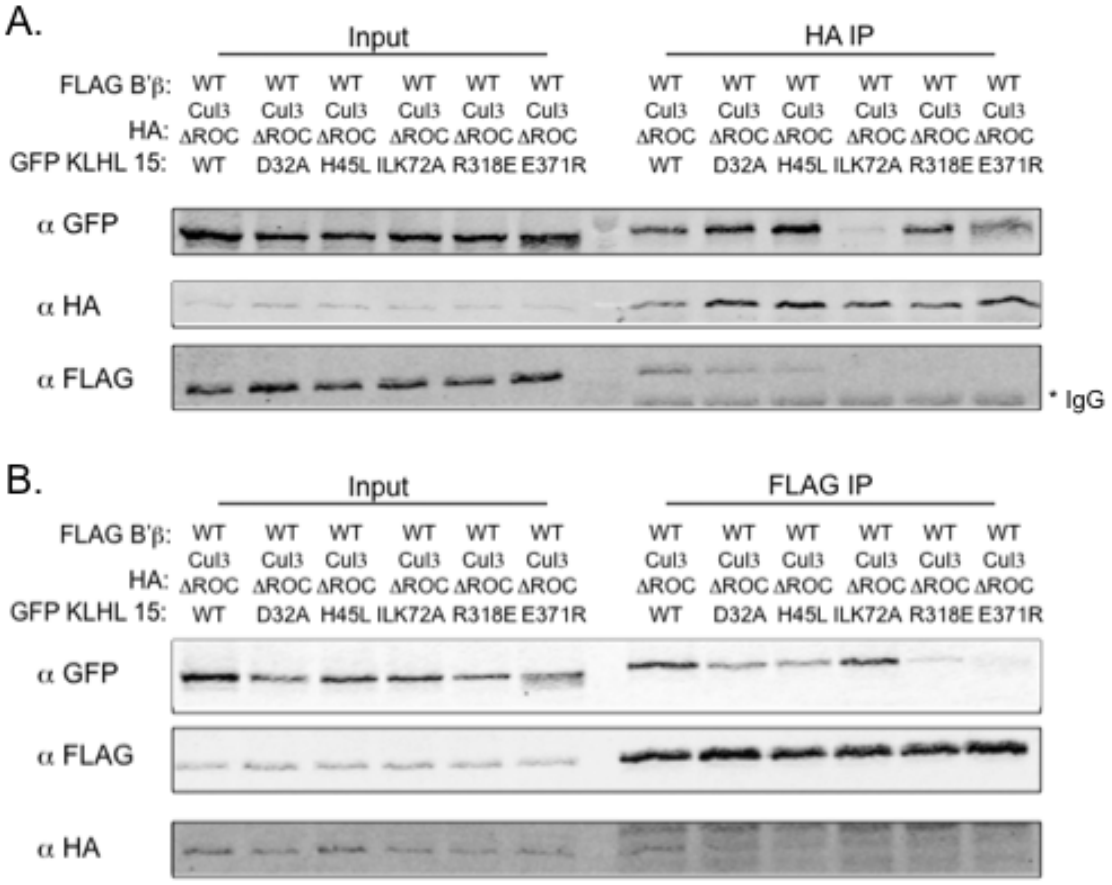

Figure 4.8 KLHL15 acts as a scaffolding, bridging the E3 ubiquitin ligase Cul3 and the substrate B'β in one complex.
Cos1 cells co-expressing HA Cul3 ΔROC, FLAG B'β and GFP KLHL15 wild type, BTB domain mutants (Asp32Ala, His45Leu, IleLeuLys72AlaAlaAla) or kelch domain mutants (Arg318Glu, Glu371Arg). ***A.*** HA IPs show only the BTB domain mutant IleLeuLys72AlaAlaAla disrupts KLHL15:Cul3 ΔROC binding. Analysis of the presence of FLAG B'β shows the substrate is present when co-expressed with KLHL15 wild type, Asp32Ala and His45Leu. ***B.*** FLAG IPs show the KLHL15 kelch domain mutants disrupt binding to B'β. HA Cul3 ΔROC is only present when co-expressed with wild type KLHL15.

CHAPTER V: CONCLUSIONS

Importance of mitochondrial function

Historically, mitochondria are best known for their role in being the "powerhouse of the cell." However, further insight into the function of the mitochondria has revealed important roles for this organelle in buffering calcium at the neuronal synapse (MacAskill & Kittler, 2010), participation in both autophagic and apoptotic cell death (Chen & Chan, 2009, Youle & Karbowski, 2005), as well as energy production through oxidative phosphorylation. Balanced mitochondrial morphology is key to maintaining proper mitochondrial function. Disruption of either mitochondrial fission or fusion results in dire consequences evident by the myriad of pathological disorders caused by mutations in mitochondrial fission and fusion proteins (Chang, et al, 2010, Palau, et al, 2009, Waterham, et al, 2007) as well as the contribution of mitochondrial dysfunction to many neurodegenerative diseases and cancer (de Moura, et al, 2010).

Involvement of phospho-regulation in maintaining mitochondrial function

The role of phosphorylation in regulating mitochondrial morphology has clearly been demonstrated by the identification of both activating and inactivating modifications on multiple residues of the mitochondrial fission protein Drp1 (Chang & Blackstone, 2007a, Cribbs & Strack, 2007, Han, et al, 2008). As inactivation of mitochondrial fission, by the PKA induced phosphorylation of Drp1 Ser656 (Chang & Blackstone, 2007a, Cribbs & Strack, 2007), is often balanced by the promotion of increased mitochondrial fusion, it was plausible that PKA induced phosphorylation of Mfn2 might in fact activate Mfn2 function (Chen, et al, 2004, Dimmer & Scorrano, 2006, Zhou, et al, 2010). In Chapter 2 I describe the characterization of Mfn2 Ser442 as a potential substrate for PKA

phosphorylation. What is clear from the analysis of direct PKA induced phosphorylation of Mfn2 on Ser442, as well as the requirement of Ser442 for PKA induced changes in mitochondrial morphology and neuroprotection, is that under the conditions studied Ser442 is not PKA phosphorylated. These results are in direct contention with recently published work describing the role of Mfn2 Ser442 in the anti-proliferative effects on Vascular Smooth Muscle cells (VSMC) (Zhou, et al, 2010). There are a number of hypotheses that can be formulated to account for the discrepancies between my findings and those of Zhou and colleagues. First, much of my work relied on cell culture model systems as well as the utilization of rat tissues, primarily the brain, while Zhou et al focused on the role of Mfn2 in the heart. It is possible that phosphorylation of Mfn2 is regulated in a tissue specific manner, due possibly to the presence (or absence) of a protein required for such regulation. Therefore it is possible Mfn2 Ser442 is PKA phosphorylated in the heart, and despite my initial examination (data not shown) I was unable to detect it. Second, it is possible that despite utilizing techniques previously employed by the lab to characterize the phosphorylation of substrate proteins I was unable to demonstrate a similar effect on Mfn2. Maybe phosphorylation of Mfn2 Ser442 is transient, or occurs in a small population of the protein pool, that the techniques described in Chapter 2 are not accurate or adequate enough to detect. Third, the role of Ser442 in regulating Mfn2 function is independent of its potential to be PKA phosphorylated. Examining the neuroprotective role of Mfn2 in hippocampal neurons demonstrated the requirement of Ser442, as either Ser442Ala/Asp mutant ablated any protective effect. Similarly, the phospho-ablating or phospho-mimicking mutations of Mfn2 have a profound effect on the proliferative function of Mfn2, while having no effect on inducing changes in mitochondrial morphology (Figure 2.5A,B and (Zhou, et al, 2010)). Taken together these results suggest Mfn2's anti-

proliferative and neuroprotective effects are not only separate from its function to promote mitochondrial elongation (Figure 2.5A,B and (Zhou, et al, 2010)) but also independent of PKA phosphorylation (Figure 5.1). However, the opposing effects of Ser442Ala and Ser442Asp on VSMC proliferation, hint at a possible role of phosphorylation (Zhou, et al, 2010). The final possibility is that Mfn2 is not PKA phosphorylated on Ser442. Despite the work of Zhou and colleagues, direct evidence of Mfn2 Ser442 phosphorylation has never been presented. This fact, along with the evidence provided in Chapter 2, strongly suggests that Mfn2 Ser442 is not PKA phosphorylated. Rather the evidence provided by Zhou et al, similar to my findings regarding the function of Mfn2 to promote neuroprotection (Figure 2.6), suggest a role of Ser442 in promoting Mfn2 function that is not related to its role in promoting mitochondrial fusion, and are independent of phosphorylation.

Involvement of independent modifications in regulating mitochondrial morphology

Given the identification of many types of posttranslational modifications on regulating Drp1 function (Figure 3.1) it was important to address the question of whether these modifications act dependently or independently to modulate Drp1 function. With the identification of Drp1 Cys663 as a nitrosylation site that activates Drp1 activity (Cho, et al, 2009) so close to the PKA phosphorylation site Ser656 that inactivates Drp1 function (Chang & Blackstone, 2007a, Cribbs & Strack, 2007), it was hypothesized that these modifications were mutually exclusive events (Figure 3.2). Evidence provided in Chapter 3 clearly demonstrates that blocking the ability of Drp1 to be nitrosylated, using a Cys663Val mutation, enhances the actions of PKA to induce Ser656 phosphorylation (Figure 3.5A) as well as to promote mitochondrial elongation

(Figure 3.3). However, direct nitrosylation of Drp1 results in no change in Ser656 phosphorylation (Figure 3.9), and is unable to block nitrosylation induced mitochondrial fragmentation (Figure 3.4). Once again, my findings were in direct contention with the previously published report, to which there are a few possible explanations. First, the methodology used by Cho et al (Cho, et al, 2009) to characterize the nitrosylation induced fragmentation was limited, and could have overlooked subtleties in the data. Characterizing mitochondria as either fragmented or not fragmented highlights only gross changes in mitochondrial morphology, rather than addressing the dynamic and highly varied shape and size of mitochondria under many conditions. The objective scoring methods used in Chapter 3 allow for the variation in morphology by classifying the mitochondria size, not just the presence or absence of fragmentation. Second, it is possible that our results are identical, however the data provided by Cho et al is itself fragmented, as they fail to show the length of mitochondria in neurons containing wild type Drp1 or the Cys663Ala under basal conditions. As demonstrated in Figure 3.3 and 3.4, the Cys663Val mutant causes elongation under basal conditions compared to wild type. Therefore, the increase in mitochondrial length following NO donor treatment may be due to a kind of buffering effect, where the elongated mitochondria are able to withstand the effects of increased NO longer, or just take longer to fragment, than smaller mitochondria. As Cho et al fail to provide mitochondrial length scores under basal conditions it is difficult to interpret their findings, in light of my results. Finally, it is clear not only from my data, but also from recently published findings that there is no functional consequence of Drp1 nitrosylation (Figure 5.1). While Drp1 is clearly nitrosylated *in vivo* following treatment of recombinant protein with NO donors, and in aged brains (Bossy, et al, 2010) there is no change in Drp1 activity following nitrosylation that results in a detectable change in function,

either directly, or through modulation of other Drp1 modifications, such as Ser656 or Ser635 phosphorylation.

Implications of regulated ubiquitination on PP2A B'β function

With the identification of the KLHL15:Cul3 ubiquitin ligase complex as novel interactors and regulators of PP2A B'β expression (Figure 5.1) come the intriguing possibilities of regulating phosphatase activity. The role of PP2A B'β in dephosphorylating and inactivating tyrosine hydroxylase, leading to decreased dopamine synthesis, has been clearly established (Saraf, et al, 2007, Saraf, et al, 2010). Identifying residues in B'β and KLHL15 that modulate the formation of the ubiquitin complex can lead to the development of small molecule targets. The residue that currently holds the most promise for pharmacological targeting is B'β Tyr52. Determining that the N-terminal portion of B'β interacts with KLHL15 (Figure 4.4) lead to the identification of the requirement of B'β Tyr52 (Figure 4.5) for the interaction to occur. Intriguingly, B'β Tyr52 has a high probability of being modified by tyrosine phosphorylation. These findings lead to a model in which the phosphorylation of B'β Tyr52 prohibits the interactions between B'β and KLHL15, leading to increased PP2A B'β stability (Figure 5.2). Therefore identifying small molecules that can specifically modulate phosphorylation of B'β Tyr52, without affecting other MAPK targets, could be a viable option in the treatment of Parkinson's disease.

Future work needs to focus on 1) demonstrating that B'β Tyr52 is indeed phosphorylated by tyrosine kinases, leading to increased PP2A B'β holoenzyme stability and 2) determining the role of mutations in B'β or KLHL15 that effect B'β:KLHL15:Cul3 on PP2A B'β substrate dephosphorylation, using the downstream dopamine synthesis as an output.

In conclusion, my thesis work has focused on the role of posttranslational modifications in regulating protein function (Figure 5.1). While I was unable to demonstrate that PKA phosphorylates Mfn2 on Ser442, this residue is clearly important for Mfn2 function that is unrelated to its role in maintaining mitochondrial morphology. Similarly, while Drp1 nitrosylation does not appear to be important for modulating Ser656 phosphorylation or GTPase activity (Bossy, et al, 2010), it is clear that the Cys663Val mutant modulates protein function, apparently by enhancing PKA induced inactivation of Drp1. These results suggest an important role of Cys663 in maintaining Drp1 function. More recently, the characterization of PP2A B'β as a target of KLHL15:Cul3 mediated ubiquitin dependent degradation opens the door for possible Parkinson's disease therapeutics by modulating PP2A B'β protein stability.

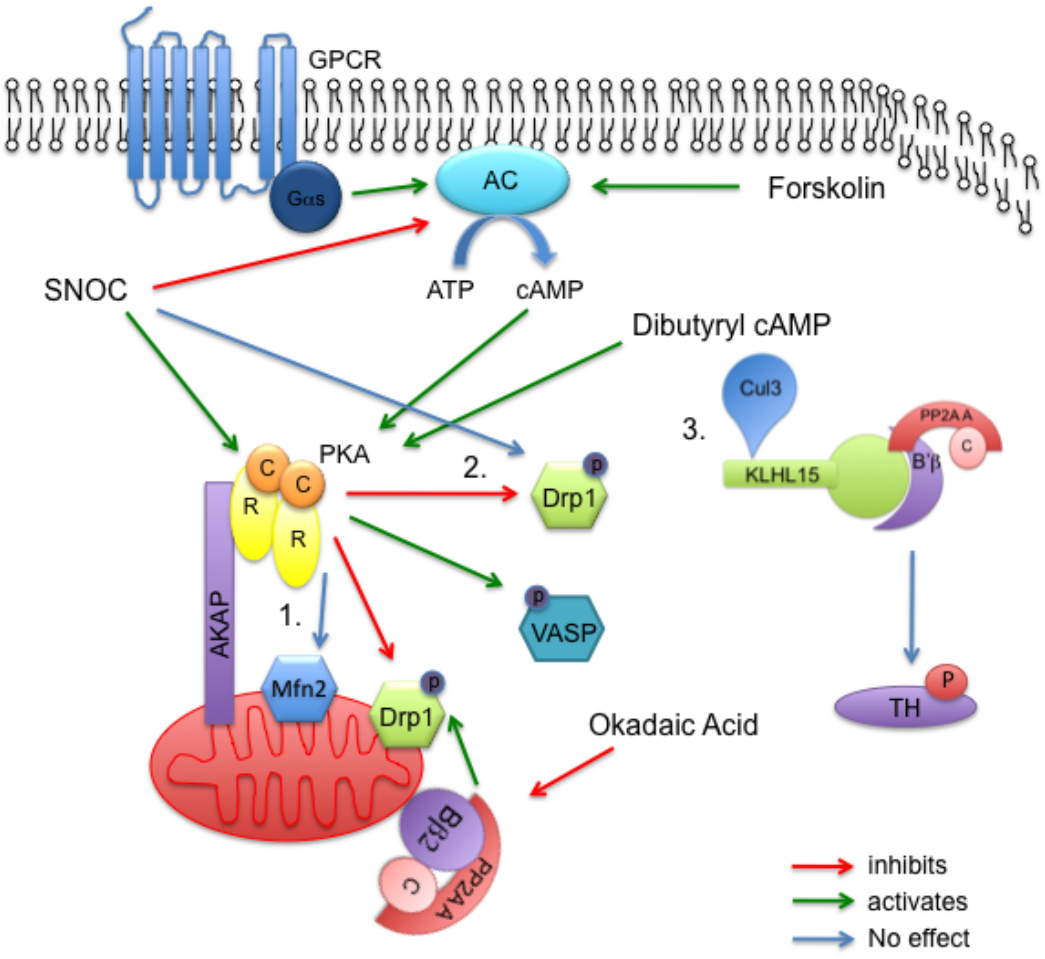

Figure 5.1 Model expanding the role of posttranslation modifications on regulating protein function, as concluded from experiments conducted herein.
Based on the results drawn from the experiments conducted in the previously discussed chapters, the following conclusions can be made; 1) Mfn2 Ser442 is important for protein function independent of mitochondria fusion and PKA phosphorylation; 2) Nitrosylation of Drp1 has no effect on PKA induced phosphorylation of Ser656, however Ser656 and Cys663 act in a similar manner to independently blunt Nitric Oxide induced mitochondrial fragmentation; 3) The formation of an E3 ubiquitin ligase complex containing Cul3, KLHL15 and PP2A B'β leads to downregulation of B'β, decreasing its ability to act on substrate proteins.

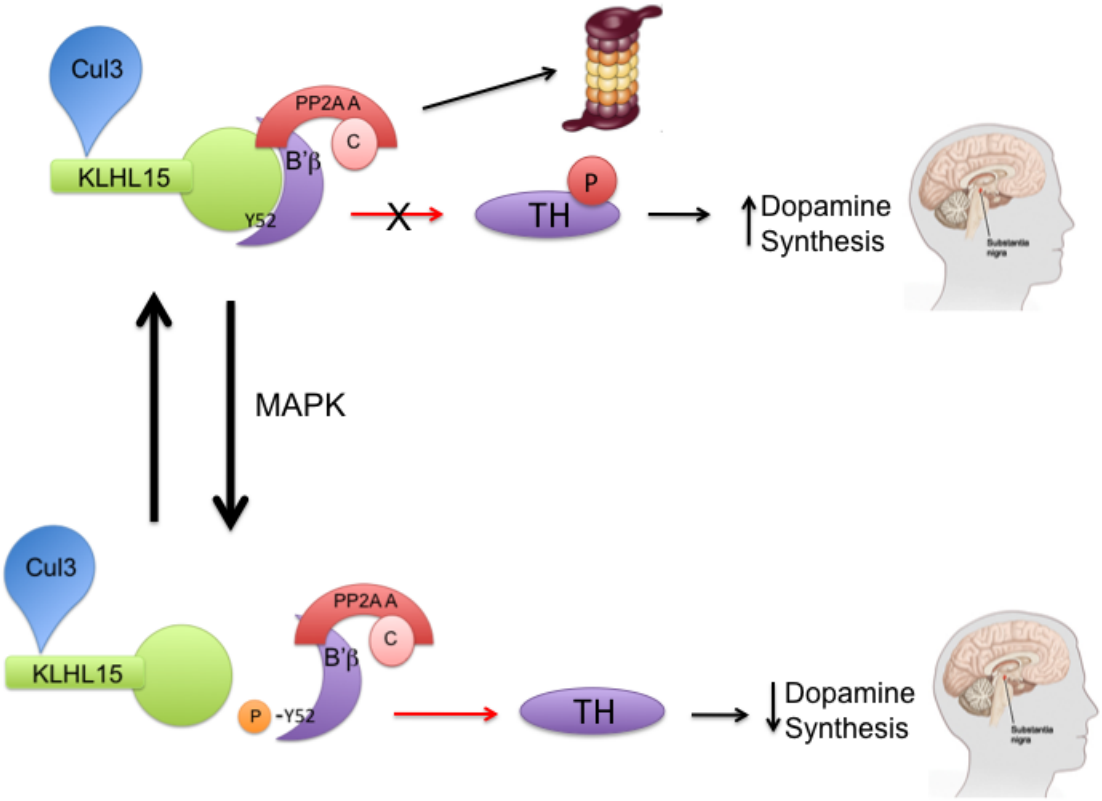

Figure 5.2 Model predicting the role of B'β Tyr52 MAPK phosphorylation in regulating PP2A B'β protein stability.
In a dephosphorylated state (top left) PP2A B'β interacts with the KLHL15:Cul3 ubiquitin ligase complex, leading to proteasomal degradation of the PP2A holoenzyme. Loss of PP2A B'β leads to maintenance of TH Ser40 phosphorylation and increased dopamine synthesis. The MAPK phosphorylation of B'β on Tyr52 is predicted to prohibit the interaction of the PP2A B'β holoenzyme with KLHL15:Cul3, causing dephosphorylation of TH Ser40, causing an overall decrease in dopamine synthesis.

REFERENCES

Adams J, Kelso R, Cooley L (2000) The kelch repeat superfamily of proteins: propellers of cell function *Trends Cell Biol* **10:** 17-24

Akhand AA, Pu M, Senga T, Kato M, Suzuki H, Miyata T, Hamaguchi M, Nakashima I (1999) Nitric oxide controls src kinase activity through a sulfhydryl group modification-mediated Tyr-527-independent and Tyr-416-linked mechanism *J Biol Chem* **274:** 25821-25826

Amati-Bonneau P, Milea D, Bonneau D, Chevrollier A, Ferre M, Guillet V, Gueguen N, Loiseau D, de Crescenzo MA, Verny C*, et al* (2009) OPA1-associated disorders: phenotypes and pathophysiology *Int J Biochem Cell Biol* **41:** 1855-1865

Andrews PW (1984) Retinoic acid induces neuronal differentiation of a cloned human embryonal carcinoma cell line in vitro *Dev Biol* **103:** 285-293

Andrews PW (1988) Human teratocarcinomas *Biochim Biophys Acta* **948:** 17-36

Banky P, Huang LJ, Taylor SS (1998) Dimerization/docking domain of the type Ialpha regulatory subunit of cAMP-dependent protein kinase. Requirements for dimerization and docking are distinct but overlapping *J Biol Chem* **273:** 35048-35055

Barsoum M, Yuan H, Gerencser A, Liot G, Kushnareva Y, Graber S, Kovacs I, Lee W, Waggoner J, Cui J*, et al* (2006) Nitric Oxide-induced mitochondrial fission is regulated by dynamin-related GTPases in neurons. **25:** 3900-3911

Beazely MA, Watts VJ (2006) Regulatory properties of adenylate cyclases type 5 and 6: A progress report *Eur J Pharmacol* **535:** 1-12

Benard G, Rossignol R (2008) Ultrastructure of the mitochondrion and its bearing on function and bioenergetics *Antioxid Redox Signal* **10:** 1313-1342

Benhar M, Forrester MT, Stamler JS (2009) Protein denitrosylation: enzymatic mechanisms and cellular functions *Nat Rev Mol Cell Biol* **10:** 721-732

Benhar M, Thompson JW, Moseley MA, Stamler JS (2010) Identification of S-nitrosylated targets of thioredoxin using a quantitative proteomic approach *Biochemistry* **49:** 6963-6969

Blom N, Gammeltoft S, Brunak S (1999) Sequence-and structure-based prediction of eukaryotic protein phosphorylation sites. **294:** 1351-1362

Bos JL (2003) Epac: a new cAMP target and new avenues in cAMP research *Nat Rev Mol Cell Biol* **4:** 733-738

Bossy B, Petrilli A, Klinglmayr E, Chen J, Lutz-Meindl U, Knott AB, Masliah E, Schwarzenbacher R, Bossy-Wetzel E (2010) S-Nitrosylation of DRP1 does not affect enzymatic activity and is not specific to Alzheimer's disease *J Alzheimers Dis* **20 Suppl 2:** S513-26

Braschi E, Zunino R, McBride HM (2009) MAPL is a new mitochondrial SUMO E3 ligase that regulates mitochondrial fission *EMBO Rep* **10:** 748-754

Brennan JP, Bardswell SC, Burgoyne JR, Fuller W, Schroder E, Wait R, Begum S, Kentish JC, Eaton P (2006) Oxidant-induced activation of type I protein kinase A is mediated by RI subunit interprotein disulfide bond formation *J Biol Chem* **281:** 21827-21836

Brummelkamp TR, Bernards R, Agami R (2002) A System for Stable Expression of Short Interfering RNAs in Mammalian Cells. **296:** 550-553

Burgoyne JR, Eaton P (2009) Transnitrosylating nitric oxide species directly activate type I protein kinase A, providing a novel adenylate cyclase-independent cross-talk to beta-adrenergic-like signaling *J Biol Chem* **284:** 29260-29268

Butt E, Abel K, Krieger M, Palm D, Hoppe V, Hoppe J, Walter U (1994) cAMP- and cGMP-dependent protein kinase phosphorylation sites of the focal adhesion vasodilator-stimulated phosphoprotein (VASP) in vitro and in intact human platelets *J Biol Chem* **269:** 14509-14517

Carlucci A, Adornetto A, Scorziello A, Viggiano D, Foca M, Cuomo O, Annunziato L, Gottesman M, Feliciello A (2008) Proteolysis of AKAP121 regulates mitochondrial activity during cellular hypoxia and brain ischaemia. **27:** 1073-1084

Cartoni R, Martinou JC (2009) Role of mitofusin 2 mutations in the physiopathology of Charcot-Marie-Tooth disease type 2A *Exp Neurol* **218:** 268-273

Cereghetti GM, Costa V, Scorrano L (2010) Inhibition of Drp1-dependent mitochondrial fragmentation and apoptosis by a polypeptide antagonist of calcineurin *Cell Death Differ*

Cereghetti GM, Stangherlin A, Martins de Brito O, Chang CR, Blackstone C, Bernardi P, Scorrano L (2008) Dephosphorylation by calcineurin regulates translocation of Drp1 to mitochondria *Proc Natl Acad Sci U S A* **105:** 15803-15808

Chang CR, Blackstone C (2007a) Cyclic AMP-dependent protein kinase phosphorylation of Drp1 regulates its GTPase activity and mitochondrial morphology *J Biol Chem* **282:** 21583-21587

Chang CR, Blackstone C (2007b) Drp1 phosphorylation and mitochondrial regulation *EMBO Rep* **8:** 1088-9; author reply 1089-90

Chang CR, Blackstone C (2010) Dynamic regulation of mitochondrial fission through modification of the dynamin-related protein Drp1 *Ann N Y Acad Sci* **1201:** 34-39

Chang CR, Manlandro CM, Arnoult D, Stadler J, Posey AE, Hill RB, Blackstone C (2010) A lethal de novo mutation in the middle domain of the dynamin-

related GTPase Drp1 impairs higher-order assembly and mitochondrial division *J Biol Chem*

Chen H, Chan DC (2009) Mitochondrial dynamics--fusion, fission, movement, and mitophagy--in neurodegenerative diseases *Hum Mol Genet* **18:** R169-76

Chen H, Chan D (2005) Emerging functions of mammalian mitochondrial fusion and fission. **Special No 2:** R283-289

Chen H, McCaffery JM, Chan DC (2007) Mitochondrial fusion protects against neurodegeneration in the cerebellum *Cell* **130:** 548-562

Chen H, Detmer SA, Ewald AJ, Griffin EE, Fraser SE, Chan DC (2003) Mitofusins Mfn1 and Mfn2 coordinately regulate mitochondrial fusion and are essential for embryonic development. **160:** 189-200

Chen K, Guo X, Ma D, Guo Y, Li Q, Yang D, Li P, Qiu X, Wen S, Xiao R*, et al* (2004) Dysregulation of HSG triggers vascular proliferative disorders. **6:** 872

Chen Q, Lin RY, Rubin CS (1997) Organelle-specific targeting of protein kinase AII (PKAII). Molecular and in situ characterization of murine A kinase anchor proteins that recruit regulatory subunits of PKAII to the cytoplasmic surface of mitochondria *J Biol Chem* **272:** 15247-15257

Chen W, Zollman S, Couderc JL, Laski FA (1995) The BTB domain of bric a brac mediates dimerization in vitro *Mol Cell Biol* **15:** 3424-3429

Chen Y, Stevens B, Chang J, Milbrandt J, Barres BA, Hell J (2008) NS21: re-defined and modified supplement B27 for neuronal cultures. **171:** 239-247

Cheng X, Ji Z, Tsalkova T, Mei F (2008) Epac and PKA: a tale of two intracellular cAMP receptors *Acta Biochim Biophys Sin (Shanghai)* **40:** 651-662

Cho DH, Nakamura T, Fang J, Cieplak P, Godzik A, Gu Z, Lipton SA (2009) S-nitrosylation of Drp1 mediates beta-amyloid-related mitochondrial fission and neuronal injury *Science* **324:** 102-105

Chung KW, Cho SY, Hwang SJ, Kim KH, Yoo JH, Kwon O, Kim SM, Sunwoo IN, Zuchner S, Choi BO (2008) Early-onset stroke associated with a mutation in Mitofusin 2. **70:** 2010-2011

Chung KW, Kim SB, Park KD, Choi KG, Lee JH, Eun HW, Suh JS, Hwang JH, Kim WK, Seo BC*, et al* (2006) Early onset severe and late-onset mild Charcot-Marie-Tooth disease with mitofusin 2 (MFN2) mutations. **129:** 2103-2118

Cipolat S, de Brito OM, Dal Zilio B, Scorrano L (2004) OPA1 requires mitofusin 1 to promote mitochondrial fusion. **101:** 15927-15932

College W (2006) Hereditary Motor Sensory Neuropathies: Charcot-Marie-Tooth Disease.

Cribbs JT, Strack S (2007) Reversible phosphorylation of Drp1 by cyclic AMP-dependent protein kinase and calcineurin regulates mitochondrial fission and cell death *EMBO Rep* **8:** 939-944

Cribbs JT, Strack S (2009) Functional characterization of phosphorylation sites in dynamin-related protein 1 *Methods Enzymol* **457:** 231-253

Dagda RK, Zhu J, Chu CT (2009) Mitochondrial kinases in Parkinson's disease: converging insights from neurotoxin and genetic models *Mitochondrion* **9:** 289-298

Dagda RK, Barwacz CA, Cribbs JT, Strack S (2005) Unfolding-resistant Translocase Targeting: A Novel mechanism for outer mitochondrial membrane localization exemplified by the B(beta)2 regulatory subunit of Protein Phosphatase 2A. **280:** 27375-27382

Dagda RK, Merrill R, Cribbs JT, Chen Y, Hell J, Usachev Y, Strack S (2008) The Spinocerebellar Ataxia12 Gene Product and Protein Phosphatase 2A Regulatory Subunit Bbeta2 Antagonizes Neuronal Survival by Promoting Mitochondrial Fission. **283:** 36241-36248

Dagda RK, Zaucha JA, Wadzinski BE, Strack S (2003) A developmentally Regulated, Neuron-specific Splice Variant of the Variable Subunit Bb Targets Protein Phosphatase 2A to he Mitochondria and Modulates Apoptosis. **278:** 24976-24985

de Moura MB, dos Santos LS, Van Houten B (2010) Mitochondrial dysfunction in neurodegenerative diseases and cancer *Environ Mol Mutagen* **51:** 391-405

Defer N, Best-Belpomme M, Hanoune J (2000) Tissue specificity and physiological relevance of various isoforms of adenylyl cyclase *Am J Physiol Renal Physiol* **279:** F400-16

Dimmer KS, Scorrano L (2006) (De)constructing Mitochondria: What For? **21:** 233-241

Dougherty B (2005) Iterative Deconvolution.

Eckert RE, Jones SL (2007) Regulation of VASP serine 157 phosphorylation in human neutrophils after stimulation by a chemoattractant *J Leukoc Biol* **82:** 1311-1321

Eichhorn PJ, Creyghton MP, Bernards R (2009) Protein phosphatase 2A regulatory subunits and cancer *Biochim Biophys Acta* **1795:** 1-15

Engelfried K, Vorgerd M, Hagedorn M, Haas G, Gilles J, Epplen JT, Meins M (2006) Charcot-Marie-Tooth neuropathy type 2A: novel mutations in the mitofusin 2 gene (MFN2). **7:**

Erlichman J, Rosenfeld R, Rosen OM (1974) Phosphorylation of a cyclic adenosine 3':5'-monophosphate-dependent protein kinase from bovine cardiac muscle *J Biol Chem* **249:** 5000-5003

Eura Y, Ishihara N, Yokota S, Mihara K (2003) Two Mitofusin Proteins, Mammalian Homologues of FZO, with Distinct Functions Are Both Required for Mitochondrial Fusion. **134:** 333-344

Figueroa-Romero C, Iniguez-Lluhi JA, Stadler J, Chang CR, Arnoult D, Keller PJ, Hong Y, Blackstone C, Feldman EL (2009) SUMOylation of the mitochondrial fission protein Drp1 occurs at multiple nonconsensus sites within the B domain and is linked to its activity cycle *FASEB J* **23:** 3917-3927

Francis SH, Corbin JD (1994) Structure and function of cyclic nucleotide-dependent protein kinases *Annu Rev Physiol* **56:** 237-272

Gluzman Y (1981) SV40-transformed simian cells support the replication of early SV40 mutants *Cell* **23:** 175-182

Guo X, Chen KH, Guo Y, Liao H, Tang J, Xiao RP (2007) Mitofusin 2 triggers vascular smooth muscle cell apoptosis via mitochondrial death pathway *Circ Res* **101:** 1113-1122

Hales KG, Fuller MT (1997) Developmentally regulated mitochondrial fusion mediated by a conserved, novel, predicted GTPase *Cell* **90:** 121-129

Han XJ, Lu YF, Li SA, Kaitsuka T, Sato Y, Tomizawa K, Nairn AC, Takei K, Matsui H, Matsushita M (2008) CaM kinase I alpha-induced phosphorylation of Drp1 regulates mitochondrial morphology *J Cell Biol* **182:** 573-585

Harder Z, Zunino R, McBride H (2004) Sumo1 conjugates mitochondrial substrates and participates in mitochondrial fission *Curr Biol* **14:** 340-345

Haycock JW (1990) Phosphorylation of tyrosine hydroxylase in situ at serine 8, 19, 31, and 40 *J Biol Chem* **265:** 11682-11691

Hemmings BA, Adams-Pearson C, Maurer F, Muller P, Goris J, Merlevede W, Hofsteenge J, Stone SR (1990) alpha- and beta-forms of the 65-kDa subunit of protein phosphatase 2A have a similar 39 amino acid repeating structure *Biochemistry* **29:** 3166-3173

Herzig S, Martinou JC (2008) Mitochondrial dynamics: to be in good shape to survive *Curr Mol Med* **8:** 131-137

Hess DT, Matsumoto A, Kim SO, Marshall HE, Stamler JS (2005) Protein S-nitrosylation: purview and parameters *Nat Rev Mol Cell Biol* **6:** 150-166

Hill J, Howlett A, Klein C (2000) Nitric oxide selectively inhibits adenylyl cyclase isoforms 5 and 6 *Cell Signal* **12:** 233-237

Hirokawa N, Takemura R (2005) Molecular motors and mechanisms of directional transport in neurons *Nat Rev Neurosci* **6:** 201-214

Horbinski C, Chu CT (2005) Kinase signaling cascades in the mitochondrion: a matter of life or death *Free Radic Biol Med* **38:** 2-11

Houslay MD, Adams DR (2003) PDE4 cAMP phosphodiesterases: modular enzymes that orchestrate signalling cross-talk, desensitization and compartmentalization *Biochem J* **370:** 1-18

Huang H, Lee T, Tzeng S, Horng J (2005) KinasePhos: a web tool for identifying protein kinase-specific phosphorylation sites. **33:** W226-229

Huang LJ, Durick K, Weiner JA, Chun J, Taylor SS (1997) Identification of a novel protein kinase A anchoring protein that binds both type I and type II regulatory subunits *J Biol Chem* **272:** 8057-8064

Huang LJ, Wang L, Ma Y, Durick K, Perkins G, Deerinck TJ, Ellisman MH, Taylor SS (1999) NH2-Terminal Targeting Motifs Direct Dual Specificity A-Kinase-anchoring Protein 1†(D-AKAP1) to Either Mitochondria or Endoplasmic Reticulum. **145:** 951-959

Ishihara N, Eura Y, Mihara K (2004) Mitofusin 1 and 2 play distinct roles in mitochondrial fusion reactions via GTPase activity. **117:** 6535-6546

Jahani-Asl A, Slack RS (2007) The phosphorylation state of Drp1 determines cell fate *EMBO Rep* **8:** 912-913

Jahani-Asl A, Cheung ECC, Neuspiel M, MacLaurin JG, Fortin A, Park DS, McBride H, Slack RS (2007) Mitofusin 2 protects cerebellar granule neurons against injury induced cell death. M703812200

James DI, Parone PA, Mattenberger Y, Martinou JC (2003) hFis1, a novel component of the mammalian mitochondrial fission machinery *J Biol Chem* **278:** 36373-36379

Janssens V, Goris J (2001) Protein phosphatase 2A: a highly regulated family of serine/threonine phosphatases implicated in cell growth and signalling *Biochem J* **353:** 417-439

Janssens V, Jordens J, Stevens I, Van Hoof C, Martens E, De Smedt H, Engelborghs Y, Waelkens E, Goris J (2003) Identification and functional analysis of two Ca2+-binding EF-hand motifs in the B"/PR72 subunit of protein phosphatase 2A *J Biol Chem* **278:** 10697-10706

Janssens V, Longin S, Goris J (2008) PP2A holoenzyme assembly: in cauda venenum (the sting is in the tail) *Trends Biochem Sci* **33:** 113-121

Jensen FC, Girardi AJ, Gilden RV, Koprowski H (1964) Infection of Human and Simian Tissue Cultures with Rous Sarcoma Virus. *Proc Natl Acad Sci U S A* **52:** 53-59

Karbowski M, Lee YJ, Gaume B, Jeong SY, Frank S, Nechushtan A, Santel A, Fuller M, Smith CL, Youle RJ (2002) Spatial and temporal association of Bax with mitochondrial fission sites, Drp1, and Mfn2 during apoptosis *J Cell Biol* **159:** 931-938

Karbowski M, Jeong S, Youle RJ (2004) Endophilin B1 is required for the maintenance of mitochondrial morphology. **166:** 1027-1039

Karbowski M, Neutzner A, Youle RJ (2007) The mitochondrial E3 ubiquitin ligase MARCH5 is required for Drp1 dependent mitochondrial division. **178:** 71-84

Karbowski M, Norris KL, Cleland MM, Jeong S, Youle RJ (2006) Role of Bax and Bak in mitochondrial morphogenesis. **443:** 658

Kim TA, Jiang S, Seng S, Cha K, Avraham HK, Avraham S (2005) The BTB domain of the nuclear matrix protein NRP/B is required for neurite outgrowth *J Cell Sci* **118:** 5537-5548

Knott AB, Perkins G, Schwarzenbacher R, Bossy-Wetzel E (2008) Mitochondrial fragmentation in neurodegeneration. **9:** 505-518

Koshiba T, Detmer SA, Kaiser JT, Chen H, McCaffery JM, Chan DC (2004) Structural Basis of Mitochondrial Tethering by Mitofusin Complexes. **305:** 858-862

Kumar S, Barthwal MK, Dikshit M (2010) Cdk2 nitrosylation and loss of mitochondrial potential mediate NO-dependent biphasic effect on HL-60 cell cycle *Free Radic Biol Med* **48:** 851-861

Lechward K, Awotunde OS, Swiatek W, Muszynska G (2001) Protein phosphatase 2A: variety of forms and diversity of functions *Acta Biochim Pol* **48:** 921-933

Lee YJ, Jeong SY, Karbowski M, Smith CL, Youle RJ (2004) Roles of the mammalian mitochondrial fission and fusion mediators Fis1, Drp1, and Opa1 in apoptosis *Mol Biol Cell* **15:** 5001-5011

Legros F, Lombes A, Frachon P, Rojo M (2002) Mitochondrial Fusion in Human Cells is Efficient, Requires the Inner Membrane Potential, and is Mediated by Mitofusins. **13:** 4343-4354

Lenaers G, Reynier P, Elachouri G, Soukkarieh C, Olichon A, Belenguer P, Baricault L, Ducommun B, Hamel C, Delettre C (2009) OPA1 functions in mitochondria and dysfunctions in optic nerve *Int J Biochem Cell Biol* **41:** 1866-1874

Leon DA, Herberg FW, Banky P, Taylor SS (1997) A stable alpha-helical domain at the N terminus of the RIalpha subunits of cAMP-dependent protein kinase is a novel dimerization/docking motif *J Biol Chem* **272:** 28431-28437

Lew JY, Garcia-Espana A, Lee KY, Carr KD, Goldstein M, Haycock JW, Meller E (1999) Increased site-specific phosphorylation of tyrosine hydroxylase accompanies stimulation of enzymatic activity induced by cessation of dopamine neuronal activity *Mol Pharmacol* **55:** 202-209

Liesa M, Palacin M, Zorzano A (2009) Mitochondrial dynamics in mammalian health and disease *Physiol Rev* **89:** 799-845

Lim I, Merrill M, Chen Y, Hell J (2003) Disruption of the NMDA receptor-PSD-95 interaction in hippocampal neurons with no obvious physiological short-term effect. **45:** 738-754

Ma Y, Taylor SS (2008) A molecular switch for targeting between endoplasmic reticulum (ER) and mitochondria: conversion of a mitochondria-targeting element into an ER-targeting signal in DAKAP1 *J Biol Chem* **283:** 11743-11751

MacAskill AF, Kittler JT (2010) Control of mitochondrial transport and localization in neurons *Trends Cell Biol* **20:** 102-112

Margulis L (1981) *Symbiosis in Cell Evolution.* Freeman W.H. and company,

Matsuzaki H, Tamatani M, Yamaguchi A, Namikawa K, Kiyama H, Vitek MP, Mitsuda N, Tohyama M (2001) Vascular endothelial growth factor rescues hippocampal neurons from glutamate-induced toxicity: signal transduction cascades *FASEB J* **15:** 1218-1220

McCright B, Rivers AM, Audlin S, Virshup DM (1996) The B56 family of protein phosphatase 2A (PP2A) regulatory subunits encodes differentiation-induced phosphoproteins that target PP2A to both nucleus and cytoplasm *J Biol Chem* **271:** 22081-22089

McCright B, Virshup DM (1995) Identification of a new family of protein phosphatase 2A regulatory subunits *J Biol Chem* **270:** 26123-26128

McMahon M, Thomas N, Itoh K, Yamamoto M, Hayes JD (2006) Dimerization of substrate adaptors can facilitate cullin-mediated ubiquitylation of proteins by a "tethering" mechanism: a two-site interaction model for the Nrf2-Keap1 complex *J Biol Chem* **281:** 24756-24768

McVey M, Hill J, Howlett A, Klein C (1999) Adenylyl cyclase, a coincidence detector for nitric oxide *J Biol Chem* **274:** 18887-18892

Meeusen S, DeVay R, Block J, Cassidy-Stone A, Wayson S, McCaffery JM, Nunnari J (2006) Mitochondrial inner-membrane fusion and crista maintenance requires the dynamin-related GTPase Mgm1 *Cell* **127:** 383-395

Merrill RA, Dagda RK, Cribbs JT, Dickey AS, Green SH, Ushachev YM, Strack S (2010) Mechanism of mitochondrial fusion by PKA/AKAP1.

Misko A, Jiang S, Wegorzewska I, Milbrandt J, Baloh RH (2010) Mitofusin 2 is necessary for transport of axonal mitochondria and interacts with the Miro/Milton complex *J Neurosci* **30:** 4232-4240

Nakamura N, Kimura Y, Tokuda M, Honda S, Hirose S (2006) MARCH-V is a novel mitofusin 2 and Drp1 binding protein able to change mitochondrial morphology.

Nangaku M, Sato-Yoshitake R, Okada Y, Noda Y, Takemura R, Yamazaki H, Hirokawa N (1994) KIF1B, a novel microtubule plus end-directed monomeric motor protein for transport of mitochondria *Cell* **79:** 1209-1220

Nemes JP, Benzow KA, Moseley ML, Ranum LP, Koob MD (2000) The SCA8 transcript is an antisense RNA to a brain-specific transcript encoding a novel actin-binding protein (KLHL1) *Hum Mol Genet* **9:** 1543-1551

Neutzner A, Youle RJ, Karbowski M (2007) Outer mitochondrial membrane protein degradation by the proteasome *Novartis Found Symp* **287:** 4-14; discussion 14-20

Palau F, Estela A, Pla-Martin D, Sanchez-Piris M (2009) The role of mitochondrial network dynamics in the pathogenesis of Charcot-Marie-Tooth disease *Adv Exp Med Biol* **652:** 129-137

Park HS, Huh SH, Kim MS, Lee SH, Choi EJ (2000) Nitric oxide negatively regulates c-Jun N-terminal kinase/stress-activated protein kinase by means of S-nitrosylation *Proc Natl Acad Sci U S A* **97:** 14382-14387

Park YY, Lee S, Karbowski M, Neutzner A, Youle RJ, Cho H (2010) Loss of MARCH5 mitochondrial E3 ubiquitin ligase induces cellular senescence through dynamin-related protein 1 and mitofusin 1 *J Cell Sci* **123:** 619-626

Perez-Torrado R, Yamada D, Defossez PA (2006) Born to bind: the BTB protein-protein interaction domain *Bioessays* **28:** 1194-1202

Petroski MD, Deshaies RJ (2005) Function and regulation of cullin-RING ubiquitin ligases *Nat Rev Mol Cell Biol* **6:** 9-20

Pierrat B, Simonen M, Cueto M, Mestan J, Ferrigno P, Heim J (2001) SH3GLB, a new endophilin-related protein family featuring an SH3 domain. **71:** 222-234

Pintard L, Willems A, Peter M (2004) Cullin-based ubiquitin ligases: Cul3-BTB complexes join the family *EMBO J* **23:** 1681-1687

Praefcke GJ, McMahon HT (2004) The dynamin superfamily: universal membrane tubulation and fission molecules? *Nat Rev Mol Cell Biol* **5:** 133-147

Qian W, Shi J, Yin X, Iqbal K, Grundke-Iqbal I, Gong CX, Liu F (2010) PP2A regulates tau phosphorylation directly and also indirectly via activating GSK-3beta *J Alzheimers Dis* **19:** 1221-1229

Reilly MM (2005) Axonal Charcot-Marie-Tooth disease: The fog is slowly lifting! **65:** 186-187

Reynolds A, Leake D, Boese Q, Scaringe S, Marshall WS, Khvorova A (2004) Rational siRNA design for RNA interference. **22:** 326

Robinson DN, Cooley L (1997) Drosophila kelch is an oligomeric ring canal actin organizer *J Cell Biol* **138:** 799-810

Rondou P, Haegeman G, Vanhoenacker P, Van Craenenbroeck K (2008) BTB Protein KLHL12 targets the dopamine D4 receptor for ubiquitination by a Cul3-based E3 ligase *J Biol Chem* **283:** 11083-11096

Rotin D, Kumar S (2009) Physiological functions of the HECT family of ubiquitin ligases *Nat Rev Mol Cell Biol* **10:** 398-409

Santel A, Frank S (2008) Shaping mitochondria: The complex posttranslational regulation of the mitochondrial fission protein DRP1 *IUBMB Life* **60:** 448-455

Santel A, Fuller MT (2001) Control of mitochondrial morphology by a human mitofusin. **114:** 867-874

Santel A, Frank S, Gaume B, Herrler M, Youle RJ, Fuller MT (2003) Mitofusin-1 protein is a generally expressed mediator of mitochondrial fusion in mammalian cells. **116:** 2763-2774

Saraf A, Oberg EA, Strack S (2010) Molecular determinants for PP2A substrate specificity: charged residues mediate dephosphorylation of tyrosine hydroxylase by the PP2A/B' regulatory subunit *Biochemistry* **49:** 986-995

Saraf A, Virshup DM, Strack S (2007) Differential expression of the B'beta regulatory subunit of protein phosphatase 2A modulates tyrosine hydroxylase phosphorylation and catecholamine synthesis *J Biol Chem* **282:** 573-580

Sarma GN, Kinderman FS, Kim C, von Daake S, Chen L, Wang BC, Taylor SS (2010) Structure of D-AKAP2:PKA RI complex: insights into AKAP specificity and selectivity *Structure* **18:** 155-166

Scheffler IE (2008) *Mitochondria* Wiley-Liss, Hoboken, N.J.

Scherer WF, Syverton JT, Gey GO (1953) Studies on the propagation in vitro of poliomyelitis viruses. IV. Viral multiplication in a stable strain of human malignant epithelial cells (strain HeLa) derived from an epidermoid carcinoma of the cervix. *J Exp Med* **97:** 695-710

Seeling JM, Miller JR, Gil R, Moon RT, White R, Virshup DM (1999) Regulation of beta-catenin signaling by the B56 subunit of protein phosphatase 2A *Science* **283:** 2089-2091

Seo AY, Joseph AM, Dutta D, Hwang JC, Aris JP, Leeuwenburgh C (2010) New insights into the role of mitochondria in aging: mitochondrial dynamics and more *J Cell Sci* **123:** 2533-2542

Shen T, Suzuki Y, Poyard M, Miyamoto N, Defer N, Hanoune J (1997) Expression of adenylyl cyclase mRNAs in the adult, in developing, and in the Brattleboro rat kidney *Am J Physiol* **273:** C323-30

Shi Y (2009) Assembly and structure of protein phosphatase 2A *Sci China C Life Sci* **52:** 135-146

Shin HW, Takatsu H, Mukai H, Munekata E, Murakami K, Nakayama K (1999) Intermolecular and interdomain interactions of a dynamin-related GTP-binding protein, Dnm1p/Vps1p-like protein *J Biol Chem* **274:** 2780-2785

Shu X, Shaner NC, Yarbrough CA, Tsien RY, Remington SJ (2006) Novel Chromophores and Buried Charges Control Color in mFruits. **45:** 9639-9647

Skroblin P, Grossmann S, Schafer G, Rosenthal W, Klussmann E (2010) Mechanisms of protein kinase a anchoring *Int Rev Cell Mol Biol* **283:** 235-330

Smirnova E, Griparic L, Shurland DL, van der Bliek AM (2001) Dynamin-related protein Drp1 is required for mitochondrial division in mammalian cells *Mol Biol Cell* **12:** 2245-2256

Smirnova E, Shurland D, Ryazantsev SN, van der Bliek AM (1998) A Human Dynamin-related Protein Controls the Distribution of Mitochondria. **143:** 351-358

Steen RL, Martins SB, Tasken K, Collas P (2000) Recruitment of protein phosphatase 1 to the nuclear envelope by A-kinase anchoring protein AKAP149 is a prerequisite for nuclear lamina assembly *J Cell Biol* **150:** 1251-1262

Stojanovski D, Koutsopoulos OS, Okamoto K, Ryan MT (2004) Levels of human Fis1 at the mitochondrial outer membrane regulate mitochondrial morphology *J Cell Sci* **117:** 1201-1210

Strack S, Chang D, Zaucha JA, Colbran RJ, Wadzinski BE (1999) Cloning and characterization of B delta, a novel regulatory subunit of protein phosphatase 2A *FEBS Lett* **460:** 462-466

Strack S, Zaucha JA, Ebner FF, Colbran RJ, Wadzinski BE (1998) Brain protein phosphatase 2A: developmental regulation and distinct cellular and subcellular localization by B subunits *J Comp Neurol* **392:** 515-527

Strack S, Cribbs JT, Gomez L (2004) Critical Role for Protein Phosphatase 2A Heterotrimers in Mammalian Cell Survival. **279:** 47732-47739

Suen D, Norris K, Youle RJ (2008) Mitochondrial dynamics and apoptosis. **22:** 1577-1590

Sugioka R, Shimizu S, Tsujimoto Y (2004) Fzo1, a protein involved in mitochondrial fusion, inhibits apoptosis *J Biol Chem* **279:** 52726-52734

Szabadkai G, Simoni AM, Chami M, Wieckowski MR, Youle RJ, Rizzuto R (2004) Drp-1-Dependent Division of the Mitochondrial Network Blocks Intraorganellar Ca2+ Waves and Protects against Ca2+-Mediated Apoptosis. **16:** 59

Taguchi N, Ishihara N, Jofuku A, Oka T, Mihara K (2007) Mitotic phosphorylation of dynamin-related GTPase Drp1 participates in mitochondrial fission *J Biol Chem* **282:** 11521-11529

Takahashi Y, Karbowski M, Yamaguchi H, Kazi A, Wu J, Sebti SM, Youle RJ, Wang H (2005) Loss of Bif-1 Suppresses Bax/Bak Conformational Change and Mitochondrial Apoptosis. **25:** 9369-9382

Takahashi Y, Meyerkord C, Wang H (2008) BARgaining membranes for autophagosome formation: Regulation of autophagy and tumorigenesis by Bif-1/Endophilin B1. **4:** 121-124

Tanaka K (2001) Alteration of second messengers during acute cerebral ischemia - adenylate cyclase, cyclic AMP-dependent protein kinase, and cyclic AMP response element binding protein *Prog Neurobiol* **65:** 173-207

Taylor SS, Buechler JA, Yonemoto W (1990) cAMP-dependent protein kinase: framework for a diverse family of regulatory enzymes *Annu Rev Biochem* **59:** 971-1005

Twig G, Elorza A, Molina AJ, Mohamed H, Wikstrom JD, Walzer G, Stiles L, Haigh SE, Katz S, Las G*, et al* (2008) Fission and selective fusion govern mitochondrial segregation and elimination by autophagy *EMBO J* **27:** 433-446

Urrutia R, Henley JR, Cook T, McNiven MA (1997) The dynamins: redundant or distinct functions for an expanding family of related GTPases? *Proc Natl Acad Sci U S A* **94:** 377-384

Vallat JM, Ouvrier RA, Pollard JD, Magdelaine C, Zhu D, Nicholson GA, Grew S, Ryan MM, Funalot B (2008) Histopathological findings in hereditary motor and sensory neuropathy of axonal type with onset in early childhood associated with mitofusin 2 mutations. *J Neuropathol Exp Neurol* **67:** 1097-1102

van den Heuvel S (2004) Protein degradation: CUL-3 and BTB--partners in proteolysis *Curr Biol* **14:** R59-61

Van Kanegan MJ, Adams DG, Wadzinski BE, Strack S (2005) Distinct protein phosphatase 2A heterotrimers modulate growth factor signaling to extracellular signal-regulated kinases and Akt *J Biol Chem* **280:** 36029-36036

Van Kanegan MJ, Strack S (2009) The protein phosphatase 2A regulatory subunits B'beta and B'delta mediate sustained TrkA neurotrophin receptor autophosphorylation and neuronal differentiation *Mol Cell Biol* **29:** 662-674

Verhoeven K, Claeys KG, Zuchner S, Schroder JM, Weis J, Ceuterick C, Jordanova A, Nelis E, De Vriendt E, Van Hul M*, et al* (2006) MFN2 mutation distribution and genotype/phenotype correlation in Charcot-Marie-Tooth type 2. **129:** 2093-2102

Viste K, Kopperud RK, Christensen AE, Doskeland SO (2005) Substrate enhances the sensitivity of type I protein kinase a to cAMP *J Biol Chem* **280:** 13279-13284

Voorhoeve PM, Hijmans EM, Bernards R (1999) Functional interaction between a novel protein phosphatase 2A regulatory subunit, PR59, and the retinoblastoma-related p107 protein *Oncogene* **18:** 515-524

Walsh C, Barrow S, Voronina S, Chvanov M, Petersen OH, Tepikin A (2009) Modulation of calcium signalling by mitochondria *Biochim Biophys Acta* **1787:** 1374-1382

Walter G, Ferre F, Espiritu O, Carbone-Wiley A (1989) Molecular cloning and sequence of cDNA encoding polyoma medium tumor antigen-associated 61-kDa protein *Proc Natl Acad Sci U S A* **86:** 8669-8672

Wang G, Moniri NH, Ozawa K, Stamler JS, Daaka Y (2006) Nitric oxide regulates endocytosis by S-nitrosylation of dynamin *Proc Natl Acad Sci U S A* **103:** 1295-1300

Wang X, Su B, Lee HG, Li X, Perry G, Smith MA, Zhu X (2009) Impaired balance of mitochondrial fission and fusion in Alzheimer's disease *J Neurosci* **29:** 9090-9103

Waterham HR, Koster J, van Roermund CW, Mooyer PA, Wanders RJ, Leonard JV (2007) A lethal defect of mitochondrial and peroxisomal fission *N Engl J Med* **356:** 1736-1741

Wong W, Scott JD (2004) AKAP signalling complexes: focal points in space and time *Nat Rev Mol Cell Biol* **5:** 959-970

Xing Y, Xu Y, Chen Y, Jeffrey PD, Chao Y, Lin Z, Li Z, Strack S, Stock JB, Shi Y (2006) Structure of protein phosphatase 2A core enzyme bound to tumor-inducing toxins *Cell* **127:** 341-353

Xu Y, Xing Y, Chen Y, Chao Y, Lin Z, Fan E, Yu JW, Strack S, Jeffrey PD, Shi Y (2006) Structure of the protein phosphatase 2A holoenzyme *Cell* **127:** 1239-1251

Yamamoto H, Hinoi T, Michiue T, Fukui A, Usui H, Janssens V, Van Hoof C, Goris J, Asashima M, Kikuchi A (2001) Inhibition of the Wnt signaling pathway by the PR61 subunit of protein phosphatase 2A *J Biol Chem* **276:** 26875-26882

Yoon Y, Krueger EW, Oswald BJ, McNiven MA (2003) The mitochondrial protein hFis1 regulates mitochondrial fission in mammalian cells through an interaction with the dynamin-like protein DLP1 *Mol Cell Biol* **23:** 5409-5420

Yoshida K (2005) Identification and characterization of a novel kelch-like gene KLHL15 in silico *Oncol Rep* **13:** 1133-1137

Youle RJ, Karbowski M (2005) Mitochondrial Fission in Apoptosis. **6:** 622

Zhou W, Chen KH, Cao W, Zeng J, Liao H, Zhao L, Guo X (2010) Mutation of the protein kinase A phosphorylation site influences the anti-proliferative activity of mitofusin 2 *Atherosclerosis* **211:** 216-223

Zhu D, Kennerson ML, Walizada G, Zuchner S, Vance JM, Nicholson GA (2005) Charcot-Marie-Tooth with pyramidal signs is genetically heterogeneous: Families with and without MFN2 mutations. **65:** 496-497

Zhu PP, Patterson A, Stadler J, Seeburg DP, Sheng M, Blackstone C (2004) Intra- and intermolecular domain interactions of the C-terminal GTPase effector domain of the multimeric dynamin-like GTPase Drp1 *J Biol Chem* **279:** 35967-35974

Zhuang M, Calabrese MF, Liu J, Waddell MB, Nourse A, Hammel M, Miller DJ, Walden H, Duda DM, Seyedin SN*, et al* (2009) Structures of SPOP-substrate complexes: insights into molecular architectures of BTB-Cul3 ubiquitin ligases *Mol Cell* **36:** 39-50

Zipper LM, Mulcahy RT (2002) The Keap1 BTB/POZ dimerization function is required to sequester Nrf2 in cytoplasm *J Biol Chem* **277:** 36544-36552

Zorzano A, Liesa M, Palacin M (2009) Role of mitochondrial dynamics proteins in the pathophysiology of obesity and type 2 diabetes *Int J Biochem Cell Biol* **41:** 1846-1854

Zuchner S, Mersiyanova IV, Muglia M, Bissar-Tadmouri N, Rochelle J, Dadali EL, Zappia M, Nelis E, Patitucci A, Senderek J*, et al* (2004) Mutations in the mitochondrial GTPase mitofusin 2 cause Charcot-Marie-Tooth neuropathy type 2A. **36:** 449